공학박사학위논문

Identification and Characterization of Cell-penetrating Peptide from 30Kc19 Protein and Its Application to Protein and Gene Delivery

30Kc19 단백질의 세포투과 펩타이드 동정과 특성 분석 및
단백질과 유전자 전달을 위한 응용

2014년 8월

서울대학교 대학원
공과대학 화학생물공학부
박 희 호

ABSTRACT

Identification and Characterization of Cell-penetrating Peptide from 30Kc19 Protein and Its Application to Protein and Gene Delivery

Hee Ho Park
School of Chemical and Biological Engineering
The Graduate School
Seoul National University

30Kc19 protein is a member of the 30K protein family, a similar structured protein found in hemolymph of *Bombyx mori*. These proteins have molecular weights of around 30 kDa, and 30Kc19 protein is the most abundant among 30K proteins (30Kc6, 30Kc12, 30Kc19, 30Kc21 and 30Kc23) in the hemolymph. Although the biological functions of the 30K proteins in silkworms have not been fully determined, several studies have recently examined their functional properties for 30Kc6 and 30Kc19. In previous studies, it was demonstrated that silkworm hemolymph and 30K proteins exhibit an anti-apoptotic effect in various cells by adding the protein to culture medium or by gene expression. 30K proteins also enhanced productions of recombinant

erythropoietin, interferon-β, and monoclonal antibody, as well as increasing glycosylation, cell growth, and viability in various cells, and also had enzyme-stabilizing effects. A recent study has shown that 30Kc19 protein has a cell-penetrating property when supplemented to the culture medium. Therefore, 30Kc19 protein is a very unique multi-functional protein, and can be applied for the delivery of therapeutic proteins, including enzymes, as it can penetrate cell membrane as well as stabilizing cargo proteins.

The dimerization propensity of the 30Kc19 in the presence of amphiphiles led to the objective of this research; the investigation on the mechanism of internalization of the 30Kc19 and the minimal effective partial sequence of the parent protein that is necessary for the cell-penetrating to occur and delivery of cargos into cells. First, dimerization propensity of the 30Kc19 protein in the presence of amphiphilic moieties; SDS and phospholipid was investigated. Native PAGE result showed that the 30Kc19 monomer formed a dimer when SDS or phospholipid was present. From the GST pull-down assay, supplementation of the 30Kc19 protein to mammalian cell culture medium showed dimerization and penetration; due to phospholipids at the cell membrane, the main components of the lipid bilayer. Mutagenesis was performed, and penetration was observed by 30Kc19 C76A and not 30Kc19 C57A, which meant Cys-57 is involved in dimerization of the 30Kc19 at the cell membrane during penetration. Then explored how the cell-penetrating 30Kc19 protein is related with phospholipids, the main cell membrane components, and elucidate the mechanism of entry of the 30Kc19 protein into animal cells for use in protein delivery system.

Based on the cell penetrating mechanism and cargo-delivery ability, hypothetical presence of cell-penetrating peptide (CPP) was assumed and endeavored in the identification of a CPP of the 30Kc19 protein originating from the silkworm. For the practical use in delivery of cell-impermeable cargo molecules, it is necessary to find a cell-penetrating domain like other cell-penetrating proteins that can efficiently deliver cargo molecules into cells. A domain was selected as the most probable candidate for CPP and several CPP candidates were tested for cell-penetrating property. From this, a new CPP; VVNKLIRNNKMNC, from 30Kc19 protein (Pep-c19) was identified and demonstrated that 30Kc19 exhibited a cell-penetrating property due to the presence of a cell-penetrating peptide at 45-57. Efficiency and toxicity of this CPP was investigated in comparison with its original protein, 30Kc19, both *in vitro* and *in vivo* and showed its superiority over its parent protein in terms of efficiency. Pep-c19 is a cell-penetrating peptide derived from the first cell-penetrating protein in insect hemolymph. Through this finding, anticipate in finding other cell-penetrating peptides from other proteins sourced from insects that have similar properties to Pep-c19.

For therapeutic application, non-covalent approach for the delivery of siRNA. The results showed that Pep-c19 was able to deliver siRNAs and have gene silencing effect along with 11R, other widely recognized CPP.

The 30Kc19 protein and Pep-c19 are a non-virus derived (e.g. TAT) and non-cytotoxic cell-penetrating protein/peptide. This study may open up new approaches and provide beneficial effects for the delivery of therapeutics in bioindustries, such as pharma- and cosmeceuticals.

Keywords: 30Kc19 protein, dimerization, cell-penetrating peptide (CPP), siRNA, recombinant protein production, *in vivo* delivery

Student number: 2007-30849

Contents

List of Figures

List of Tables

List of Abbreviations

ALT : aspartate aminotransferase

Antp : Antennapedia homeodomain or Penetratin

Arg : arginine

AST : alanine aminotransferase

BBB : blood brain barrier

BCA : bicinchronic acid

BSA : bovine serum albumin

BME : β-mercaptoethanol

BUN : blood urea nitrogen

CHAPS : 3-[(3-cholamidopropyl)dimethylammonio]-1-propanesulfonate

CLC : Cake-Loving Company

CLSM : confocal laser scanning microscopy

CPP : cell-penetrating peptide

CTAB : cetyl trimethylammonium bromide

DMEM : Dulbecco's modified Eagle's medium

dsRNA : double-stranded ribonucleic acid

DW : deionized water

E. coli : *Escherichia coli*

EDTA : ethylenediaminetetraacetic acid

EGFP : enhanced green fluorescent protein

EMBOSS : The European Molecular Biology Open Software Suite

FBS : fetal bovine serum

FGFR3 : fibroblast growth factor receptors 3

FITC : fluorescein isothiocyanate

GFP : green fluorescent protein

GST : glutathione-S-transferase

HCl : hydrochloric acid

HEK 293 : human embryonic kidney 293

HeLa: Henrietta Lacks

HIV-1 : human immunodeficiency virus-1

HRP : horseradish peroxidase

HSV-1 : herpes simplex virus-1

IPTG : isopropyl 1-thio-β-D-galactopyranoside

LOOPP : Learning, Observing and Outputting Protein Patterns

MAP : model amphipathic peptide

MTS : membrane translocation sequence

mRNA : messenger ribonucleic acid

MTT : 3,(4,5-dimethylthiazol-2-yl)2,3-diphenyltetrazolium

naCPP : non-amphipathic cell-penetrating peptide

OCT : optimal cutting temperature

paCPP : primary amphipathic cell-penetrating peptide

PAGE : polyacryl amide gel electrophoresis

PBS : phosphate buffered saline

PS : penicillin-streptomycin

PTD : protein transduction domain

R : arginine

RIPA : radioimmunoprecipitation assay

RISC : ribonucleic acid-induced silencing complex

RNA : ribonucleic acid

RNAi : ribonucleic acid interference

saCPP : secondary amphipathic cell-penetrating peptide

SD : standard deviation

SDS : sodium dodecyl sulfate

SST : serum separating tube

siRNA : short interfering ribonucleic acid

TAT : trans-activator of transcription

TP : Transportan

T X-100 : Triton X-100

Chapter 1.

Research background and objectives

Chapter 1. Research background and objectives

The 30Kc19 protein, a member of the 30K protein family, is a similar structured protein found in silkworm hemolymph, *Bombyx mori* [1]. It is the most abundant among 30K proteins (30Kc6, 30Kc12, 30Kc19, 30Kc21 and 30Kc23) in hemolymph with molecular weights of about 30 kDa [2]. These "30K proteins" are synthesized in fat body cells and accumulate in the hemolymph during the fifth instar larval to early pupal stages [3, 4]. They are then transferred from the hemolymph to fat body cells during metamorphosis from larva to pupa and are deposited there until use [5, 6].

The biological functions of the 30K proteins in silkworms have not been fully determined, although several studies have recently examined their functional properties [6, 7]. In previous studies, it was demonstrated that silkworm hemolymph and 30K proteins exhibit an anti-apoptotic effect in various cells by adding the protein to culture or medium by gene expression [8-20]. Other than the anti-apoptotic effect, 30K proteins also enhance production of recombinant erythropoietin, interferon-β, and monoclonal antibodies; increase glycosylation, cell growth, and viability in various cells; and have an enzyme-stabilizing effect [21-28]. A recent study has shown that 30Kc19 protein has a cell-penetrating property when supplemented to the culture medium [29]. Therefore, the 30Kc19 protein is a very unique multifunctional protein that can be applied for the delivery of therapeutic proteins including enzymes, as it can penetrate cell membranes and stabilize cargo proteins. However, the exact mechanism of penetration to animal cells has not been fully

determined and hence is necessary to understand the molecular mechanism of cell penetration for the practical use of the 30Kc19 protein. In addition, for the practical use in delivery of cell-impermeable cargo molecules, it is necessary to find a cell-penetrating domain like other cell-penetrating proteins that can efficiently deliver cargo molecules into cells.

In this research, dimerization propensity of the 30Kc19 protein in the presence of amphiphilic moieties; SDS and phospholipid was investigated. Then explored how the cell-penetrating 30Kc19 protein is related with phospholipids, the main cell membrane components, and elucidate the mechanism of entry of the 30Kc19 protein into animal cells for use in protein delivery system. Furthermore, I endeavored in the identification of a cell-penetrating peptide of the 30Kc19 protein (Pep-c19), originating from the silkworm. A domain was selected as the most probable candidate for CPP and several CPP candidates were tested for cell-penetrating property. Then, efficiency and toxicity of this CPP was investigated in comparison with its original protein, 30Kc19, both *in vitro* and *in vivo*.

In summary, the objectives of this study are:

1. Investigation of dimerization propensity of the 30Kc19 protein in the presence of amphiphilic moieties and the mechanism of entry into mammalian cells.
2. Prediction and identification of cell-penetrating peptide (CPP) of the 30Kc19 protein (Pep-c19)

3. Application of Pep-c19 for protein delivery *in vitro* and *in vivo* systems
4. Application of Pep-c19 for siRNA delivery *in vitro* system

The 30Kc19 protein and Pep-c19 are a non-virus derived (e.g. TAT) and non-cytotoxic (polyarginine) cell-penetrating protein/peptide. In this study, efforts have led to finding of cell-penetrating mechanism of the 30Kc19 protein and its relationship with dimerization phenomenon, identification of Pep-c19 for protein delivery *in vitro* and *in vivo*, and its potential for therapeutic protein delivery. This study may open up new approaches for the delivery of therapeutics in bioindustries, such as pharma- and cosmeceuticals.

Chapter 2.

Literature review

Chapter 2. Literature review

2.1 Cell-penetrating peptides (CPPs)

Biological molecules, including proteins, small molecules, nucleic acids, antibodies, nanoparticles, and drugs enter into the cells through lipid bilayer or the nucleus across nuclear membrane to utilize their given actions in the cells. Generally however, cell membrane restricts intracellular and intranuclear delivery of molecules except for certain circumstances and specific conditions. To overcome problems of conventional intracellular delivery, various techniques have been developed. A conventional procedure for delivering genetic material is to use viral vectors, but treating genetic disorders with this method has met with only limited success [30]. Alternative nonviral methods, such as electroporation, microinjection, pH-sensitive or cationic liposomes have been developed for conventional drug delivery. However, limitations in terms of efficiency, applicable to only some molecules, or requirement of special tools were shown [31-33].

2.1.1 Terminology, classification, and structure of CPPs

A unified terminology and classification of the carrier peptides has not yet been developed. In the past two decades, as well as cell-penetrating proteins, the so-called “cell-penetrating peptides (CPPs)” have gained increasing attention. These new class of peptides are generally less than 30 amino acids in length, and are comprised of cationic and/or hydrophobic residues, which can

penetrate into cells [34, 35]. In 1988, Green and Frankel first discovered that TAT CPP derived from HIV-1 virus move across the cell membrane [36, 37]. They demonstrated the ability of TAT protein, derived from human immunodeficiency virus-1 (HIV-1), to penetrate into cells in a receptor-independent and concentration-dependent manner [36-38]. Since then, penetratin CPP derived from Antennapedia of *Drosophila melanogaster* in 1994 [39, 40], and VP22 CPP derived from herpes simplex virus in 1997 [41, 42] were discovered.

Recently, classification of CPPs has been suggested which can be arranged in three classes: protein derived CPPs, model peptides, and designed CPPs [43]. Protein derived CPPs generally consist of the minimal effective partial sequence of the parent cell-penetrating protein, and are known also as “protein transduction domains (PTDs)” or “membrane translocation sequences (MTSs)”. Model CPPs comprise of sequences that have been designed with the aim of producing well defined α-helical structures with amphipathic properties or of mimicking the structures of known CPPs. Designed CPPs are generally chimeric peptides composed of a hydrophilic and a hydrophobic domain of different origin. The structures and origins of major representative CPPs are shown in Table 2.1.1.

As demonstrated, CPPs from different classes have different amino acid sequence motifs. However, two common features can be seen, which are all CPPs appear to be a positive charge and amphipathicity. All known CPPs are net positively charged at physiological pH, and comprised of approximately 17% [44] to 100% (polyarginines [45, 46]) of positively charged amino acids. All

CPPs are amphipathic with the exception of polycationic homopolymers (polyarginines, polylysines and polyornithines [46-48]. Some CPPs adopt amphipathic character when in an α-helical structure, as for instance the model amphipathic peptide (MAP) [49], while others have distinct hydrophobic and hydrophilic parts, as, for instance, the chimeric transportan CPP [50].

2.1.2 Mechanism of penetration

The exact mechanism responsible for the uptake of CPPs and their cargos has not yet been fully established and has been the subject of considerable study for the past decades. In spite of some common features of these peptides, particularly their highly cationic nature and hydrophobicity, it was proposed that penetration mechanism is not the same for CPPs of different types. A number of experiments on CPP penetration in cell lines have been carried out under non-endocytotic and no active transport environment, where efficient penetration was observed at low temperatures at 4 °C and in the presence of many different inhibitors of endocytosis [40, 49-62]. However, recent studies showed that the role of endocytosis in internalization of CPP cannot be neglected [63, 64]. At least for some CPPs endocytosis could be an exclusive or alternative mechanism of internalization. It was shown that the internalization of penetratin peptides into the live cells is related to endocytotic processes [65] and that Tat derived CPPs do not enter live cells at low temperature [60] and are not internalized into liposomes [66]. Recently it was suggested that Tat derived

Table 2.1.1 Examples of cell-penetrating peptides (CPPs)

Name Sequence	**Class** Origin	Ref.
Tat CGRKKRRQRRRPPQC	**Protein-derived CPP** Human immunodeficiency virus-1 trans-activating transcriptional activator (HIV-1 TAT); amino acids 48-60	[51]
Antp (Penetratin) RQIKIWFQNRRMKWKK	**Protein-derived CPP** *Drosophila* Antennapedia homeodomain; amino acids residues 43-58	[40]
MAP (Model amphipathic peptide) KLALKLALKALKAALKLA-amide	**Model peptide**	[49]
$(Arg)_7$ (R7) RRRRRRR	**Model peptide**	[46]
MPG GALFLGFLGAAGSTMGAWSQPKSKRKV	**Designed CPP** Peptide derived from fusion sequence of HIV-1 gp41 protein coupled to peptide derived from the nuclear localization sequence of SV40 T-antigen	[67]
Transportan (TP) GWTLNSAGYLLGKINLKALAALAKISIL-amide	**Designed CPP** Minimal active part of galanin (amino acids l–12) coupled to mastoparan via Lys	[50]

CPPs enter cells primarily by lipid raft-mediated macropinocytosis that is stimulated by cell-surface binding of Tat derived CPPs, which is an another form of endocytosis [68, 69].

On the other hand, an inverted micelle mechanism was suggested for penetratin and Tat, in which positively charged peptides interact with negatively charged phospholipids to change part of the membrane into an inverted micelle structure that can open on either the intracellular or the extracellular side of the membrane [40, 64]. The cell-penetrating peptide that has an α-helical structure, for instance MAP and, partly, transportan [70] , could be associated with pore formation when in contact with membrane [71, 72].

Based on the known processes that occur during internalization, CPPs were classified based on their mechanisms of entry (Table 2.1.2) and a hypothetical lipid binding of CPPs as function of their amphipathic property and lipid headgroup charge was constructed (Fig. 2.1.2) [73]. As can be seen in the figure, internalization of CPP varies depending on their classification. The first step of internalization is the interaction of CPP with the cell surface. Primary amphipathic CPPs (paCPPs) penetrate into membranes of high and low anionic lipid content and induce membrane leakage. Secondary amphipathic CPPs (saCPPs) undergo structural change and then membrane insertion occurs. In contrast, no headgroup binding happens for non-amphipathic CPPs (naCPPs), thus no insertion but transmembrane electrical field enables the internalization of CPPs. It has been shown that cationic CPPs (naCPP) bind electrostatically to the exposed negative-charged lipid bilayer of cell membrane, which stimulates the macropinocytic uptake of CPPs and its cargos into macropinosomes and

endosomal escape into cytoplasm. The endosomal escape process is likely to be dependent on the pH drop in endosomes and along with other factors, which perturbs the endosomal membrane, thus release of CPPs and its cargo into cytoplasm. To date, a number of studies are now emphasizing the role of endocytosis [60, 74, 75], and in particular macropinocytosis [68, 76, 77], direct penetration [78, 79], and inverted micelle [80-82].

2.1.3 Penetration of CPPs *in vitro* and *in vivo*

The transport of CPPs across membranes has been studied *in vitro* cells and in tissues *in vivo*. Various mammalian cells have been used, including primary cells and cell lines. CPPs successfully penetrated in primary cells from brain and spinal cord of rat [40], aorta of calf [83], endothelium of umbilical vein from porcine and human [49], and in osteoclasts [84]. But mostly, cell lines have been used.

For penetration to occur, no special cell cultivating procedures are needed with cell lines. Cells are usually grown to a certain % of confluence in dishes, wells, or μ-well plates and then can be incubated with CPP containing solution, which in most cases is cell culture medium. When the penetration of CPP is monitored directly by confocal microscopy or other imaging techniques, the cells are usually fixed by formaldehyde or paraformaldehyde, both of which are milder fixation agents than acetone, and methanol [85, 86]. It has been argued recently that even mild fixation can affect the internalization of some CPPs and artifacts may occur [60]. However, with or without the fixation process, it still

Table 2.1.2 Classification of CPPs based on their mechanism.

Classification	**Name** Sequence
Primary amphipathic CPPs (paCPPs)	**Transportan (TP)** GWTLNSAGYLLGKINLKALAALAKKIL
Secondary amphipathic CPPs (saCPPs)	**Antp (Penetratin)** RQIKIWFQNRRMKWKK **MAP** KLALKLALKALKAALKLA
Non-amphipathic CPPs (naCPPs)	**Tat** YGRKKRRQRRR **$(Arg)_7$ (R7)** RRRRRRR

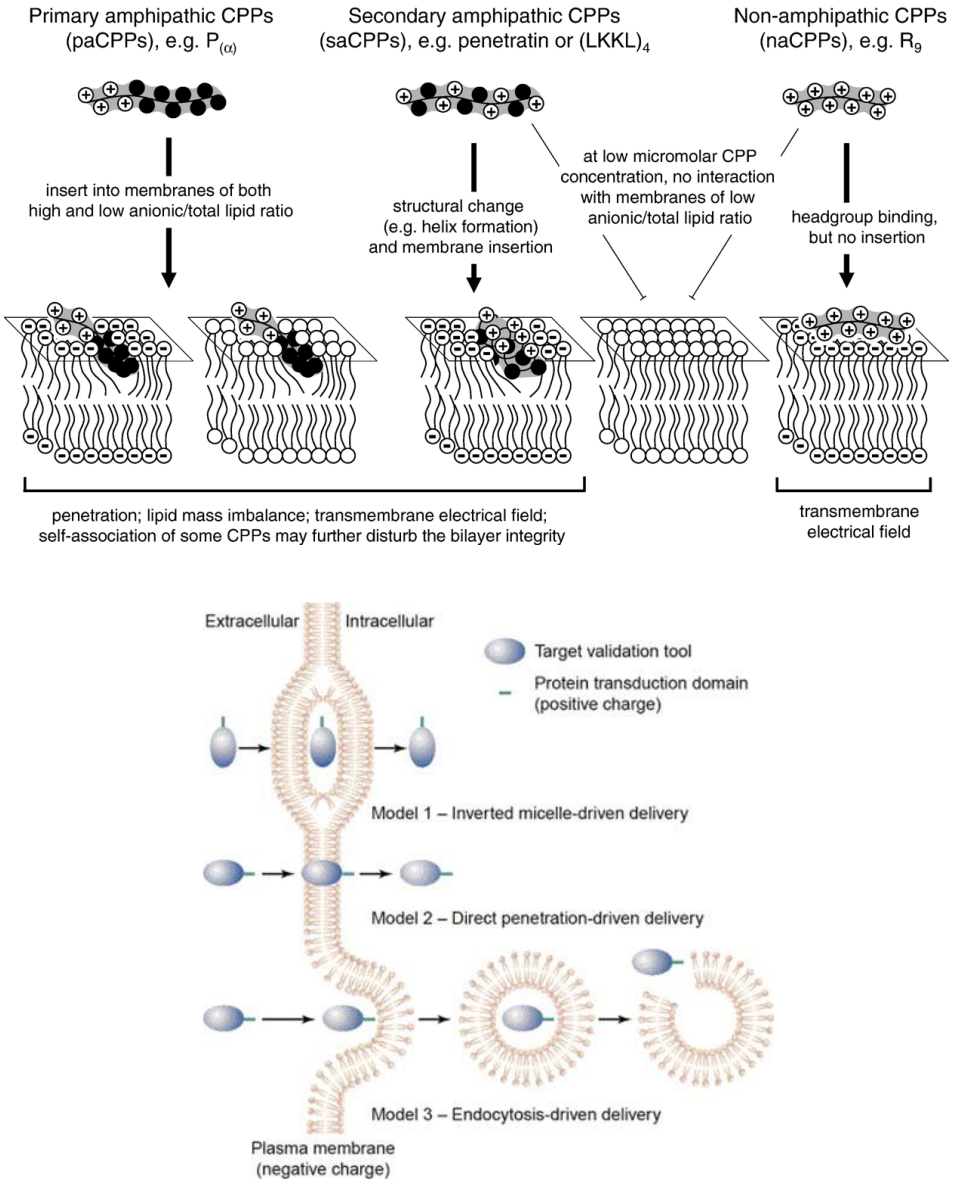

Figure 2.1.2 (a) Schematic view of the lipid binding of CPPs as function of their amphipathic property and lipid headgroup charge [73]. (b) Mechanisms of penetration across the plasma membrane [87].

enabled Tat and transportan to penetrate into various cell lines (Bowes, Jurkat, HeLa, Caco-2) [50, 55, 57, 58, 60, 62].

Some penetration experiments have been performed *in vivo* in whole organisms and a small number of experiments *ex vivo* in isolated tissue. *Ex vivo* tissue experiments were performed mainly in isolated blood vessels. Most *in vivo* experiments were carried out with penetratin and Tat. Besides the blood vessel cells, penetratin was successfully used *in vivo* to enter peritoneally and to reach brain and spinal cord cells [88]. In some cases, it also by passed the blood–brain barrier [89-91]. Tat was used *in vivo* to deliver active cargo enzyme in cells from all tissues of mouse [92].

2.1.4 Penetration of CPPs with cargos

The CPPs encompass ability to penetrate rapidly into living mammalian cells, and hence, are used to deliver various functional cargo molecules (Figure 2.1.4). The main applicative potential is the possibility of attaching biologically active cargos and delivering it into cells through penetration. Cargos can be attached in many ways; the most common link between the CPP and cargos is usually a covalent bond. When the cargos are either a peptide or protein, CPP-cargos are most often synthesized or expressed as fusion protein [93-95]. Or alternatively, a suitable amino acid as a linker or molecule as a spacer can be used. To couple cargos to CPPs such as transportan, the thiol group of cysteine can be used [50, 89]. The thiol group of cysteine gets reduced in the reductive environment, thus when present in the cell the disulfide bridge will readily get cleaved between

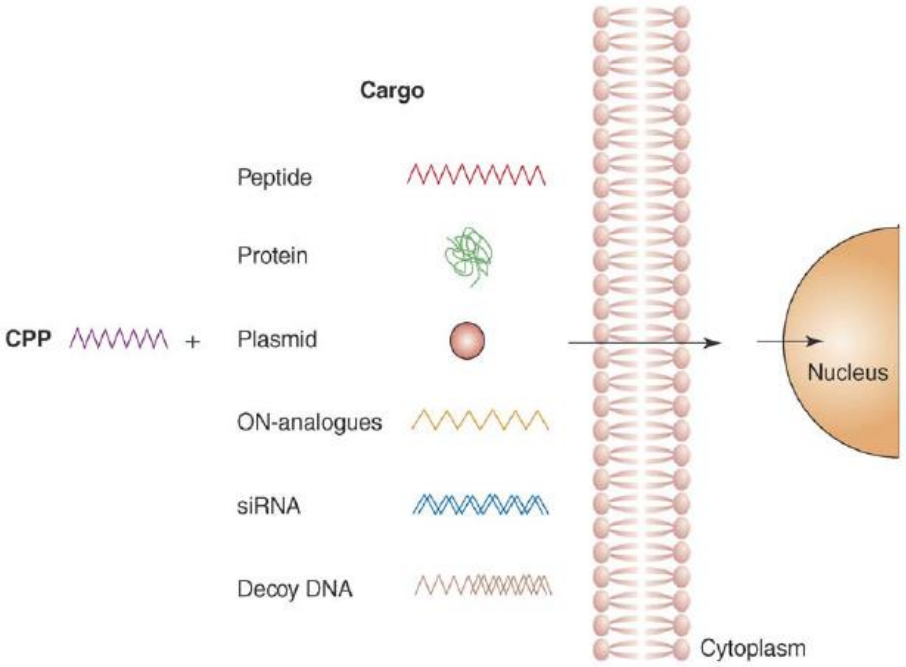

Figure 2.1.4 Intracellular delivery of cargos using cell-penetrating peptide [96].

CPPs and cargos, resulting in the release of cargos. Cargos can also be attached to CPPs by non-covalent bonds, such as biotin-conjugated CPPs to avidins [56]. A large number of cargos have been effectively delivered into cells using CPPs, such as proteins [97-100], small molecules [46, 101, 102], nucleic acids [103-105], antibodies [106, 107], and nanoparticles [108-111]. Unlike conventional methods, the delivery of cargo molecules using CPPs did not appear to vary by different cell types and efficiently delivered into cells by almost 100% [112]. The penetration was also accomplished within a relatively short period of time (less than 10 min).

2.1.5 Toxicity of CPPs

To be used as vehicles for drug delivery, the toxicity of CPPs must be kept at a minimum. The *in vitro* toxicity of CPPs has been more frequently characterized than *in vivo* studies. For *in vitro* toxicity, toxic effects on membranes of cells and organelles, and toxic effects resulting from the specific interaction of CPPs with cell components have been observed. It has been noticed that CPPs from the class of model peptides, such as MAP, and some designed CPPs, such as transportan, resemble in structure the antimicrobial lytic peptides that kill microbial cells by disrupting their cell membranes [113, 114]. For concentrations over 1 μM of MAP, it exerted strong toxic effects on various cell lines [49, 83] by the trypan blue exclusion [115], MTT [116], and fluorescein leakage [83] tests. Lower toxicity was observed for transportan, which showed toxicity from 5 μM concentration, by the glucose leakage test in

BMC cells [117]. Penetratin is known to cause little disruption to membranes [117], whereas Tat appears to cause no disruption to cell membranes [51, 117]. Because most CPPs have net positive charge, binding to negative charge such as polyanions is presumed. This was confirmed with penetratin, which interacted with heparin, nucleic acids, and polysialic acid [118, 119]. It may be possible that the interaction is important for internalization but whether it is the cause of side effects *in vivo* is not known. Various toxic effects have been observed for other CPPs. Transportan is derived from galanin and mastoparan and thus encompasses some properties of both peptides. It inhibits binding of galanin to galanin type-1 receptor and changes the activities of heterotrimeric G-proteins [50]. It was shown that transportan inhibs GTPase activity with Gs. Although this was not observed with other types of G-proteins, this could be a serious problem to use transportan as a drug delivery vehicle. It must be noticed that the inhibition of GTPase occurs at 10 times higher concentrations than those used in delivery experiments. Nevertheless, the problem was overcome by truncating transportan, resulting in transportan-10 which has no effect on G-proteins [52]. Tat-peptide is derived from HIV transcription factor Tat protein. As well as activating gene expression and replication, it is also involved in a number of processes including apoptosis [120, 121] and angiogenesis [122]. Some of these effects can be produced also with Tat derived CPPs [123]. No toxicity and undesirable side effects have been detected in most *in vivo* applications of CPPs [46, 89, 92]. However, when 10 μg or more of penetratin was applied in rat by intrastriatal injection, neurotoxic cell death and recruitment of inflammatory cells in brain was detected; an effect which was

much decreased at a dose of 1 μg [90].

The protein delivery was initially achieved by conjugation with Antp into various cells, including neurons [124]. Antp-fusion proteins are easily delivered for proteins with a size smaller than 100 amino acid residues; however cytotoxicity was a concern, as penetratin showed toxicity in the brain. In the case of trans-activating transcriptional activator (TAT) derived from HIV-1, it is the most intensely studied and widely used cell-penetrating peptide till date. In the first exon of HIV-1 TAT, a region coding from 48-60 amino acid residues was found to be the domain responsible for cell penetration and nuclear localization [116, 123, 125]. Like penetratin, TAT has been used to deliver functional proteins of large size into the cells and *in vivo* mice for the treatment of cancer, inflammation and other diseases [81, 126-133]. However, it should be noted that efficiency of penetration CPPs depend on the size and type of cargo being delivered. This is most noticeably demonstrated by difficulties in delivering large and anionic cargos, such as macromolecules and siRNAs.

Intracellular delivery by CPPs has shown enormous potentials to deliver a wide range of functional molecules, such as nucleic acids, nanoparticles, and drugs both *in vitro* and *in vivo* [134-136]. Although several CPPs have been identified, it remains important to find new peptides that are efficient vehicles for the delivery of cargos, and with low toxicity because some have toxic effects on membranes of cells and organelles, including toxic effects resulting from the specific interaction of CPPs with cell components [35]. Moreover, lack of cell- and tissue-specific targeting makes CPPs difficult to be applicable *in vivo* delivery. Despite these problems, CPPs offer an easy alternative for

intracellular delivery of molecules *in vitro* and *in vivo* with more economical viability.

2.1.6 Detecting internalization of CPPs

CPPs are peptides, hence cannot usually be observed directly and must be either labelled or attached to cargos in which we can detect for detection of the small amounts that are internalized in cells. Labelled CPPs or cargos can be detected by fluorescence emission, fluorescence quenching, radioactivity, specific labelling with dyes or by enzymatic activity of the cargo. Some detection methods are very convenient for visualizing CPPs internalized in cells but the drawback is that it does not have a rapid response time for kinetic studies, such as visualization of internalized biotinylated transportan by labelled streptavidin, using confocal microscopy [50]. That is why in most cases, the internalization kinetic studies are performed by the CPP itself or the cargo molecules in CPP-cargo molecules that have been labelled by fluorophores or radioactive isotopes.

Radioactively labelled cargo molecules can be used for the detection. The main advantage of this method is that the delivery of a cargo molecule into cells can be traced directly and that there may be a large variety of commercially available labelled compounds for use as cargo, such as commercially available radiolabelled antineoplastic agent, ^{14}C-doxorubicin that is coupled to penetratin [91]. The highly sensitive and directly traceable by using radioactively labelled CPP or CPP-cargo construct is the main advantage of this method over others.

However, the disadvantage is that it requires separating the internalized cell fraction of the labelled compound from the bulk that remains in the incubation solution. Thus this method is improper and not suitable for kinetic experiments that require continuous monitoring of the amount of cell-internalized CPPs or CPP-cargo molecules.

Fluorophores, such as fluorescein and fluorescein derivatives are frequently used for the detection [83, 91, 137]. After incubating cells with labelled CPPs, the medium is removed and the concentration of labelled CPPs inside the cells determined directly [138], by fluorescence flow cytometry [53], or internalized CPPs from cell lysate can be detected using HPLC [49].

CPP uptake can be monitored in real time by using confocal laser scanning microscopy (CLSM) [125]. Attached cells are incubated with fluorescently labelled peptide and the time course analysis of the fluorescence inside and outside the cells is monitored.

The fluorescence-based methods have a drawback in that sensitivity is lower than the radioactivity-based methods. The detection limit of fluorescence methods is close to the concentrations where some CPPs, such as MAP and transportan can disturb membranes [117]. For these CPPs, internalization at lower concentrations (< 0.1 μM) would be much advised. This can be easily resolved by use of radioactively labelled CPPs.

Chapter 3.

Experimental procedures

Chapter 3. Experimental procedures

3.1 Construction of plasmid

Total RNA was isolated from *Bombyx mori* silkworm at the fifth-instar larval stage using RNeasy (Qiagen, Valencia, CA, USA), and 30Kc19 cDNA was obtained by RT-PCR. The 30Kc19 gene was amplified using PCR, and the DNA fragment was inserted into the pET-23a expression vector (Novagen, Madison, WI, USA) with a T7 tag at the N-terminus and a 6-His tag at the C-terminus. The GST-30Kc19 ORFs were cloned from the pGEX-4T-1 vector (GE Healthcare, Uppsala, Sweden) into the N-terminal of 30Kc19 in the pET-23a vector. The GST-30Kc19 fusion protein contained two amino acids (Glu and Phe) derived from the EcoRI sequence (GAATTC) between GST and 30Kc19. Point mutation of pET-23a/30Kc19 was requested and performed by Enzynomics and pET-23a/30Kc19 C57A and pET-23a/30Kc19 C76A were constructed. For GFP-30Kc19, ORFs of GFP were cloned from pCMV-AC-GFP vector (Origene, Rockville, MD, USA) to N-terminal of 30Kc19 in pET-23a vector. The GFP-30Kc19 contained two amino acids (Glu, Phe) derived from the EcoRI sequence (GAATTC) between GFP and 30Kc19. Truncated forms of 30Kc19; $30Kc19_{1\text{-}120}$ and $30Kc19_{121\text{-}239}$ were also constructed. For GFP-30Kc19, ORFs of GFP were cloned from pCMV-AC-GFP vector (Origene, Rockville, MD, USA) to N-terminal of 30Kc19 in pET-23a vector. The GFP-30Kc19 contained two amino acids (Glu, Phe) derived from the EcoRI sequence (GAATTC) between GFP and 30Kc19. GFP-Pep-c19; $30Kc19_{42\text{-}57}$ sequence at the C-terminus of GFP was constructed to pET-23a vector.

3.2 Production and purification of proteins and peptides

The constructed vectors were transformed into *E. coli* BL21 (DE3, Novagen) and cells were grown in LB-ampicillin medium at 37℃. Isopropyl 1-thio-β-D-galactopyranoside (IPTG, 1 mM) was used for induction. *E. coli* were then further incubated at 37℃ for the production of protein, except for GFP-30Kc19, for which 30℃ was selected as the induction temperature. After centrifugation, the cells were harvested and disrupted by sonication. Following cell lysis, all recombinant proteins except GST-fusion protein were purified from the supernatant using a HisTrap HP column (GE Healthcare), dialyzed against 20 mM Tris-HCl buffer (pH 8.0) using a HiTrap Desalting column (GE Healthcare) with purity > 90% (data not shown), and stored at −70℃ until use. For the GST-fusion protein, the purified protein was dialyzed against PBS (pH 7.4) and 300 mM NaCl and stored at −70℃ until use. The quantitative analysis of proteins was performed using a Micro BCA kit (Thermo Fisher Scientific Inc., Rockford, IL, USA). N-terminal FITC-linked CPP candidates and Pep-c19 with purity of 90% were ordered from Peptron (Daejeon, Korea), and were diluted and stored at −70 °C until use. 11R and Pep-c19 peptides with purity of 90% were ordered from Peptron (Daejeon, Korea), and were diluted and stored at −70 °C until use.

3.3 Reducing SDS-PAGE, non-reducing SDS-PAGE, and native PAGE

All reducing SDS-PAGE, non-reducing SDS-PAGE, and native PAGE were

conducted using 12% polyacrylamide gels unless otherwise indicated. For the reducing condition, samples were mixed with reducing sample buffer containing SDS and β-mercaptoethanol (BME) (pH 6.8), and for non-reducing condition, samples were mixed with non-reducing sample buffer without BME. 15 min pre-incubation of 30Kc19 proteins with SDS, detergents, and materials was performed prior to loading. The reducing condition samples with the reducing buffer were denatured by boiling. For the native condition, samples were mixed with native sample buffer without any denaturing reagent. After electrophoresis, each sample was separated according to size (reducing or non-reducing) or pattern (native). The polyacrylamide gel was immersed in Coomassie blue staining solution and then immersed in destaining solution for analysis.

A 42 kDa and 67 kDa sized ovalbumin and BSA (Sigma, St. Louis, MO, USA) were used as standards for the molecular weight assay of the recombinant 30Kc19 protein. SDS (Sigma) was dissolved and diluted with deionized water (DW) according to the appropriate concentration for the molecular weight assay. CTAB, Triton X-100 and CHAPS detergents (all from Sigma) were dissolved in DW and stored in frozen aliquots until use. Dextran sulfate sodium salt (Fluka) was dissolved in DW and used in the experiment. L-α-Phosphatidyl choline (Sigma) was used as the phospholipid. It was dissolved in chloroform and stored at −20℃ until use. Prior to the experiment, the chloroform was removed with nitrogen gas and diluted with DW. Five controlled cycles of freeze-thawing were carried out to form unilamellar vesicles.

3.4 Cell culture

HEK 293, HeLa, HEK 293-EGFP stable cell line cells were maintained in a humidified atmosphere of 5% CO_2 at 37 ℃ in DMEM (Gibco, Invitrogen, Carlsbad, CA, USA), supplemented with 10% (w/v) fetal bovine serum (FBS, Gibco) and 1% (v/v) penicillin streptomycin (PS, Gibco). For the 4 ℃ experiment, cells were pre-incubated at 4 ℃ for 1 h before proteins were added.

3.5 Immunoblot analysis

HEK 293 cells were maintained in a humidified atmosphere of 5% CO_2 at 37℃ in DMEM supplemented with 10% (w/v) fetal bovine serum (FBS, Gibco, Grand Island, NY, USA) and 1% (v/v) penicillin streptomycin (PS, Gibco). Protein was added to the culture medium and incubated for 6 h at 37℃ in a humidified atmosphere of 5% CO_2. After the incubation, cells were washed with PBS three times, treated with trypsin-EDTA (Sigma), then washed three times with PBS for strict distinction between intracellular and membrane-bound proteins. Cells were treated with trypsin-EDTA to distinguish between intracellular and membrane-bound proteins (Sigma). The collected cells were washed three times in PBS. Cell extracts were collected with RIPA buffer (50 mM Tris-HCl (pH 7.4), 150 mM NaCl, 1% Triton X-100, 0.1% SDS, protease inhibitor cocktail) at 4 ℃ for 1 h followed by centrifugation. Each cell extract containing an equal amount of protein was resolved by PAGE and examined by immunoblot analysis. Anti-30Kc19 rabbit antibody was prepared using the following procedure. 30Kc19 was first purified from silkworm hemolymph

using a two-step chromatography purification method (size exclusion and ion exchange). Anti-30Kc19 polyclonal antibody was produced by immunizing a rabbit with the purified 30Kc19 protein, which was subsequently purified by Protein G chromatography (AbFrontier, Seoul, Korea). 30Kc19 was detected using this anti-30Kc19 antibody. Other primary antibodies, Anti-β tubulin mouse monoclonal antibody, anti-EGFP rabbit polyclonal antibodies, and anti-His tag mouse monoclonal antibody were used (all from Santa Cruz Biotechnology, Santa Cruz, CA, USA). For the secondary antibody, following antibodies were used; HRP-conjugated antibody and Alexa 488-conjugated antibody (Invitrogen, Carlsbad, CA, USA).

3.6 Quantitative internalization analysis

Internalization of FITC-linked Pep-c19 and GFP-Pep-c19 protein was measured by fluorescence intensity using a microplate reader (Tecan GENiosPro, Tecan, Durham, NC, USA). HeLa cells were seeded on 96-well plate (Nunc Lab-Tek, Thermo Scientific) and incubated overnight. FITC-linked peptides or protein were added to the culture medium and were incubated in 37 ℃ in humidified atmosphere of 5% CO_2. Unless indicated otherwise, after incubation, cells were washed vigorously three times with PBS to minimize the possible presence of membrane-bound peptides and fluorescence was measured with excitation at 485 nm (20 nm bandwidth) and emission at 535 nm (25 nm bandwidth) with a gain of 60 or excitation at 535 nm (25 nm bandwidth) and emission at 612 nm (10 nm bandwidth) with a gain of 60. If indicated, cells

were washed vigorously with PBS three times and treated with trypsin-EDTA for removal of membrane-bound proteins, and then fluorescence of cell lysate was measured.

3.7 GST pull-down assay

Purified GST-tagged proteins were prebound to resin by incubating the proteins with GST-bind resin for 2 h at 4 ℃ in PBS (pH 7.4), 300 mM NaCl, and a protease inhibitor mixture. The prebound resin was washed three times with the same buffer solution. Then, samples were analyzed by immunoblotting with the anti-30Kc19 rabbit antibody, followed by an HRP-conjugated anti-rabbit antibody.

3.8 Construction of HEK 293 stable cell-line expressing EGFP

HEK 293 stable cell line expressing EGFP was constructed by selection using G-418. Transfection was performed 3 days after plating using the Lipofectamine 2000 (Invitrogen) according to the manufacturer's instructions. HEK 293 cell was transfected with pEGFP-N1 and 1 day after transfection, the cells were transferred into media containing G-418 (1 mg/ml) and continuously cultured for 2 weeks. Only EGFP expressing colonies were selectively transferred to fresh media containing G-418 (0.5 mg/ml) based on green fluorescence.

3.9 Formation of CPP/siRNA complex

Synthetic siRNAs for EGFP siRNA sequence used: EGFP sense strand: Thiol-ACUACCAGCAGAACACCCC (dTdT), and EGFP antisense strand: (dTdT) UGAUGGUCGUCUUGUGGGG-Cy3, all purchased from Bioneer Co., Korea with routine process protocol set up by the company.

The prepared siRNAs were mixed with CPPs (11R or Pep-c19) in DMEM and incubated for 15 min at room temperature for the formation of CPP/siRNA complexes.

3.10 Gel shift/retardation assay for CPP/siRNA complex

The complex formation was monitored by 2% (w/v) agarose gel in TAE buffer electrophoresis using molecular markers. Following electrophoresis, the gels were stained with 0.5 mg/ml ethidium bromide for 20 min and analyzed on a UV illuminator to identify the locations of siRNA.

3.11 Cell viability assay

To assess cytotoxicity of the CPP/siRNA complex, HEK 293-EGFP cells were seeded on a 96-well plate at 70% confluency, and CPP/siRNA in DMEM were added and incubated for 24 h and 72 h at 37 °C in a 5% CO_2 incubator. Then 0.5 mg/ml MTT (3,(4,5-dimethylthiazol-2-yl)2,3-diphenyltetrazolium) was added to the media and incubated for 2 h. The formazan crystals that developed were solubilized with dimethyl sulfoxide (Sigma–Aldrich), and

absorbance was measured at 560 nm using the ELISA reader.

3.12 Immunocytochemistry and live cell analysis

For immunocytochemistry, cell penetration of the protein was visualized using either confocal microscopy or fluorescence microscopy. HeLa cells were seeded on 8-well chamber slides (Nunc Lab-Tek, Rochester, NY, USA) and incubated overnight. Protein was added to the culture medium then HeLa cells were incubated for 6 h at 37℃ in a humidified atmosphere of 5% CO_2. After the incubation, the cells were treated with trypsin-EDTA (Sigma) and washed three times with PBS, fixed in 4% paraformaldehyde for 20 min, and incubated for 10 min with 0.25% Triton X-100 in PBS for permeabilization. The fixed cells were blocked with 3% BSA in 0.1% PBS-T for 1 h and then incubated with anti-30Kc19 polyclonal rabbit antibody (Ab Frontier), anti-T7 tag rabbit antibody (Abcam, Cambridge, UK), or anti-His tag mouse monoclonal antibody (Santa Cruz). Then, either Rhodopsin-conjugated anti-rabbit antibody (Jackson ImmunoResearch, West Grove, PA, USA) or Alexa Fluor 488-conjugated anti-rabbit antibody (Invitrogen) was used for the secondary antibody. Nuclei of cells were stained with Hoechst 33342 for 10 min. For confocal microscopy, a confocal laser microscope (EZ-C1, Nikon, Tokyo, Japan) was used to observe intracellular fluorescence, and images were taken using the manufacturer's software (Nikon).

For live cell analysis, cell penetration was visualized using confocal laser microscopy (EZ-C1, Nikon, Japan). HeLa cells were seeded on 8-well chamber

slide (Nunc Lab-Tek, Thermo Scientific) and were incubated overnight. FITC-linked peptide or protein was added to the culture medium and was incubated for 4 h at 37 ℃ in a humidified atmosphere of 5% CO_2. Nuclei of cells were then stained with Hoechst 33342 for 10 min. Cells were washed vigorously with PBS three times to minimize the possible presence of membrane-bound peptides and then live cell intracellular fluorescence images were taken by the manufacture's software (Nikon, Japan).

3.13 Inhibitors of endocytosis

When cell-penetrating efficiency was performed in the presence of cytochalasin B (25 μM), sucrose (100 nM), or nystatin (25 μg/ml) (all purchased from Sigma-Aldrich), cells were preincubated with these inhibitors of endocytosis for 1 h prior to supplementation of 30Kc19 protein or Pep-c19 to culture medium. Incubation was performed for 6 h, after which cells were extensively washed analyzed by immunocytochemistry method as mentioned previously using spectrofluorometer in order to determine the intracellular penetration efficiency.

3.14 *In vivo* penetration of Pep-c19

To investigate the *in vivo* penetration of Pep-c19, GFP-30Kc19 and GFP-Pep-c19 proteins were each dissolved in PBS and intraperitoneally injected to 5-week-old female ICR mice with an average weight of about 25 g (3.5 μmol/kg). Following 12 h incubation time, mice were euthanized and organs

were collected. Then, the organs were frozen with optimal cutting temperature (OCT, Miles Laboratories, Elkhart, IN, USA) compound and tissues were sectioned at a thickness of 10 μm using microtome-cryostat (Microm, Walldorf, Germany) and were stored at −70 °C until further analysis for confocal microscopy.

3.15 *In vivo* toxicity analysis

To investigate the *in vivo* toxicity of Pep-c19, serum biological parameters were determined. 30Kc19 protein and Pep-c19 were dissolved in PBS and were intraperitoneally injected to 5-week-old female ICR mice with an average weight of about 25 g (0.2 μmol/kg or 2 μmol/kg). Mice were euthanized after 14 days, and blood samples were collected by heart-puncture method, and were maintained in serum separating tube (SST) at room temperature for 30 min. Following centrifugation for 10 min at 300 × g to obtain serum, samples were analyzed. As a parameter of kidney function, blood urea nitrogen (BUN) and creatinine levels were determined. For liver function, serum aspartate aminotransferase (AST) and alanine aminotransferase (ALT) activities were determined. The blood samples were delivered to Neodin Medical Institute (Seoul, Korea) where all biological parameters were determined and analyzed.

Chapter 4.

Dimerization of the 30Kc19 protein in the presence of amphiphilic moieties and importance of Cys-57 during cell penetration

Chapter 4. Dimerization of the 30Kc19 protein in the presence of amphiphilic moieties and importance of Cys-57 during cell penetration

4.1 Introduction

As mentioned previously, although the biological functions of the 30K proteins in silkworms have not been fully determined, several studies have recently examined their functional properties for 30Kc6 and 30Kc19 [6, 7]. In previous studies, it was demonstrated that gene expression or addition of recombinant 30K proteins to culture medium produced from *Escherichia coli* (*E. coli*) exhibited anti-apoptotic effects in various cells [8-20]. 30K proteins also enhanced productions of recombinant erythropoietin, interferon-β, and monoclonal antibody, as well as increasing glycosylation, cell growth, and viability in various cells, and also had enzyme-stabilizing effects [21-28].

Recently, the recombinant 30Kc19 protein, originating from silkworm hemolymph of *Bombyx mori* has attracted attention due to its cell-penetrating property and use in a protein delivery system [139]. 30Kc19 protein, is comprised of 239 amino acids in total, has all-α helix in N-terminal domain and all-β sheet in C-terminal domain (Figure 4.1) [140, 141]. Therefore, 30Kc19 protein is a very unique multi-functional protein, and can be applied for the delivery of therapeutic proteins, including enzymes, as it can penetrate cell membrane as well as stabilizing cargo proteins. It is necessary to understand the molecular mechanism of cell penetration for the practical use of the 30Kc19

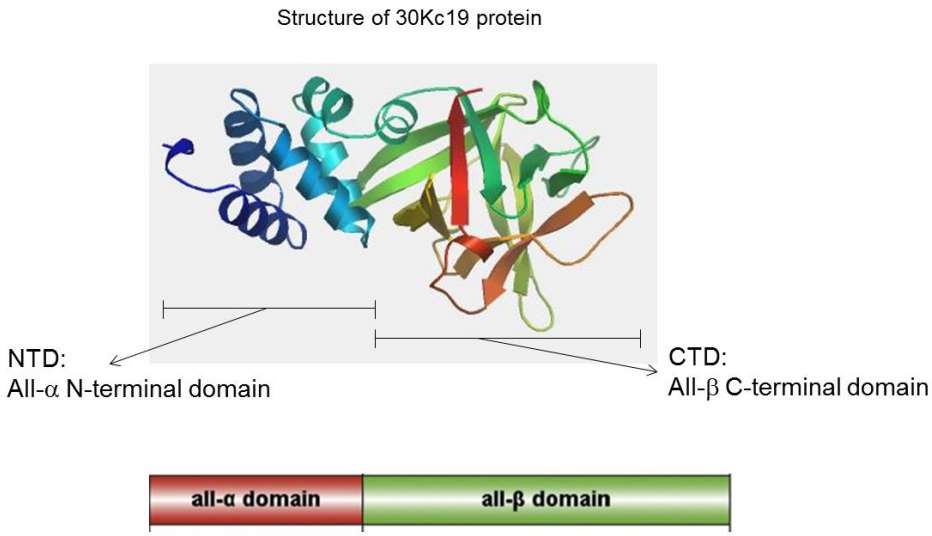

Figure 4.1 Structure of the 30Kc19 protein. 30Kc19 protein, comprised of 239 amino acids in total, has all-α helix in N-terminal domain and all-β sheet in C-terminal domain.

protein. However, the exact mechanism of penetration to animal cells has not been fully determined and this observation of penetration across cell membrane has raised questions concerning the interaction of the protein-lipid bilayer.

Herein, a dimerization propensity of the 30Kc19 protein in the presence of either SDS or phospholipids is reported. Then, investigated how the cell-penetrating 30Kc19 protein is related with phospholipids, the main cell membrane components, and elucidated the mechanism of entry of the 30Kc19 protein into animal cells for use in protein delivery system.

4.2 Cell-penetrating property of the 30Kc19 protein

The 30Kc19 protein has recently shown a cell-penetrating property in various types of cells when supplemented to culture medium, and was found to be the first cell-penetrating protein in insect hemolymph that exhibited a cell-penetration property both *in vitro* and *in vivo* [139]. In this study, I investigated the cell-penetrating property and the intracellular penetration mechanism of the 30Kc19 protein. First, 30Kc19 protein was added to culture medium and immunocytochemistry analysis showed that 30Kc19 was able to penetrate cells from rhodamine red color (Figure 4.2). 30Kc19 protein was localized in the cytoplasm of the cell and was not able to penetrate the nucleus.

4.3 Dimerization of the 30Kc19 protein is promoted by SDS

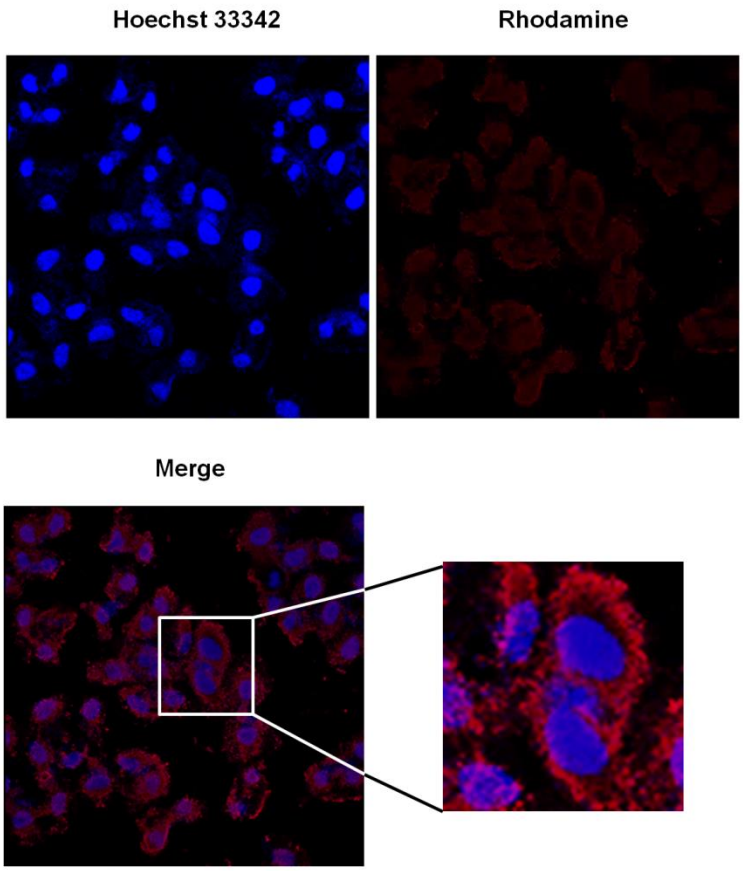

Figure 4.2 Cell-penetrating property of the 30Kc19 protein. HeLa cells were supplemented with the 30Kc19 protein in culture medium for 6 h. The cell-penetrating ability of the 30Kc19 protein was analyzed by immunocytochemistry, which showed internalization of 30Kc19 protein. The internalized protein was visualized by Rhodopsin-conjugated anti-rabbit antibody (red), and nuclei were visualized with Hoechst 33342 (blue). Supplementing the cell culture medium with the protein was conducted in a quantity of 0.4 mg/ml.

Recently, a dimerization propensity of the 30Kc19 protein was seen during characterization assay using PAGE analysis, and believed its relevance with cell penetration. Previously, the 30Kc19 protein was run on PAGE under reducing and non-reducing conditions and observed the dimerization propensity. Under the reducing condition, a monomer and a faint dimer band were seen. In contrast, not only a 30 kDa sized monomer protein was detected under a non-reducing condition but also a clear 60 kDa dimer sized protein was detected.

These results demonstrated that the properties of the 30Kc19 protein are similar to other peptides under reducing and non-reducing conditions, dimer was considered to be due to the non-reducing environment in the presence of SDS [81, 142]. To confirm whether this was the case, 30Kc19 was pre-treated with different concentrations of SDS for 10 min and was then loaded on native PAGE. A monomer band was detected when no SDS was mixed with the protein. However, both a monomer and dimer were detected when the SDS concentration was increased to 0.1% (Figure 4.3(a)). A shift from the monomer to the dimer was detected in 0.1% SDS, and almost all monomers shifted to the dimer at 0.5% SDS. Therefore, 30Kc19 originally existed as a monomer and dimerized in the presence of SDS. Additional experiments were carried out to verify this for other well-known standard proteins such as ovalbumin and BSA. Ovalbumin and BSA were loaded on native PAGE but showed no significant difference in pattern as the concentration of SDS increased when compared with that of 30Kc19 (Figure 4.3(b)). This result shows that there was an increase in the size of 30Kc19, indicating dimerization of the protein. 30Kc19 protein exists as a monomer and that SDS causes dimerization of the 30Kc19.

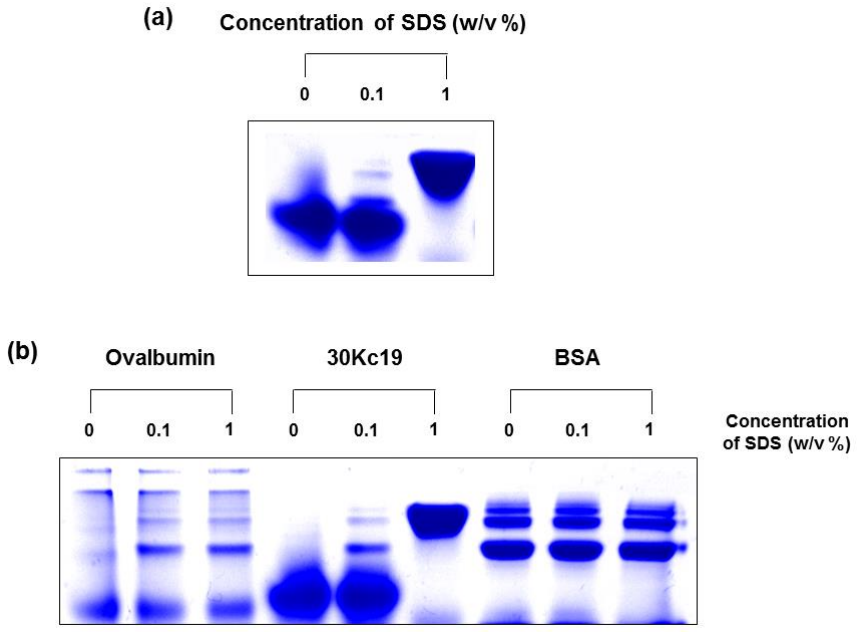

Figure 4.3 Monomer and dimer forms of 30Kc19. (a) Native PAGE result of the 30Kc19 protein pre-treated with different SDS concentrations. (b) Native PAGE result of the ovalbumin, 30Kc19, and BSA proteins, each pre-treated with different SDS concentrations.

4.4 Dimerization of the 30Kc19 protein is promoted by phospholipid

Dimerization propensity was seen for 30Kc19 when SDS was mixed with the protein. It was unclear whether this occurred because SDS is a surfactant. SDS is an anionic (negative) detergent; hence, cationic, non-ionic, and zwitterionic detergents were selected and tested for dimerization [143]. When the cationic surfactant CTAB was mixed with the 30Kc19 protein, no dimerization was observed (Figure 4.4(a)). In fact, because CTAB is a positively charged detergent, the 30Kc19-CTAB mixture did not progress on PAGE. Triton X-100 and CHAPS, which are non-ionic and zwitterionic surfactants, respectively, resulted in no dimerization of 30Kc19, indicating that dimerization of 30Kc19 is not just dependent on the surfactant nature of SDS and that it could be due to the anionic property of SDS. We hypothesized that dimerization may have been caused by the negative SDS charge. Hence a well-known polyanionic material, dextran sulfate, was used in various concentrations to determine the reason for the change in the 30Kc19 pattern. However, when dextran sulfate was added, no difference in the 30Kc19 pattern was seen (Figure 4.4(b)). We found L-α-phosphatidylcholine, a phospholipid, which is similar in structure and properties to SDS, has an amphiphilic moiety and is a component of the cell membrane with similar structural properties to SDS (Figure 4.4(c)). When a low concentration of phospholipid (1 mM) was mixed with the 30Kc19 protein, no major tendency for a pattern shift was detected. However, as the concentration increased, a significant difference in the 30Kc19 protein pattern was detected

and dimers were seen (Figure 4.4(d)). When the lipid concentration reached 10 mM, most of the monomeric 30Kc19 protein was in a dimer form. This result showed that majority of 30Kc19 shifted towards the dimer as the 30Kc19 protein was mixed with increasing concentrations of phospholipid. This observation paralleled with the results shown when the 30Kc19 protein was mixed with SDS, a material with similar properties to phospholipid.

4.5 Dimerization of 30Kc19 during cell penetration

Previously, our group identified the cell-penetrating property of the 30Kc19 protein when it is supplemented in culture medium [139]. Phospholipids are a major component of the cell membrane lipid bilayer. I hypothesized the possible relevance of 30Kc19 dimerization with phospholipids and the cell-penetrating property of the 30Kc19 protein. Also the mechanism of entry of the 30Kc19 protein into animal cells through an interaction with the cell membrane was elucidated. First, an immunoblot against the 30Kc19 protein incubated with or without SDS is shown as a reference for the pattern analysis (Figure 4.5(a), left). As expected, the ratio of 30Kc19 dimer to monomer increased by adding SDS to the solution. HEK 293 cells were incubated with 0, 0.2, and 0.4 mg/ml recombinant 30Kc19 protein. The cells were treated with trypsin and then washed multiple times to remove plasma membrane-bound protein. The cells were then lysed and the lysate was loaded onto native PAGE followed by an immunoblot against the 30Kc19 protein. Penetration of the 30Kc19 protein into the cell was observed, and detected an increased amount of intracellular

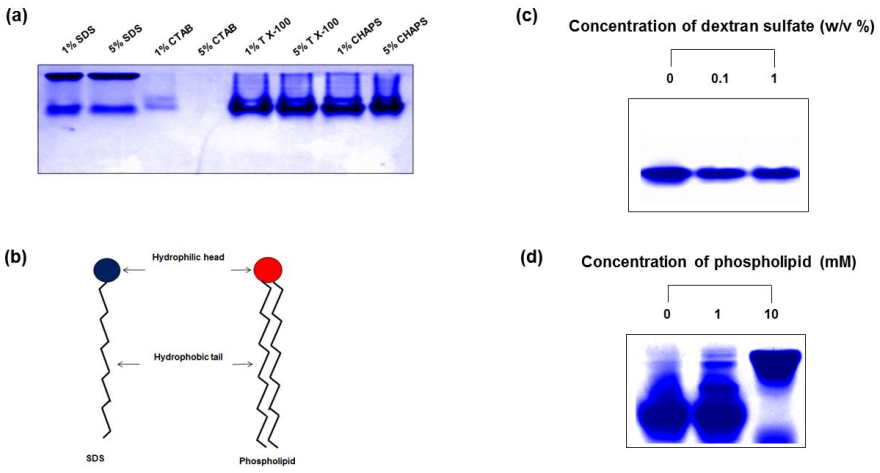

Figure 4.4 Monomer and dimer forms of 30Kc19. (a) Native PAGE result of the 30Kc19 protein pre-treated with different classes of anionic (SDS), cationic (CTAB), non-ionic (T X-100), and zwitterionic (CHAPS) surfactant detergents. (b) Native PAGE result of the 30Kc19 protein pre-treated with negative material, dextran sulfate. (c) Schematic diagram showing similarity of SDS and phospholipids. (d) Native PAGE result of the 30Kc19 protein pre-treated with different phospholipid concentrations.

30Kc19 protein as the concentration was raised in the culture medium (Figure 4.5(a), right). Interestingly, the 30Kc19 protein was found mainly as a dimer in the cell lysate, indicating that the 30Kc19 monomer protein in the medium dimerized during cell penetration or in the cytosol. Then, the dimerized form of the 30Kc19 protein in the cytosol using a GST pull-down assay followed by a reducing PAGE immunoblot was further confirmed. GST-30Kc19 was produced in *E. coli* and loaded on reducing PAGE (Figure 4.5(b)). A 60 kDa sized monomer GST-30Kc19 protein was detected under reducing conditions, and confirmed that the protein was expressed and purified successfully. Then, the 30Kc19 protein, the GST-30Kc19 protein, or 30Kc19 protein plus GST-30Kc19 protein, respectively was added to HEK 293 cell culture medium. The cell lysates were loaded onto reducing PAGE, and confirmed that both the 30Kc19 protein and GST-30Kc19 penetrated the cells (Figure 4.5(c)). When the 30Kc19 protein-treated cell lysate was subjected to the GST pull-down assay, no 30Kc19 protein was detected, as expected, whereas the GST-30Kc19 protein was detected when the GST-30Kc19 protein-treated cell lysate was used. However, when the cell lysate treated with both the 30Kc19 protein and GST-30Kc19 protein was subjected to the GST pull-down assay, the 30Kc19 protein was detected. Based on these results, it was concluded that the 30Kc19 protein formed a dimer with 30Kc19 of GST-30Kc19 during penetration and remained a dimer inside the cells (Figure 4.5(d)). Therefore, it is suggested that the 30Kc19 protein interacted with phospholipid on the plasma membrane and formed a dimer and this allowed the 30Kc19 protein to penetrate the cells.

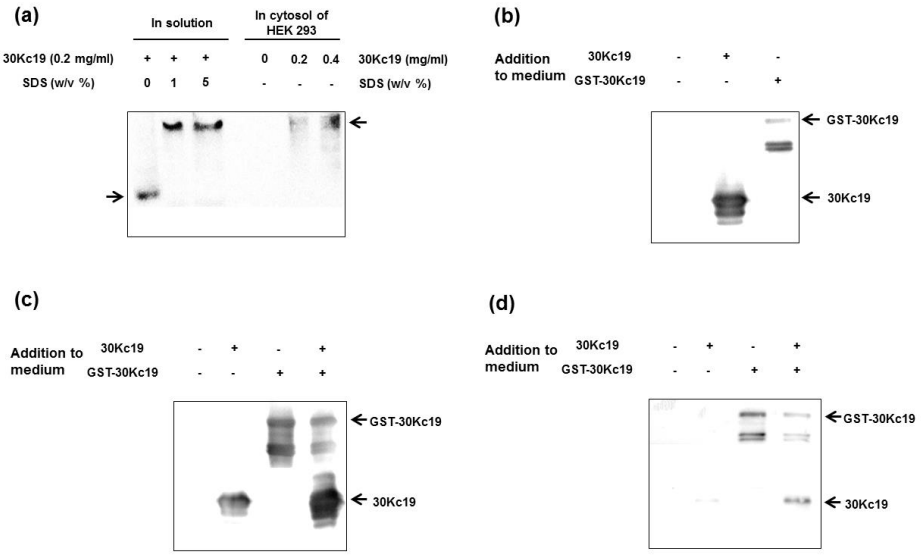

Figure 4.5 Dimerization of 30Kc19 during cell penetration. (a) Native PAGE immunoblot result of the 30Kc19 protein pre-treated with SDS (left) and cell lysate supplemented with 30Kc19 in culture medium for 6 h (right). (b) Reducing SDS-PAGE result of the 30Kc19 and GST-30Kc19 fusion proteins in solution. (c) Reducing PAGE immunoblot result of the HEK 293 cell lysate, supplemented with the 30Kc19 protein only, the GST-30Kc19 protein only, or the 30Kc19 plus GST-30Kc19 proteins in culture medium for 6 h. (d) HEK 293 cells were supplemented with the 30Kc19 protein only, the GST-30Kc19 protein only, or the 30Kc19 plus the GST-30Kc19 proteins in culture medium for 6 h. Reducing PAGE immunoblot result of the cell lysate GST pull-down assay. Proteins were supplemented in the culture medium in equal molar quantities of 0.2 and 0.4 mg/ml for the 30Kc19 protein and GST-30Kc19 protein, respectively.

4.6 Importance of 30Kc19 Cys-57 for cell penetration

I was convinced that the 30Kc19 protein dimerizes during cell penetration but were unsure exactly how the 30Kc19 protein homodimerizes during penetration. A similar result was demonstrated with the peptide hormone resistin in which a disulfide-linked homodimer was converted to a monomer under reducing conditions and conversion of a single cysteine to alanine abolished the dimerization [144, 145]. The 30Kc19 protein has two cysteine residues, Cys-57 and Cys-76 (Figure 4.6(a)). There is high probability that one of these cysteines is involved in dimerization of the 30Kc19 protein. Thus, a point mutation in pET-23a/*30Kc19* was requested and pET-23a/*30Kc19 C57A* and pET-23a/*30Kc19 C76A* were constructed (Enzynomics). Expression and purification of the 30Kc19 C57A and 30Kc19 C76A proteins were performed by the same method as for the 30Kc19 protein, and they were analyzed by reducing SDS-PAGE (Figure 4.6(b)). The result showed that both proteins were expressed successfully. Then, the 30Kc19 protein, the 30Kc19 C57A protein, and the 30Kc19 C76A protein were added in equal amounts (0.4 mg/ml) to culture medium containing HEK 293 cells. The cell lysates were loaded onto reducing PAGE, and confirmed that the 30Kc19 protein and 30Kc19 C76A penetrated the cells by immunoblot analysis. However, the 30Kc19 C57A protein-treated cell lysate showed no sign of the penetration, indicating that the 30Kc19 protein cannot penetrate cells without Cys-57 (Figure 4.6(c)). Additionally, the dimerization propensity on native PAGE of 30Kc19 C57A and 30Kc19 C76A by immunoblot analysis was checked (Figure 4.6(d)). Similar to

the wild-type 30Kc19 protein, 30Kc19 C57A, and 30Kc19 C76A showed no signs of dimerization in the absence of cell penetration (Figure 4.6(d)). However, when each of the protein-treated HEK 293 cell lysates was loaded onto native PAGE for immunoblot analysis, we observed that only the 30Kc19 protein and 30Kc19 C76A penetrated the cells and existed as dimers inside the cells (Figure 4.6(d)). Immunocytochemistry of the 30Kc19 proteins was used to confirm penetration of 30Kc19 and 30Kc19 C76A but not 30Kc19 C57A. Note that 30Kc19 C57A was not detected inside the cells, but 30Kc19 C76A managed to penetrate the cells (Figure 4.6(e)). Thus, conversion of this cysteine to alanine at 57 abolished dimerization of 30Kc19, indicating that a single disulfide bond was necessary to connect the two 30Kc19 proteins into a homodimer and that 30Kc19 protein can only penetrate the cell membrane by dimerization. The cysteine residue at 57 is critical for cell penetration, which means it is involved in dimer formation between the 30Kc19 proteins. Although one can presume formation of multimer, this is quite unlikely because only monomer and dimer were shown in non-reducing PAGE analysis indicating that multimer is not formed.

However, one cannot rule out the possibility that dimer was formed during cell lysis and PAGE steps. Although it is highly unlikely that oxidation occurred and dimer was formed during this step; certainty can be made by *in vivo* analysis using BiFC or time-course analysis as supplementary data.

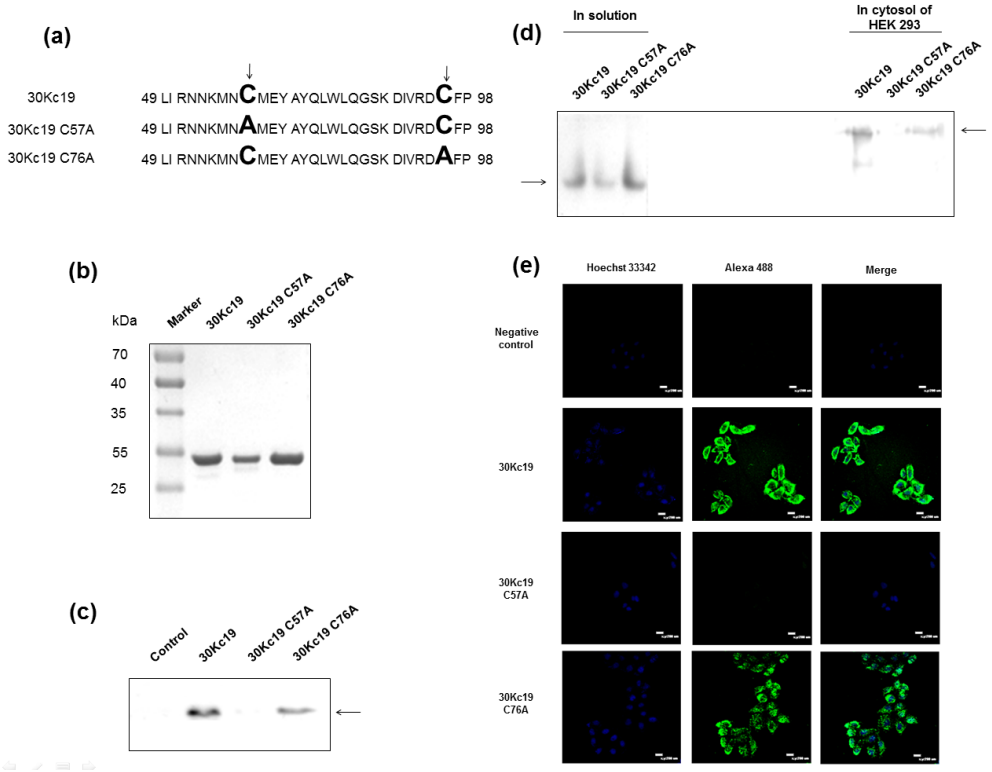

Figure 4.6 Importance of 30Kc19 Cys-57 for cell penetration. (a) Alignment of 30Kc19 and mutated 30Kc19 Cys and Ala residues highlighted in bold. (b) Reducing SDS-PAGE result of the 30Kc19 protein, 30Kc19 C57A, and 30Kc19 C76A. (c) Reducing PAGE immunoblot result of the HEK 293 cell lysate supplemented with each protein. (d) Native PAGE immunoblot result of each protein (left), and the HEK 293 cell lysate supplemented with each protein (right). Monomeric and dimeric species are indicated by arrows. (e) HeLa cells were supplemented with each protein. The cell penetration was analyzed by visualized by Alexa Fluor 488 (green), and nuclei were visualized with Hoechst 33342 (blue). Equal molar quantity of 0.4 mg/ml and 6 h for all proteins.

4.7 Intracellular penetration in the presence of inhibitors of endocytosis

Cells were treated with inhibitors of endocytosis; cytochalasin B, sucrose, and nystatin, for the disruption of microfilaments/inhibition of macropinocytosis, inhibition of clathrin-mediated endocytosis, and disruption of caveolar structure and function, respectively [102]. When cells were given a hyperosmolar condition by sucrose treatment, no markedly difference in the penetration ability of the 30Kc19 protein was seen (Figure 4.7). This showed that 30Kc19 protein does not penetrate by clathrin-mediated endocytosis. However, treatment of cytochalasin B or nystatin slightly lowered the cell-penetrating ability of the 30Kc19 protein, which demonstrates that 30Kc19 protein penetrates cells by macropinocytosis and caveolin-mediated endocytosis. But because the level of decrease in the penetration is low when cytochalasin B or nystatin was treated, it may be possible that the 30Kc19 protein internalizes by other methods of entry.

4.8 Intracellular cargo delivery using the 30Kc19 protein

A recent study has shown that 30Kc19 protein has a cell-penetrating property when supplemented to the culture medium [139]. In order to examine the ability of 30Kc19 protein to deliver foreign proteins into the cell, a GFP was selected because of its cell-impermeable property and ability to give out its own green fluorescence. This is useful because both intracellular delivery of cell-

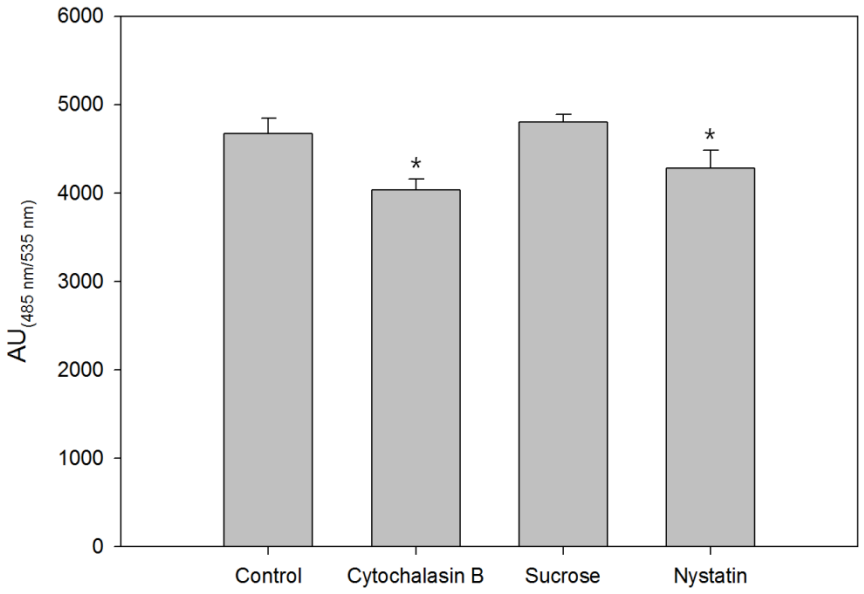

Figure 4.7 Intracellular penetration in the presence of inhibitors of endocytosis. Cells were pre-incubated for 1 h with different modulators of endocytosis; cytochalasin B (25 μM) for the disruption of microfilaments/inhibition of macropinocytosis, sucrose (100 mM) for the inhibition of clathrin-mediated endocytosis, and nystatin (25 μg/ml) for the disruption of caveolar structure and function. Protein was supplemented to the medium and after 6 h of incubation, HeLa cells were fixed with paraformaldehyde. The intracellular 30Kc19 protein was visualized by Alexa Fluor 488-conjugated anti-rabbit antibody fluorescence was measured using spectrofluorometer (ex. 485 nm/em. 535 nm). *$p < 0.001$, compared with the control group (n = 4). Error bars represent standard deviation.

impermeable cargo is possible and also because of ease of assay via intracellular fluorescence. Thus, GFP-30Kc19 protein expressed from *E. coli*, purified, and was added to culture medium. The results showed that when the 30Kc19 protein is fused with GFP, it was able to penetrate and deliver its cargo protein into cells (Figure 4.8). This means that we can utilize the 30Kc19 protein for successful intracellular delivery of cargo proteins. Also, it demonstrates that *in vivo* delivery of cargos to tissues and organs may be achieved using this 30Kc19 protein as a fusion partner. Other than cargo proteins, it is expected that 30Kc19 protein may also intracellularly deliver cell-impermeable cargo molecules such as oligonucleotides when conjugated to the 30Kc19 protein.

4.9 Penetration mechanism of the 30Kc19 protein

We observed that the dimerization characteristic of the 30Kc19 protein was similar to a representative PTD, Antennapedia (Antp) [34]. This Antp PTD also exhibits a very similar pattern during interactions with SDS and cell membranes [40]. Dimerization of Antp also has the characteristic of penetrating inside cell in an energy independent manner. In addition, dimerization propensities of the fibroblast growth factor receptors 3 (FGFR3) transmembrane domains in detergents and in lipid bilayers were observed previously [146]. Like the 30Kc19 protein, cysteine was involved in the propensity for dimerization, which suggests that the nature of the hydrophobic environment plays an important role in defining the structure and characteristic of proteins. The

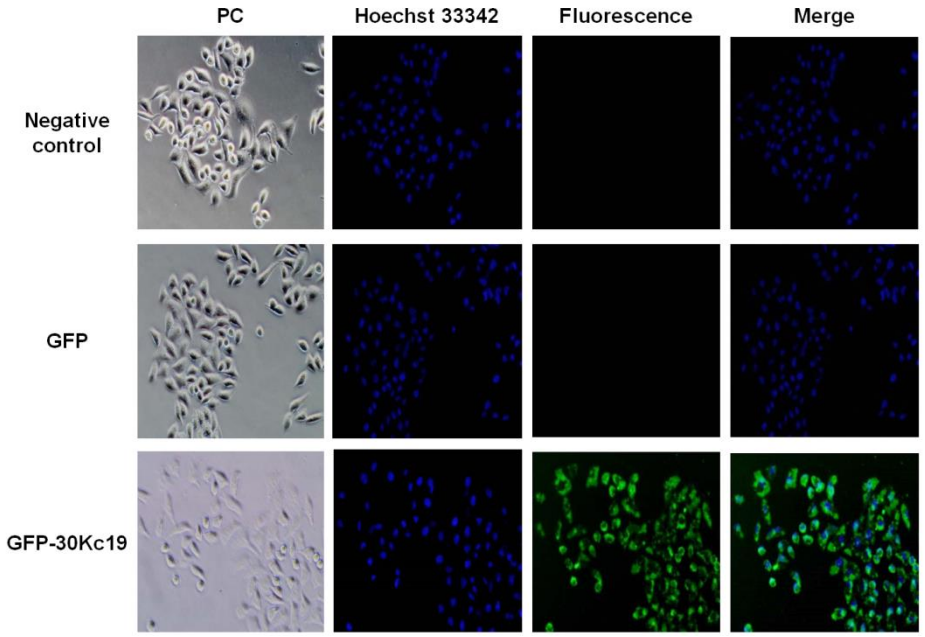

Figure 4.8 Intracellular cargo delivery using the 30Kc19 protein. HeLa cells were supplemented with the GFP or GFP-30Kc19 fusion protein in culture medium for 6 h. Ability of the 30Kc19 protein to intracellularly deliver GFP fusion protein (GFP-30Kc19) was analyzed by immunofluorescence, which showed internalization of GFP-30Kc19 protein. The internalized protein was visualized by its own signal of GFP protein, and nuclei were visualized with Hoechst 33342 (blue). Supplementing the cell culture medium with the protein was conducted in an equal molar quantity of 5 μM.

capability of the 30Kc19 protein to propensity for dimerization is thought to be similar manner to TM domain of FGFR3. Others reported that Penetratin (Antp) penetrates into cells by hydrophobic amino acids which insert into the core of cell membrane and cause change in the orientation of the negatively charged phospholipid head group [147]. To cross cell membranes efficiently is thought to be similar manner to Antp's mechanism of entry into cells (Figure 4.9).

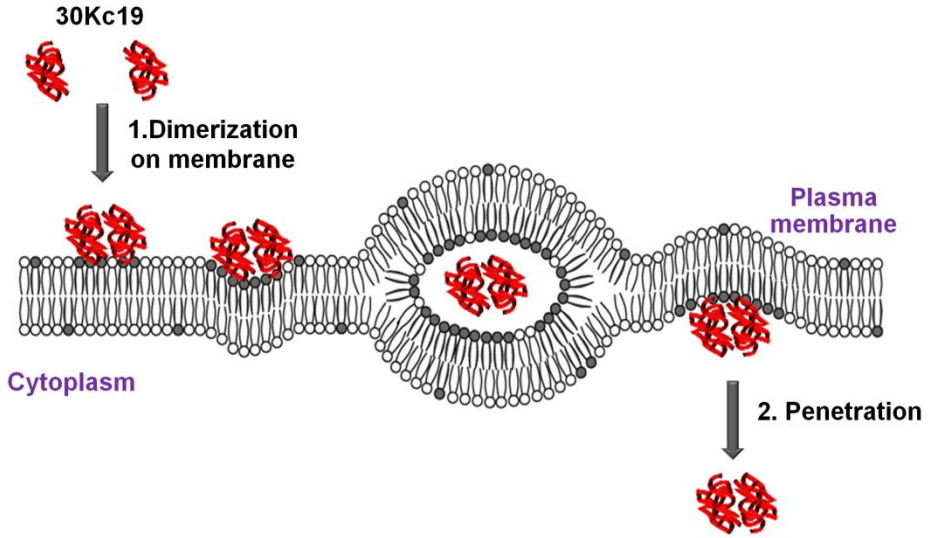

Figure 4.9 Schematic diagram of 30Kc19 protein monomer that dimerizes at the surface of the cell membrane and penetrates the cell as a dimer. The capability of the 30Kc19 protein to cross the cell membrane efficiently is thought to be similar to other CPP mechanism of entry into cells. The 30Kc19 protein is arbitrarily represented as a dimer in this model. The protein recruits negatively charged phospholipids (black circles) at the plasma membrane. The hydrophilic cavity accommodates the protein and releases it into the cytoplasm.

4.10 Conclusions

Recently, the recombinant 30Kc19 protein, originating from silkworm hemolymph of *Bombyx mori* has attracted attention due to its cell-penetrating property and use in a protein delivery system. However, this observation of penetration across cell membrane has raised questions concerning the interaction of the protein-lipid bilayer. Here, a dimerization propensity of the 30Kc19 protein was seen in the presence of amphiphilic moieties; SDS or phospholipid. Native PAGE showed that the 30Kc19 monomer formed a dimer when SDS or phospholipid was present. In the GST pull-down assay, supplementation of the 30Kc19 protein to mammalian cell culture medium showed dimerization and penetration; due to phospholipids at the cell membrane, the main components of the lipid bilayer. Mutagenesis was performed, and penetration was observed by 30Kc19 C76A and not 30Kc19 C57A, which meant Cys-57 is involved in dimerization of the 30Kc19 at the cell membrane during penetration.

Chapter 5.

Prediction and identification of cell-penetrating peptide of the 30Kc19 protein (Pep-c19)

Chapter 5. Prediction and identification of cell-penetrating peptide of the 30Kc19 protein (Pep-c19)

5.1 Introduction

In the past two decades a new class of peptides has gained increasing attention. These so-called "cell-penetrating peptides" are usually less than 30 amino acids in length, and are comprised of cationic and/or hydrophobic residues [34, 35]. These cell-penetrating peptides have the ability to penetrate rapidly into living mammalian cells, and hence, can be used to deliver various functional cargo molecules, such as proteins [97-100], small molecules [46, 101, 102], nucleic acids [103-105], antibodies [106, 107], and nanoparticles [108-111] (Figure 5.1). The exact mechanism responsible for the uptake of CPPs and their cargoes has not yet been fully established; however, a number of studies are now emphasizing the role of endocytosis [60, 74, 75], and in particular macropinocytosis [68, 76, 77], direct penetration [78, 79], and inverted micelle [80-82]. Proteins and peptides have been found to move across the cell membrane since the initial discovery of TAT CPP derived from HIV-1 virus in 1988 [36, 37], penetratin CPP derived from Antennapedia of *Drosophila melanogaster* in 1994 [39, 40], and VP22 CPP derived from herpes simplex virus in 1997 [41, 42]. Although several CPPs have been identified, it remains important to find new peptides that are efficient vehicles for the delivery of cargos, and with low toxicity because some have toxic effects on membranes of cells and organelles, including toxic effects resulting from the specific interaction of CPPs with cell components [35].

Although the biological functions of the 30K proteins in silkworms have not been fully determined, several studies have recently examined their functional properties for 30Kc6 and 30Kc19 [6, 7]. A recent study has shown that 30Kc19 protein has a cell-penetrating property when supplemented to the culture medium [29]. Therefore, 30Kc19 protein is a very unique multi-functional protein, and can be applied for the delivery of therapeutic proteins, including enzymes, as it can penetrate cell membrane as well as stabilizing cargo proteins. However, for the practical use in delivery of cell-impermeable cargo molecules, it is necessary to find a cell-penetrating domain like other cell-penetrating proteins that can efficiently deliver cargo molecules into cells.

Here, a cell-penetrating peptide of 30Kc19 protein (Pep-c19), originating from the silkworm is reported. It demonstrates how CPP candidates were selected, and tested for identification of a peptide domain that has a cell-penetrating property.

5.2 Presence of CPP in the 30Kc19 protein

30Kc19 protein, comprised of 239 amino acids in total, has all-α helix in N-terminal domain and all-β sheet in C-terminal domain as shown in Figure 5.2(a) [140, 141]. Recently, our group has shown cell-penetrating property in various types of cells, as well as the ability to deliver cargo proteins into the

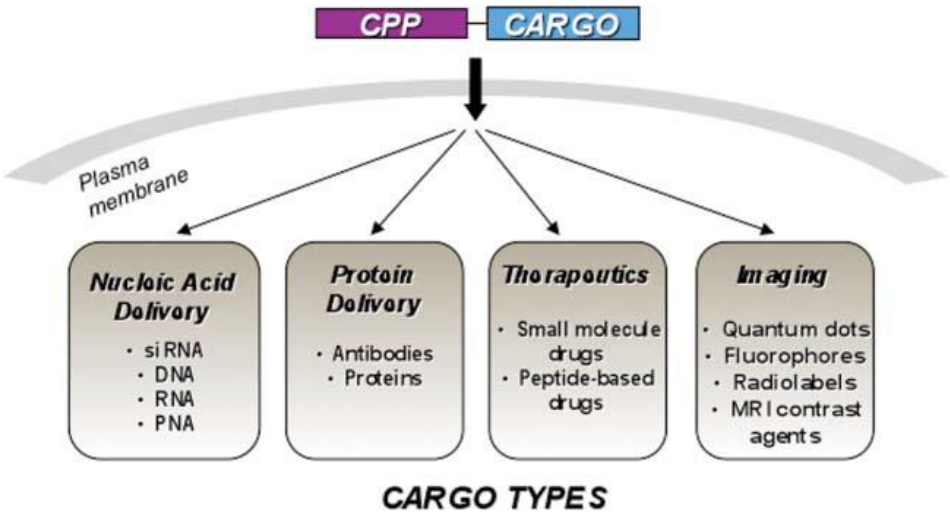

Figure 5.1 Schematic diagram of application of cell-penetrating peptides as molecular delivery vehicles [148].

cells when supplemented to culture medium. It was found to be the first cell-penetrating protein in insect hemolymph that exhibited a cell-penetration property both *in vitro* and *in vivo* [139]. In this study, the presence of CPP within the 30Kc19 protein was first investigated. To determine whether penetration of 30Kc19 is dependent on the structure of the protein itself, and to confirm the presence of CPP in the 30Kc19 protein, N- and C-terminal truncated forms of 30Kc19 protein were constructed (Figure 5.2(b)), expressed and purified. The soluble forms of $30Kc19_{1-120}$ and $30Kc19_{121-239}$ were seen from the Western-blot analysis (Figure 5.2(c)). However, $30Kc19_{1-120}$ was expressed more as soluble form and $30Kc19_{121-239}$ was expressed less as soluble form. This indicates that $30Kc19_{121-239}$ is mostly produced as misfolded proteins; inclusion bodies and refolding into bioactive forms is necessary. Hence only soluble forms of proteins were used. HEK 293 cell was used for Western-blot analysis as in previous study to compare the cell-penetrating ability of $30Kc19_{1-120}$ and $30Kc19_{121-239}$ with the 30Kc19 protein [139]. When cells were incubated with soluble form of N-terminal truncated 30Kc19 ($30Kc19_{1-120}$) at both 37 ℃ and 4 ℃, 30Kc191-120 protein was found in the cell (Figure 5.2(d)). Unlike the $30Kc19_{1-120}$ protein, $30Kc19_{121-239}$ protein was not found in the cell and further experiments were not carried out (data not shown). This raised a question of the possible presence of a cell-penetrating peptide within the 30Kc19 protein. It was likely that the N-terminal truncated domain was responsible for the cell-penetrating property of 30Kc19 protein, which meant that CPP may exist in this domain.

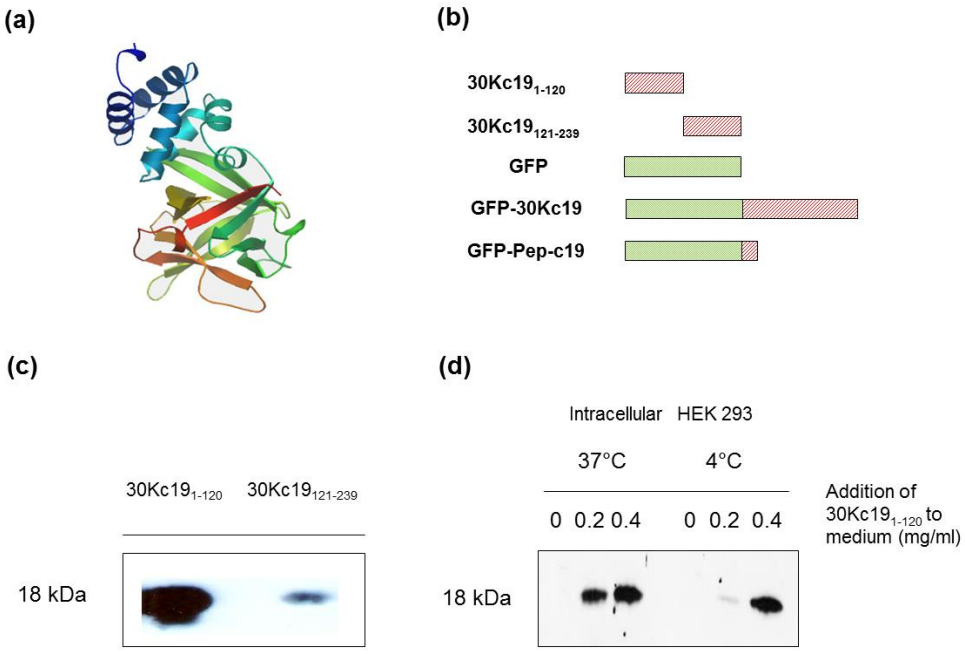

Figure. 5.2 Cell-penetrating property of 30Kc19 protein and demonstration of potential presence of cell-penetrating peptide in the 30Kc19 protein. Unless indicated otherwise, 0.2 mg/ml of proteins were used in the culture medium and were incubated with HEK 293 cells for 4 h. All figures are the results from immunoblots of whole cell lysate using the anti-30Kc19 antibody. (a) 3D representation structure of 30Kc19 protein using Swiss-model program. (b) Schematic diagram of the proteins related to this work. (c) Truncated 30Kc191-120 and 30Kc19$_{121-239}$ proteins. (d) Cell-penetrating property of truncated 30Kc19 protein at low temperature. When the cells were incubated with 30Kc19$_{1-120}$ at 4 ℃ as well as 37 ℃, 30Kc19 protein was detected in both cases.

5.3 Identification of 30Kc19 CPP (Pep-c19)

The possible location of CPP within the 30Kc19 protein was predicted. Most CPPs have common characteristics, in that they have relatively high positive charge from basic amino acids such as arginine and lysine, and also have relatively high hydrophobicity from hydrophobic residues [34, 35]. Also, taking penetratin from Antennapedia into account, evaluation was performed that CPPs are also likely to be found in the secondary structure of helix motif and surface with relatively high accessibility [149, 150]. Then the 30Kc19 sequence was analyzed for high frequency of basic amino acids, as well as hydrophobic amino acids in close proximity. Helix motif, positive surface charge, hydrophobicity, and relative surface accessibility were analyzed and showed that $30Kc19_{45\text{-}55}$ satisfied the characteristics and hence, it was selected as being the most probable candidate for the CPP within in the 30Kc19 protein.

In order to examine whether this region of 30Kc19 domain encompasses CPP, 17 peptides conjugated with FITC were synthesized (Figure 5.3(a)). We extended the peptide sections starting from 41 to 57 because of hydrophobic amino acids at 41 (Val) and 42 (Ile), and Cys at 57. We expected hydrophobic amino acid is an important factor because $Antp_{43\text{-}58}$ sequence (RQIKIWFQNRRMKWKK) contains 6 hydrophobic amino (Ile, Ile, Trp, Phe, Met, Trp) acids in total. In addition, it was expected that cysteine may be an important factor because of previous report that it may be involved in the process of internalization via formation of dimer [142]. HeLa cell was used for intracellular fluorescence analysis as in previous study [139]. To narrow down

the search for cell-penetrating peptide, each FITC-linked peptide was added to culture medium and cells were later washed vigorously with PBS several times to remove any cell-bound peptides. Intracellular fluorescence from each peptide was measured using a spectrofluorometer. Out of 3 sections; $30Kc19_{x\text{-}55}$, $30Kc19_{x\text{-}56}$, and $30Kc19_{x\text{-}57}$, each showed high fluorescence, as indicated (Figure 5.3(b)). However, because washes in PBS may not be sufficient to remove some membrane-bound peptides, 2 peptides from each section were selected (red arrow), and thus, 6 peptides; $30Kc19_{41\text{-}55}$, $30Kc19_{42\text{-}55}$, $30Kc19_{41\text{-}56}$, $30Kc19_{42\text{-}56}$, $30Kc19_{44\text{-}57}$, $30Kc19_{45\text{-}57}$ were closely examined for their cell-penetrating ability by using confocal microscopy. The results showed that 2 peptides; $30Kc19_{44\text{-}57}$ and $30Kc19_{45\text{-}57}$, were visualized in cytoplasm and were able to penetrate the plasma membrane (Figure 5.3(c)). The results are similar to HIV-TAT and Antp [69, 151]. On the other hand, 4 peptides; $30Kc19_{41\text{-}55}$, $30Kc19_{42\text{-}55}$, $30Kc19_{41\text{-}56}$ and $30Kc19_{42\text{-}56}$, were unable to penetrate the cell, and some actually formed membrane-bound aggregates (data not shown), which could explain the fluorescence given out in Figure 5.3(b). The formation of aggregates could have risen from the hydrophobic amino acids; Val-41 and Ile-42, where the number of hydrophobic amino acids in those 4 peptides was too many to allow for stability and solubility in the culture medium. $30Kc19_{45\text{-}57}$ is shorter in length than $30Kc19_{44\text{-}57}$, and thus, $30Kc19_{45\text{-}57}$ was chosen as the CPP of 30Kc19 protein. Thus, $30Kc19_{45\text{-}57}$, which will be named “Pep-c19”, was found to be the cell-penetrating peptide from 30Kc19 protein that efficiently penetrated cells when supplemented into medium for mammalian cell culture.

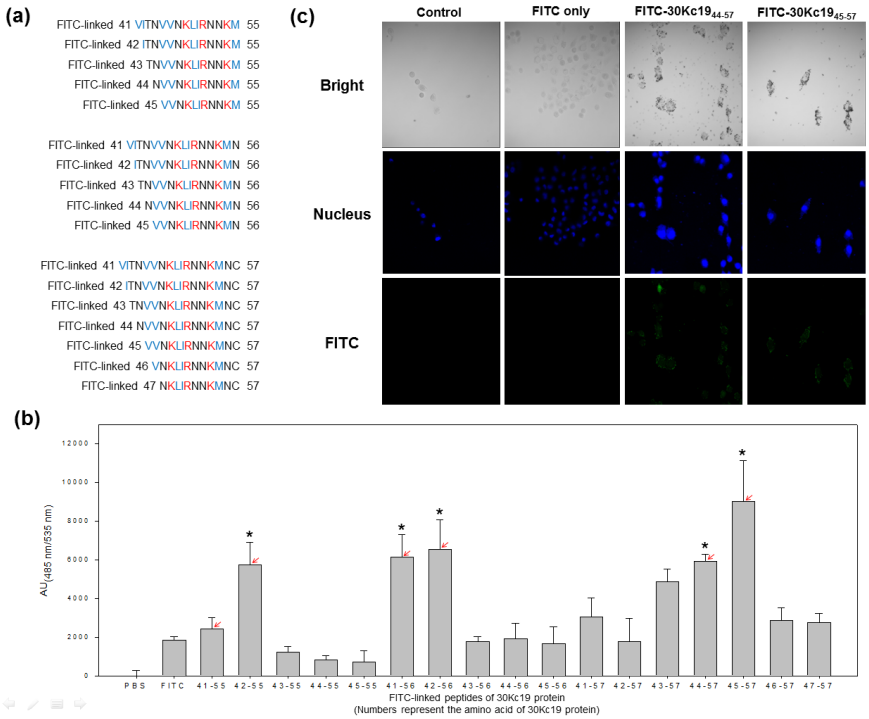

Figure 5.3 Identification of Pep-c19. (a) FITC-linked peptides were selected based on the computational results for the cell-penetrating ability. (b) Intracellular fluorescence of 30Kc19$_{x-y}$ CPP candidates was measured using spectrofluorometer (ex. 485 nm/em. 535 nm). *p < 0.001, compared with the FITC-treated group (n = 6). Error bars represent standard deviation. (c) Confocal microscopy image of the cell internalization of 30Kc19$_{x-y}$ CPP candidates in living cells. In all cases, HeLa cells were incubated for 4 h with the same molar concentration of 30Kc19$_{x-y}$ peptides (10 μM). The cell internalization of 30Kc19$_{x-y}$ peptides were visualized by FITC fluorescence (Green) and nuclei were visualized by Hoechst 33342 (Blue). x and y denote the amino acid number of 30Kc19 protein.

5.4 Intracellular penetration in the presence of inhibitors of endocytosis

It was notable that Pep-c19 successfully penetrates into cells and tissues upon addition to culture medium and intraperitoneal injection to mice, respectively. However, the mode of intracellular penetration was still unknown. Hence, inhibitors of endocytosis were used to find out how the Pep-c19 penetrates into cells. Prior to the treatment of FITC-Pep-c19 peptide, HeLa cells were treated with inhibitors of endocytosis; cytochalasin B, sucrose, and nystatin, for the disruption of microfilaments/inhibition of macropinocytosis, inhibition of clathrin-mediated endocytosis, and disruption of caveolar structure and function, respectively (Figure 5.4) [102]. Sucrose was treated to give cells a hyperosmolar condition, but no markedly difference in the penetration ability of the Pep-c19 was seen. This showed that Pep-c19 does not penetrate by clathrin-mediated endocytosis. However, when cytochalasin B or nystatin was treated to cells, slightly lowered cell-penetrating ability of the Pep-c19 was seen, which demonstrates that it penetrates cells by macropinocytosis and caveolin-mediated endocytosis. Others reported that cytochalasin B reduced the cellular uptake of CPP by half [152], and nystatin reduced the CPP reporter β-gal activity by 50% in various cells [153]. The mechanism of entry of Pep-c19 is similar to other CPPs, but Pep-c19 involves 2 uptake pathways. In our current studies, we are undergoing molecular mechanism study of Pep-c19 for clarification of endosomal escape property.

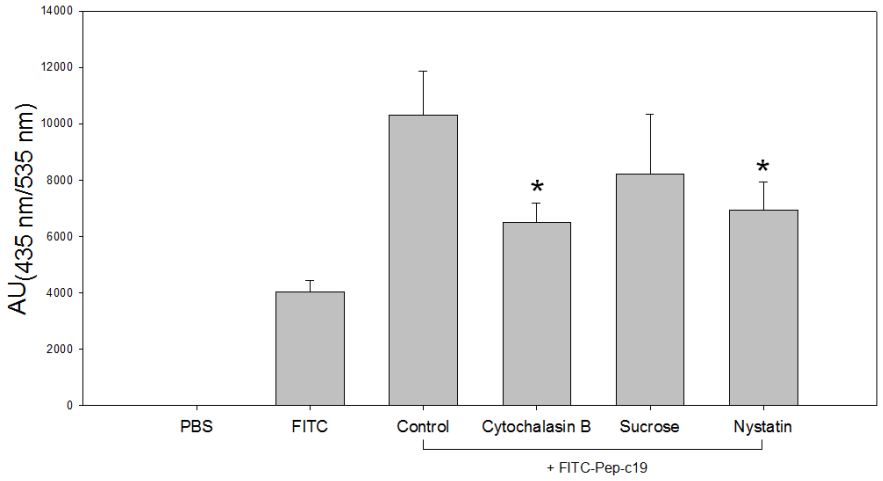

Figure. 5.4 Intracellular penetration in the presence of inhibitors of endocytosis. HeLa cells were pre-incubated for 1 h with various endocytosis inhibitors; cytochalasin B (25 μM) for the disruption of microfilaments/inhibition of macropinocytosis, sucrose (100 mM) for the inhibition of clathrin-mediated endocytosis, and nystatin (25 μg/ml) for the disruption of caveolar structure and function. FITC-linked Pep-c19 peptide was supplemented to the medium and after 6 h of incubation, HeLa cells were vigorously washed three times with PBS. The intracellular FITC-Pep-c19 was measured by green fluorescence using spectrofluorometer (ex. 485 nm/em. 535 nm). *$p < 0.05$, compared with the control group (n = 3). Error bars represent standard deviation.

5.5 Comparison of Pep-c19 with other cell-penetrating peptides

Well-known cell-penetrating peptides derived from protein transduction domains are Tat from human immunodeficiency virus-1 (HIV-1) [36, 37], VP22 from herpes simplex virus-1 (HSV-1) [41, 42], and Antp (also known as Penetratin) from Antennapedia homeodomain [39, 40]. In this research, a new cell-penetrating peptide was found from the third helix of *Bombyx mori* silkworm hemolymph. Pep-c19, in comparison with other CPPs in terms of the primary structure, Pep-c19 CPP contains less positive amino acids (3 in the sequence) than other CPPs (TAT has 8, VP22 has 9, Antp; has 7) (Table 5.5). Instead, Pep-c19 has more hydrophobic acids (6 in the sequence) than the most of other CPPs (TAT has 0, VP22 has 1, Antp has 6). With the secondary structure, Antp's homeodomain is comprised of 60 residues and it is consisted of 3 alpha-helices. Third alpha-helix is responsible for penetration (Antp), which is similar to our Pep-c19, because it is also from the third alpha helix of the 30Kc19 protein. HSV-1 protein has a size that is a little bigger than the 30Kc19 protein, 38 kDa, and VP22 is located at the very last 34 residues. These CPPs have been used to transduce proteins into cells and tissues and for some (Tat and Antp) even across blood brain barrier but efficiency various depending on the cargo that is attached to the CPPs [154]. Though advantages and disadvantages exist among the CPPs, the major advantage of Pep-c19 is that it is not a virus-derived cell-penetrating peptide meaning it is applicable as a therapeutic tool, short length, and is not toxic.

Table 5.5 Comparison of Pep-c19 with other cell-penetrating peptides.

Name	Origin	Sequence (No. of amino acid)	Features
Tat	Human immunodeficiency virus-1 trans-activating transcriptional activator (HIV-1 TAT); residues 48-60	GRKKRRQRRRPPQ (13)	Able to transduce 15 – 120 kDa proteins into cells with high efficiency (~100%). *In vivo* delivery after 4 h into various tissues and across BBB.
VP22	Herpes simplex virus-1 protein 22 (HSV-1); residues 266-301	DAATATRGRSAASRPTERPRA PARSASRPRRPVD (34)	38 kDa size with last 34 residues responsible for penetration. Efficacy varies with cell type but quite inefficient.
Antp (Penetratin)	Antennapedia homeodomain; residues 43-58	RQIKIWFQNRRMKWKK (16)	Consists of 3 alpha-helices. Third helix responsible for penetration; *in vivo* delivery into brain within 30 min.
Nona-arginine (R9)	Polyarginine	RRRRRRRRR (9)	Polyarginine peptides of 4-16 residues tested with 8 and 9 being optimal. Able to transduce molecules into a variety of cells in culture.
Pep-c19	*Bombyx mori* 30Kc19 protein; residues 45-57	VVNKLIRNNKMNC (13)	28 kDa size with 13 residues in third helix responsible for penetration; *in vivo* delivery into various tissues except brain.

(Red color: positive amino acid, blue color: hydrophobic amino acid) [154]

5.6 Conclusions

A new CPP; VVNKLIRNNKMNC, from 30Kc19 protein was identified and demonstrated that 30Kc19 exhibited a cell-penetrating property due to the presence of a cell-penetrating peptide at 45-57. The mode of intracellular penetration was evaluated by the use of inhibitors of endocytosis to find out how the Pep-c19 penetrates into cells. Sucrose was treated to give cells a hyperosmolar condition, but no markedly difference in the penetration ability of the Pep-c19 was seen. This showed that Pep-c19 does not penetrate by clathrin-mediated endocytosis. However, when cytochalasin B or nystatin was treated to cells, slightly lowered cell-penetrating ability of the Pep-c19 was seen, which demonstrates that it penetrates cells by macropinocytosis and caveolin-mediated endocytosis. The results strongly suggest that Pep-c19 has great potential for the efficient delivery of micro- and macromolecules including drugs and proteins to target tissues for therapeutic purposes. Since Pep-c19 is a cell-penetrating peptide derived from the first cell-penetrating protein that has been found in insect hemolymph, anticipate that other cell-penetrating peptides will be identified from other proteins in insects.

Chapter 6.

In vitro and *in vivo* protein delivery system using cell-penetrating peptide of the 30Kc19 protein (Pep-c19)

Chapter 6. *In vitro* and *in vivo* protein delivery system using cell-penetrating peptide of the 30Kc19 protein (Pep-c19)

6.1 Introduction

The transport of CPPs across membranes has been studied *in vitro* cells and in tissues *in vivo*. Various mammalian cells have been used, including primary cells and cell lines. CPPs successfully penetrated in primary cells from brain and spinal cord of rat [40], aorta of calf [83], endothelium of umbilical vein from porcine and human [49]. But in most cases, cell lines have been used.

For penetration to occur *in vitro*, no special cell cultivating procedures are needed with cell lines. Cells are usually grown to a certain % of confluence in dishes, wells, or μ-well plates and then can be incubated with CPP containing solution, which in most cases is cell culture medium.

Only a few penetration experiments have been performed *in vivo* in whole organisms and even fewer *ex vivo* in isolated tissue. *Ex vivo* tissue experiments were performed mainly in isolated blood vessels. Most *in vivo* experiments were carried out with penetratin and Tat. Besides the blood vessel cells, penetratin was successfully used *in vivo* to enter peritoneally and to reach brain and spinal cord cells [88]. In some cases, it also by passed the blood–brain barrier [89-91]. Tat was used *in vivo* to deliver active cargo enzyme in cells from all tissues of mouse [92]. Proper kinetic experiments are mostly obtained with cells from cell lines because although *ex vivo* and *in vivo* experiments showed clear physiological responses are important for understanding the

mechanism of internalization, and particularly for demonstrating the drug delivery potential of CPPs, these experiments are not suitable for studies of kinetics of internalization because of difficulties in obtaining sufficient kinetic data under well-defined and reproducible experimental conditions.

Hence, for the practical use in delivery of cell-impermeable cargo molecules, it is necessary to characterize CPP-conjugated cargos whether it can efficiently deliver cargo molecules into cells both *in vitro* and *in vivo* (Figure 6.1).
Here, the cell-penetrating peptide of 30Kc19 protein (Pep-c19), originating from the silkworm is tested for cell-penetrating property. The efficiency and toxicity of this "Pep-c19" in comparison with its original protein, 30Kc19, both *in vitro* and *in vivo* are also investigated.

6.2 *In vitro* protein delivery of protein-conjugated Pep-c19

In order to examine the ability of Pep-c19 to deliver foreign proteins into the cell as well as its cell-penetrating efficiency, a GFP-Pep-c19 as well as GFP and GFP-30Kc19 was expressed in *E. coli* and purified (Figure 6.2(a)). HeLa cell was used for fluorescence analysis as in previous study to compare the cargo-delivering ability of Pep-c19 with the 30Kc19 protein [139]. Each protein was added to culture medium of HeLa cells and the increase in intracellular GFP-Pep-c19 was determined to be dependent on the concentration of the protein in the culture medium. The efficiency of the Pep-c19 was higher than the GFP-30Kc19, even after vigorous washing with PBS for the removal of any cell-bound proteins (Figure 6.2(b)). The increase in the intracellular penetrated

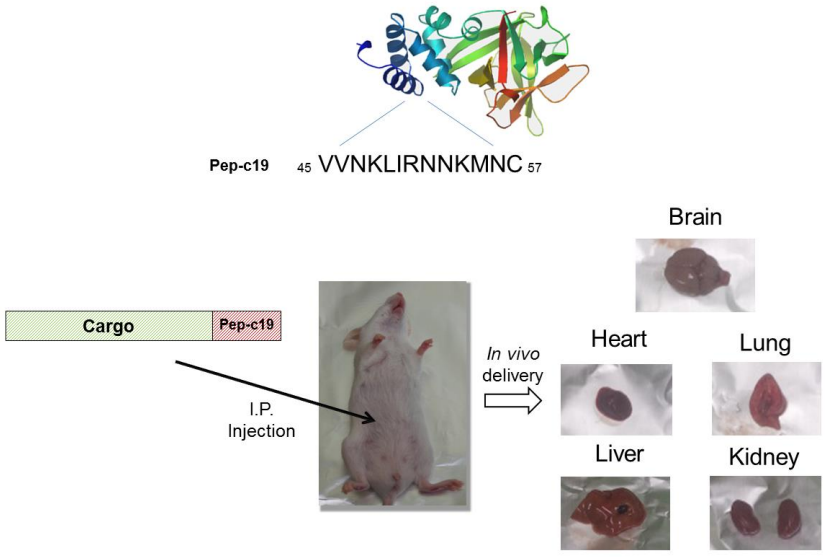

Figure. 6.1 Intraperitoneal injection of Pep-c19 and organ preparation from mice for *in vivo* delivery.

GFP-Pep-c19 was dependent on the time of the protein in the culture medium, and the efficiency of the Pep-c19 was also higher than the GFP-30Kc19, after vigorous washing with PBS (Figure 6.2(c)). Then, each protein was added to the culture medium of HeLa cells and immunocytochemistry was performed. Similar to GFP-30Kc19, GFP-Pep-c19 also penetrated into the cells. Live cell images were taken under confocal microscope after vigorous washing with PBS to exempt membrane-bound proteins and possible artifacts from fixation process of immunocytochemistry, where cell surface-bound proteins could be moved into cells [155]. The confocal images indicated that GFP-Pep-c19 successfully penetrated inside the living cells (Figure 6.2(f)). Similar to Figure 5.3(c), it was worthwhile to notice that GFP-Pep-c19 was visualized in a punctate form. It was shown that internalized foreign proteins fused with the cell-penetrating peptide were observed as punctate forms [151, 156]. Quantification of the intracellular fluorescence from the cell lysate was performed to fully exclude the possible membrane-bound proteins. Protein-treated cells were treated with trypsin-EDTA for removal of membrane-bound proteins and then fluorescence of cell lysate was measured (Figure 6.2(f)). The result showed that both GFP-30Kc19 and GFP-Pep-c19 proteins were located in the cell lysate, but more GFP-Pep-c19 was found inside the cell. These results demonstrated that Pep-c19 can, not only penetrates itself, but it is also able to deliver impermeable cargo proteins, such as GFP into the cell with higher efficiency than the whole 30Kc19 protein.

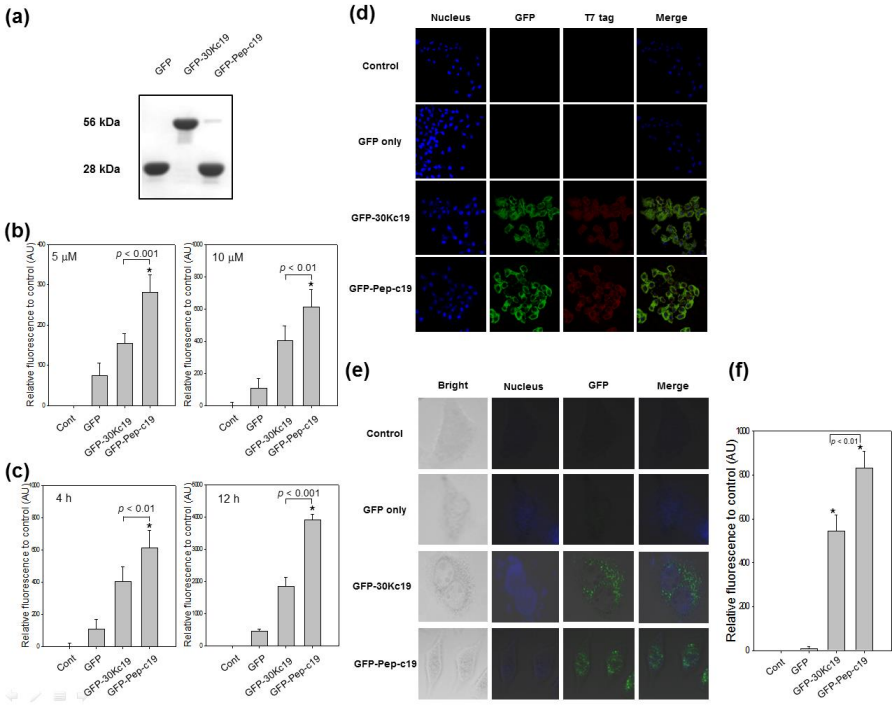

Figure 6.2 Delivery of GFP into the cells by Pep-c19. (a) SDS-PAGE result of proteins. (b) Intracellular fluorescence in dose-dependent (4 h) and (c) time-dependent (10 μM) manner was measured using spectrofluorometer (ex. 488 nm/em. 515 nm) (n = 6). (d) Immunocytochemistry image of the HeLa cell internalization of GFP-Pep-c19 using confocal microscopy. (e) Confocal microscopy image in living cells. The GFP-Pep-c19 was visualized by GFP fluorescence (Green) and nuclei were visualized by Hoechst 33342 (Blue) (4 h, 10 μM) (f) Intracellular fluorescence of GFP-Pep-c19 (10 μM, 6 h) was measured after trypsin-EDTA for removal of membrane-bound proteins using spectrofluorometer (ex. 488 nm/em. 515 nm) (n = 3). Error bars represent standard deviation.

6.3 *In vivo* protein delivery of protein-conjugated Pep-c19

Previously, CPPs have been used to successfully deliver cell-impermeable cargos such as proteins [97-100], small molecules [46, 101, 102], nucleic acids [103-105], antibodies [106, 107], and nanoparticles [108-111] either *in vitro* and *in vivo*. To investigate *in vivo* penetration and efficiency in comparison with the whole 30Kc19 protein, we intraperitoneally injected each protein to 5-week-old ICR mice, and the organs, including brain, heart, lung, kidney, and liver, were isolated 12 h after injection [92, 157, 158]. In order to avoid an artifact and to address the potential issue caused by fixation process from immunohistochemistry, fluorescence images were taken without the fixation process, and thus, the penetration of GFP-Pep-c19 into tissues was analyzed by the fluorescence from the GFP protein. No fluorescence was detected for the native GFP in tissues (Figure 6.3, top panel). Fluorescence was detected in all the tissues except the brain (Figure 6.3 (a), (b), (c), (d)), isolated from the mouse that were injected with GFP-30Kc19 and GFP-Pep-c19, although the fluorescence intensities varied among tissues (Figure 6.3, middle panel). For GFP-Pep-c19, we observed that fluorescence intensity was much higher than that from GFP-30Kc19 in tissues (Figure 6.3, bottom panel). This indicates that Pep-c19 penetrated and delivered cargo into various tissues across the blood vessel barriers with a high efficiency. No fluorescence was detected for all groups in the brain tissue, indicating the both the 30Kc19 and Pep-c19 are unable to penetrate and deliver cargos across the blood brain barrier (BBB) (Figure 6.3(e)).

6.4 Toxicity test for the long-term administration of Pep-c19

Previously, it was shown that 30K proteins do not show any toxic effect *in vitro* cell cultures and *in vivo* study [10, 13, 16, 17, 139]. To examine *in vivo* toxicity of Pep-c19, we measured the toxicity parameters that represent toxicity in kidney and liver. Toxicity in kidney is shown by increase in the levels of blood urea nitrogen (BUN) and creatinine, whereas toxicity on liver is shown by increase in the levels of aspartate aminotransferase (ALT) and alanine aminotransferase (AST) [159, 160]. The level of BUN, creatinine, ALT and AST from the blood serum of Pep-c19-injected mice were analyzed by Neodin Institute. We injected 3 different mice with 0.2 μmol/kg and 2 μmol/kg of each protein, every day, for 14 days, and evaluated the toxicity. After 2 weeks of injection, no apparent differences in the body weights and behaviors of mice were observed in any of the groups (data not shown). Toxicity results showed that high dose and long-term administration of Pep-c19 did not cause statistically significant or meaningful differences between 30Kc19 protein and Pep-c19 from all four toxicity parameters (Figure 6.4). In all tests, the *p*-values between the control group and the 30Kc19-injected group and Pep-c19-injected group were mostly higher than 0.1. These results indicate that long-term administration of Pep-c19 did not cause significant toxicity *in vivo*. Previously, it was reported that Tat and VP22 are non-toxic both *in vitro* [51, 161, 162] and Tat is non-toxic *in vivo* [92]. In another group, toxicity was evaluated *in vivo* by applying peptides to the cornea 4 times daily for 7 days. At very high

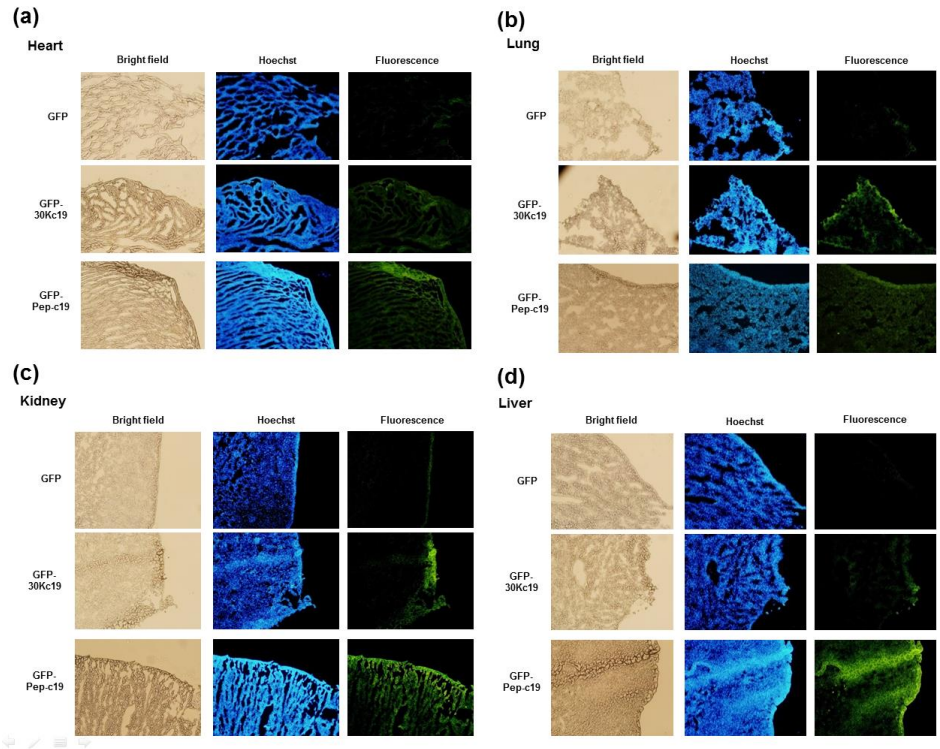

Figure 6.3.1 *In vivo* delivery of GFP into various tissues by Pep-c19. Proteins were dissolved in PBS with 10 mg/ml, 20 mg/mg, 10 mg/ml, respectively, and were intraperitoneally injected into female 5-week-old ICR mice (25 g). Same molar amount of GFP, GFP-30Kc19, and GFP-Pep-c19 were injected into mice (3.5 μmol/kg; 100 mg/kg mouse for GFP, 200 mg/kg mouse for GFP-30Kc19, 100 mg/kg mouse for GFP-Pep-c19). As a control experiment, the same volume of PBS was injected into mice. After 12 h of injection, the organs; heart, lung, kidney, and liver were collected, and tissues were sectioned to 10 μm width using a microtome-cryostat. The penetrated GFP-Pep-c19 was visualized by GFP fluorescence (Green), and nuclei were visualized by Hoechst 33342 (Blue).

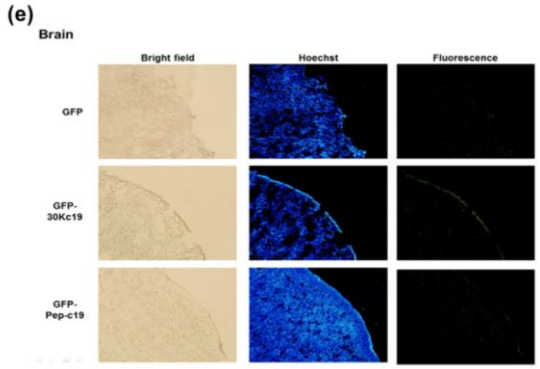

Figure 6.3.2 *In vivo* delivery of GFP into brain tissues by Pep-c19. Proteins were dissolved in PBS with 10 mg/ml, 20 mg/mg, 10 mg/ml, respectively, and were intraperitoneally injected into female 5-week-old ICR mice (25 g). Same molar amount of GFP, GFP-30Kc19, and GFP-Pep-c19 were injected into mice (3.5 μmol/kg; 100 mg/kg mouse for GFP, 200 mg/kg mouse for GFP-30Kc19, 100 mg/kg mouse for GFP-Pep-c19). As a control experiment, the same volume of PBS was injected into mice. After 12 h of injection, the brain was collected, and tissues were sectioned to 10 μm width using a microtome-cryostat. The penetrated GFP-Pep-c19 was visualized by GFP fluorescence (Green), and nuclei were visualized by Hoechst 33342 (Blue).

concentrations, the Antennapedia peptide showed no toxicity, whereas Tat caused some mild eyelid swelling [163]. The results in Figure 6.4 show that Pep-c19 has similar non-toxic property. Therefore, it is anticipated that Pep-c19 could be utilized as an efficient and nontoxic carrier for the delivery of biological molecules into tissues *in vivo*. Other than fusing the CPP with the cargo, the non-conjugation approach may also be adapted for the delivery of cell-impermeable cargos; for instance siRNA, by mixing the CPP and siRNA and forming CPP/siRNA complex.

Regarding the mechanism of entry for 30Kc19 and Pep-c19, it was found that Cys-57 plays a crucial role in the dimerization and penetration. Because Cys-57 is the final jigsaw puzzle of the Pep-c19 sequence, the mode of penetration is expected to be similar for both cases.

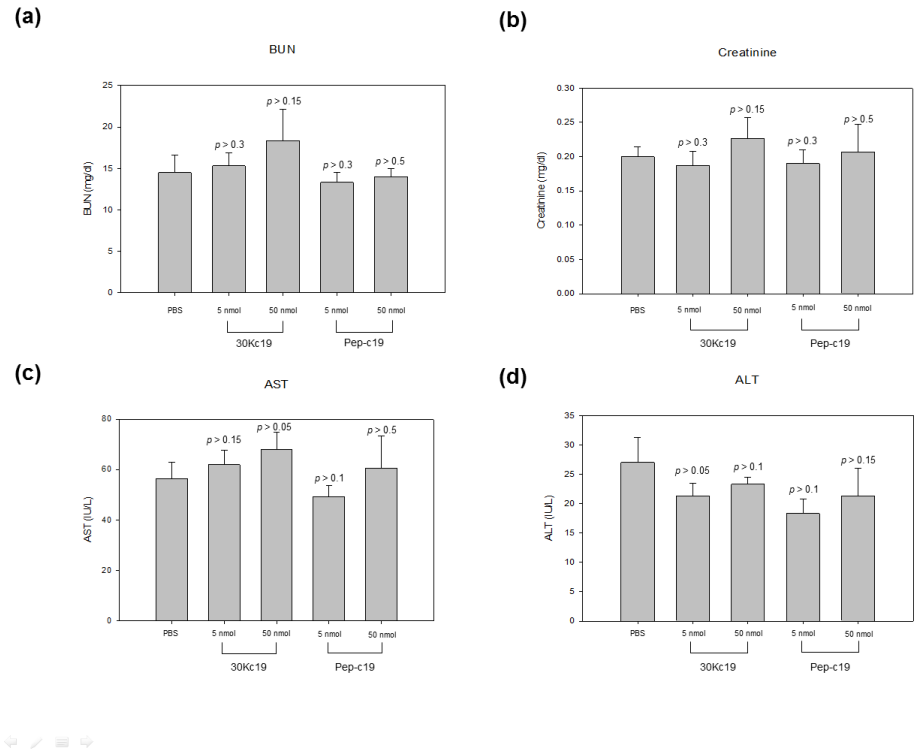

Figure 6.4 Toxicity test for the long-term administration of Pep-c19. 30Kc19 and Pep-c19 were injected to mice daily (0.2 μmol/kg and 2 μmol/kg) for 14 days. For the control experiment, the same volume of PBS was injected. 3 different mice were used for each experiment (n = 3). To evaluate serum biological parameters, blood serum were collected from mice. (a), (b) To analyze the kidney function, blood urea nitrogen (BUN) and creatinine levels were determined. (c), (d) As a parameter of the liver function, aspartate aminotransferase (AST) and alanine aminotransferase (ALT) activities were determined. The *p*-values on each bar were evaluated by comparing with the control group (PBS-treated). Error bars represent the standard deviation.

6.5 Conclusions

The newly identified CPP; VVNKLIRNNKMNC, from 30Kc19 protein was analyzed for its ability to penetrate and deliver cargo molecules *in vitro* and *in vivo*. In this study, Pep-c19 was fused to the C-terminal of the cargo protein and intracellular delivery was successful. But similar intracellular delivery is expected if Pep-c19 is located at N-terminal of the cargo protein. When Pep-c19 was intraperitoneally injected into mice, Pep-c19 successfully delivered cargo proteins into various organ tissues with higher efficiency than the 30Kc19 protein itself, and without toxicity in kidney and liver. However, no fluorescence was detected for all groups in the brain tissue, indicating the both the 30Kc19 and Pep-c19 are unable to penetrate and deliver cargos across the blood brain barrier (BBB). In any case, results strongly suggest that Pep-c19 could be utilized as an efficient and nontoxic carrier for the delivery of biological molecules into target organ tissues for therapeutic purposes *in vivo*.

Chapter 7.

In vitro siRNA delivery system using cell-penetrating peptide of the 30Kc19 protein (Pep-c19)

Chapter 7. *In vitro* siRNA delivery system using cell-penetrating peptide of the 30Kc19 protein (Pep-c19)

7.1 Introduction

In 1998, Andrew Fire first discovered RNA interference (RNAi) and since then it has now spread to become a standard protocol [164]. RNAi responses are initiated by delivery of short sequence of nucleotides called "short interfering RNAs (siRNAs)" into the cytoplasm of cells. Cytoplasmic siRNAs then combine with RNA-induced silencing complex (RISC) which then recognizes and degrades target mRNAs [165] (Figure 7.1). However, due to their size (larger than 10 kDa) and strong negative charge, siRNAs cannot enter cells on their own and therefore require a delivery vehicle. Although many materials, such as cationic lipids and polymers have been developed to deliver siRNAs, these delivery agents cannot introduce siRNAs into the entire population of cells and in a non-cytotoxic fashion, especially primary cells. Hence, siRNA delivery into cells remains the rate-limiting step problem for development of RNAi.

These siRNAs can be beneficial for modulating expression of specific gene of interest with treatment of diseases such as viral infection, cancer, and genetic disorders [164, 166-169]. In clinical practice, however, therapeutic application of siRNA has been hindered due to limited stability, poor cellular uptake *in vivo*, and lack of a reliable delivery method [170-172]. The main obstacle in practical application of siRNA as a molecular medicine is the where it can lead sequence-specific mRNA degradation. siRNAs are impermeable to cells

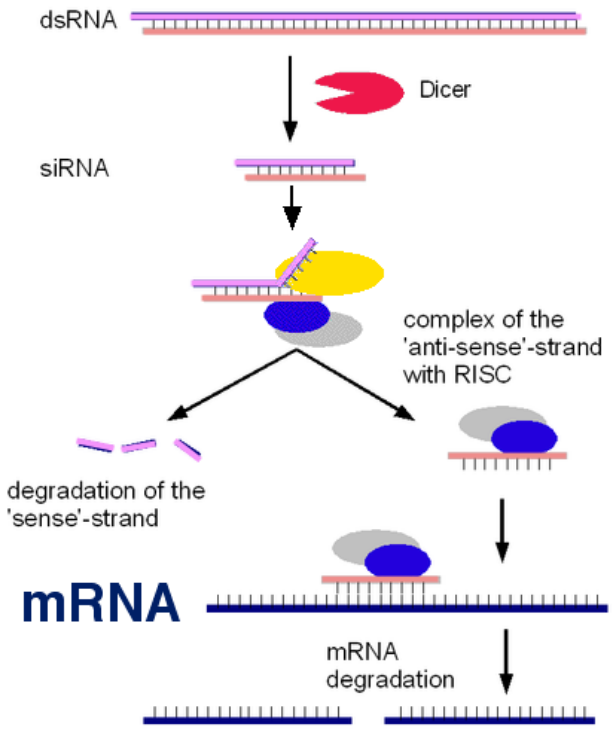

Figure 7.1 Principle of RNAi. RNAi are long double-stranded RNA (dsRNA) molecules complementary to mRNA sequences. When siRNAs enter the cell, RISC-siRNA complex forms which can induce suppression of specific genes of interest (mRNA) [173].

without the use of transfection reagents or techniques that may damage the plasma membrane. Adenoviruses, liposomes, and cationic polymers can be useful delivery systems [174-177]. Viral vector-based siRNA delivery overcomes the problem of poor transfection, but clinical application of viral vectors is hampered by concerns about serious inflammatory side effects [175, 177, 178]. Conjugating or entrapping the siRNAs to or in a nano-carrier such as a water soluble polymer, cationic lipid, or liposome is less toxic than use of viral vectors. However, there are still problems of low efficiency, and the siRNAs have to escape the endosome [174, 176]. Therefore, search for a safe and highly effective delivery system for siRNA-based molecular medicine continues. With this in mind, a new approach using ‘‘cell penetrating peptide (CPP)’’ for systemic siRNA delivery seems promising.

Some researchers have reported that the formation of covalently bound conjugates between CPPs and siRNA offers another potential delivery strategy. For this strategy to work, a CPP [179-181], transportan [180], or Tat [103, 181] should be linked to a siRNA. However, the binding of CPPs to siRNA is difficult [182].

Another proposed method is the formation of non-covalent electrostatic bonds between siRNA and CPPs, including arginine-rich peptides [183, 184], MPG peptide [185] and its analogue [102], and penetratin analogue [186].

The preparation of such CPP-siRNA complexes is technically simple, because these are formed through electrostatic interaction in an aqueous solution which requires no purification. Although some researchers have demonstrated successful delivery of siRNA into cells using this method, the non-covalent

complexes may reduce the penetration efficiency of CPPs.

To address the siRNA delivery problem, Pep-c19 CPP was used because previously CPPs was shown to rapidly transport macromolecules into the entire population of cells in a non-cytotoxic manner via macropinocytosis, a specialized type of fluid phase endocytosis that all cells appear to perform [187].

Here, the cell-penetrating peptide of 30Kc19 protein (Pep-c19), originating from the silkworm for the delivery of siRNA is presented. Through non-covalent biding between the Pep-c19 and siRNA, Pep-c19/siRNA complex was formed for its gene silencing effect in comparison with a well-known CPP, 11R. The cargo delivery efficiency as well as cytotoxicity of the CPP/siRNA complexes were determined *in vitro*.

7.2 Formation of non-covalent CPP/siRNA complexes

Non-covalent CPP/siRNA complexes were made by mixing CPP and siRNA together and incubated for 15 min at room temperature. 0.5 μg of siRNA was used and molar excess CPPs were mixed. 2% (w/v) agarose gel in TAE buffer was used for gel shift/retardation assay and electrophoresis was conducted. The siRNA began to disappear at 20-fold molar excess for 11R and 50-fold molar excess Pep-c19 (Figure 7.2). This demonstrated that 11R forms 11R/siRNA complex at lower molar excess than the Pep-c19/siRNA. The reason being could be because 11R is more positively charged than the Pep-c19 due to the presence of more positive-charged amino acids (Arginine) than the Pep-c19, which has only 3 positive amino acids in the sequence (K, R, K).

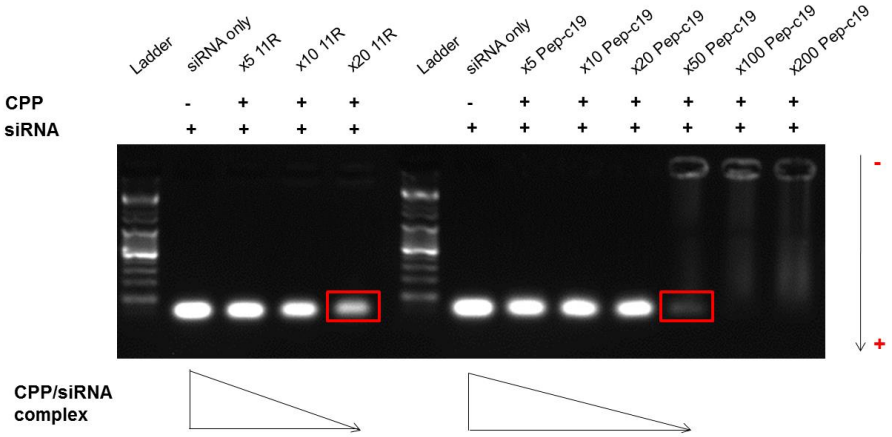

Figure 7.2 Gel shift/retardation assay for CPP to form complexes with siRNA. 0.5 μg of siRNA was used and molar excess CPPs were mixed and incubated for 15 min at room temperature for the formation of CPP/siRNA complex. 2% (w/v) agarose gel in TAE buffer was used.

7.3 Internalization of non-covalent CPP/siRNA complexes in HeLa cells

Internalization of non-covalent CPP/siRNA complexes was analyzed in HeLa cells. HeLa cells were seeded on 24 well and 20- and 50-fold molar excess CPPs to 100 nM siRNA were preincubated for the formation of CPP/siRNA complex. CPP/siRNA complexes were added to the culture medium and incubated for 1 h at 37 °C in 5% CO_2. Cells were thoroughly washed 3 times with PBS and any non-specific binding to the membrane was removed by trypsin treatment. Cells were collected, lysed with RIPA buffer, and the lysate was analyzed for the presence of Cy3, linked to 3´end of siRNA. Fluorescence was analyzed using spectrofluorometer (ex 535 nm, em 612 nm) and then it was normalized to the total protein amount of cells. The fluorescence of internalized Pep-c19/siRNA complex was 2.3 fold and 3.5 fold higher than the siRNA, as compared with 2.1 fold and 1.68 fold higher for 11R/siRNA, the former 20-fold and latter 100-fold molar excess of CPPs to siRNA, respectively (Figure 7.3). This demonstrated that Pep-c19 is more efficient in internalizing and delivering siRNA to cells than 11R CPP.

7.4 Effect of CPP/siRNA complex on the fluorescence of HEK 293-EGFP cells

The gene silencing effect of internalized CPP/siRNA complexes were analyzed in HEK 293-EGFP cells. HEK 293-EGFP cells were seeded on 24 well and 20- and 100-fold molar excess CPPs to 100 nM siRNA were

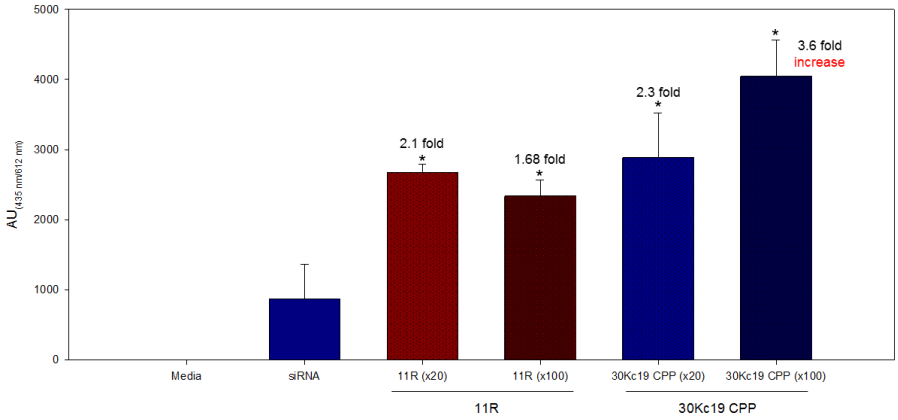

Figure 7.3 Internalization of non-covalent CPP & siRNA-Cy3 complexes in HeLa cells. 100 nM siRNA was used. 2 and 10 μM of CPPs were mixed with siRNA to form CPP/siRNA complexes by preincubating for 15 min at room temperature. CPP/siRNA complex was added to culture medium for 1 h and were washed vigorously with PBS. Trypsin was added to remove any prebound complexes to cell membrane. Cells were collected, lysed and cell lysate was analyzed for the presence of Cy3 using spectrofluorometer (Ex 535, Em 612nm). Data were normalized to total protein amount of cells. Experiment was performed in triplicate. *$p < 0.01$. Error bars represent standard deviation.

preincubated for the formation of CPP/siRNA complex. CPP/siRNA complexes were added to the culture medium and incubated for 24 h and 72 h at 37 ℃ in 5% CO_2. Cells were thoroughly washed 3 times with PBS and any non-specific binding to the membrane was removed by trypsin treatment. Cells were collected, lysed with RIPA buffer, and the lysate was analyzed for the amount of EGFP by fluorescence. Fluorescence was analyzed using spectrofluorometer (ex 485 nm, em 535 nm) and then it was normalized to the total protein amount of cells. The fluorescence of EGFP in cells treated with 11R/siRNA complex for 24 h was reduced 13.6% and 14.8% for 20-fold and 100-fold molar excess CPPs to siRNAs, respectively (Figure 7.4.1(a)). For Pep-c19/siRNA complex, the fluorescence of EGFP in cells was reduced 17.3% and 20.1% for 20-fold and 100-fold molar excess CPPs to siRNAs, respectively. However, the fluorescence of EGFP in cells treated with 11R/siRNA complex for 72 h was reduced 18.9% and 17.8% for 20-fold and 100-fold molar excess CPPs to siRNAs, respectively (Figure 7.4.1(b)). For Pep-c19/siRNA complex, the fluorescence of EGFP in cells was reduced 17.7% and 18.2% for 20-fold and 100-fold molar excess CPPs to siRNAs, respectively. This demonstrated that Pep-c19 and 11R have similar gene silencing effect in cells. This was verified again by Western blot were for 72 h were thoroughly washed 3 times with PBS and any non-specific binding to the membrane was removed by trypsin treatment. Cells were collected, lysed with RIPA buffer, and the lysate was analyzed for the amount of EGFP by Western blot analysis (Figure 7.4.2 (a)). β tubulin was used as standard. For 11R/siRNA treated cells, no comparative difference was seen in the amount of EGFP protein than the control.

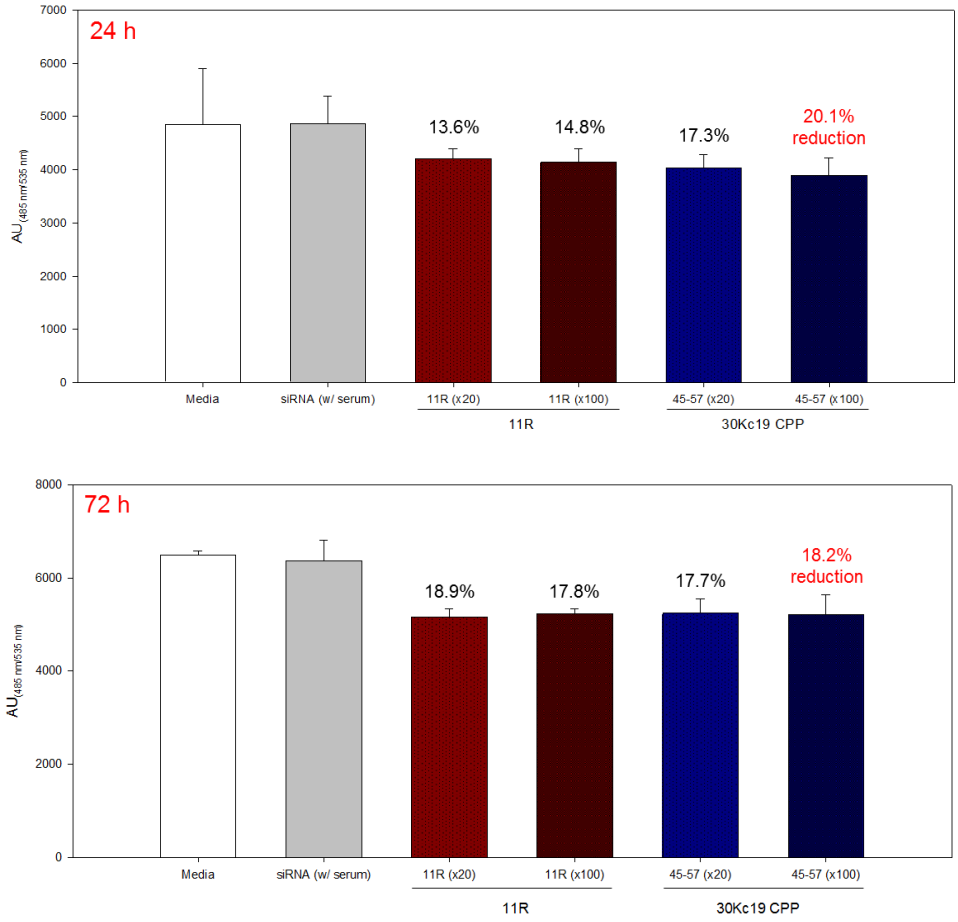

Figure 7.4.1 Gene silencing effect of non-covalent CPP-EGFP siRNAs delivered in HEK 293-EGFP cells. 100 nM siRNA was used. 2 and 10 μM of CPPs were mixed with siRNA to form CPP/siRNA complexes. (a) 24 h ($p < 0.01$) and (b) 72 h ($p < 0.05$). Cells were collected, lysed and cell lysate was analyzed for the presence of EGFP using spectrofluorometer (ex 485, em 535 nm). Data were normalized to total protein amount of cells. n = 3.

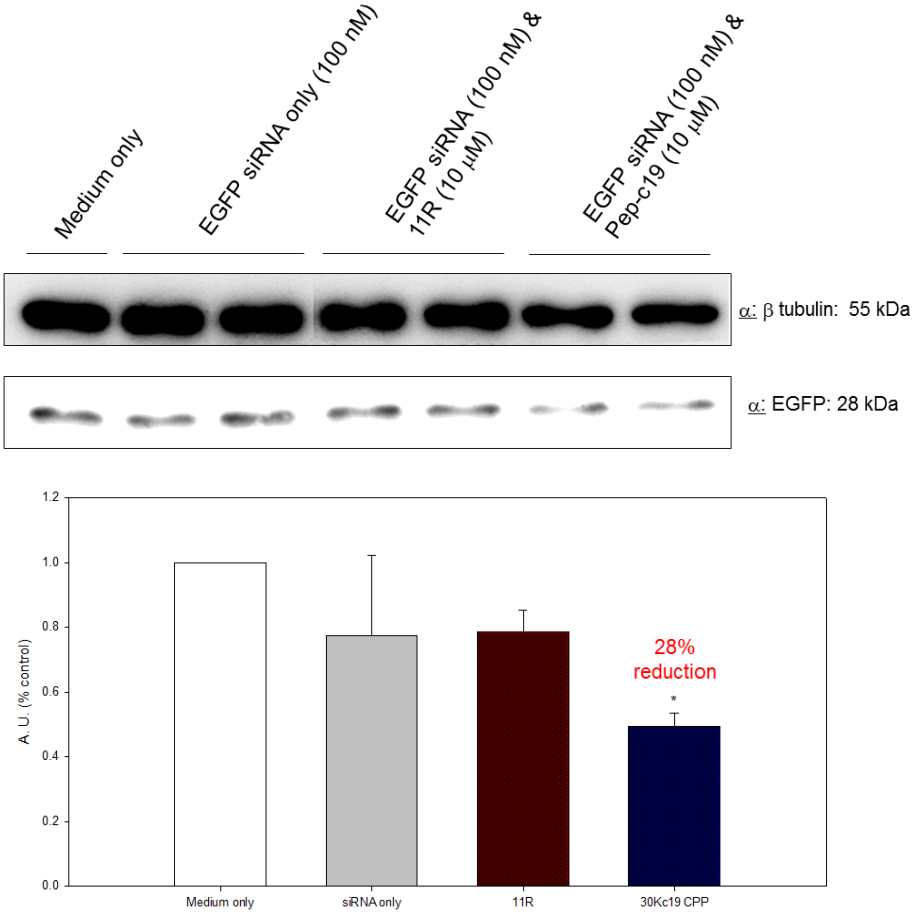

Figure 7.4.2 Gene silencing effect of non-covalent CPP-EGFP siRNAs delivered in HEK 293-EGFP cells. 100 nM siRNA. 10 μM of CPPs were mixed with siRNA to form CPP/siRNA complexes. 72 h. (a) Cell lysate was analyzed for the presence of EGFP using Western blot analysis. Primary antibodies are β tubulin and EGFP antibody. Data were normalized to β tubulin content in cells. n = 2. (b) Western blot data was converted quantitatively by ImageJ. *$p < 0.25$. Error bars represent standard deviation.

However, for Pep-c19/siRNA treated cells showed lower amount of EGFP protein in cells, and 28% reduction was seen than the control (Figure 7.4.2 (b)). This data demonstrated that Pep-c19/siRNA complex has more gene silencing effect than 11R/siRNA complex in cells.

7.5 Cytotoxicity of CPP/siRNA complex

The cytotoxicity of internalized CPP/siRNA complexes was analyzed in HEK 293-EGFP cells. HEK 293-EGFP cells were seeded on 24 well and 20- and 100-fold molar excess CPPs to 100 nM siRNA were preincubated for the formation of CPP/siRNA complex. CPP/siRNA complexes were added to the culture medium and incubated for 24 h and 72 h at 37 ℃ in 5% CO_2. Cells were thoroughly washed 3 times with PBS. Then 0.5 mg/ml MTT (3,(4,5-dimethylthiazol-2-yl)2,3-diphenyltetrazolium) was added to the media and incubated for 2 h. The formazan crystals that developed were solubilized with dimethyl sulfoxide (Sigma−Aldrich), and absorbance was measured at 560 nm using the ELISA reader. The viability of cells treated with 11R/siRNA complex for 24 h was reduced 89.0% and 84.6% for 20-fold and 100-fold molar excess CPPs to siRNAs, respectively (Figure 7.5(a)). For Pep-c19/siRNA complex, the viability of cells was reduced 96.2% and 88.9% for 20-fold and 100-fold molar excess CPPs to siRNAs, respectively. For 72 h incubation, the viability of cells treated with 11R/siRNA complex was reduced 88.6% and 77.5% for 20-fold and 100-fold molar excess CPPs to siRNAs, respectively (Figure 7.5(b)). For Pep-c19/siRNA complex, the viability of cells was reduced 82.9% and 80.8% for 20-fold and 100-fold molar excess CPPs to siRNAs, respectively. This

demonstrated that Pep-c19 and 11R have similar cytotoxicity in cells and more cytotoxicity was seen for longer period of incubation for 72 h than 24 h.

With regards to cell penetration, cell-penetrating mechanism of Pep-c19 is thought to be similar with 30Kc19 protein as mentioned previously, hence is expected to form a dimer at the cell membrane during penetration. When siRNA is mixed with Pep-c19, a non-covalent CPP/siRNA complex is formed prior to internalization. Thus, for Pep-c19/siRNA complex, it is thought to form a dimer with one another.

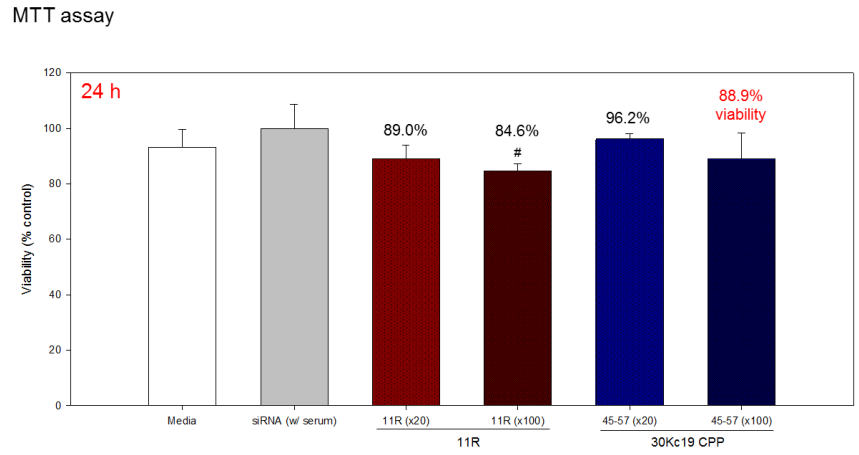

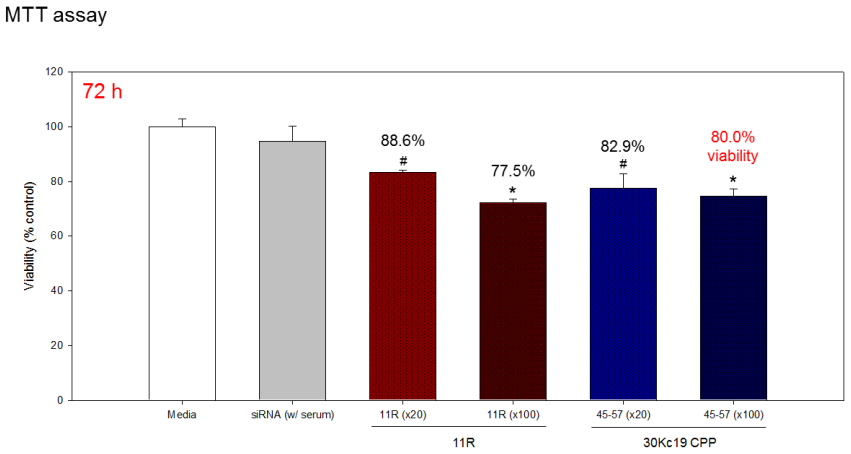

Figure 7.5 Cytotoxicity of non-covalent CPP-EGFP siRNAs delivered in HEK 293-EGFP cells. 100 nM siRNA. 2 and 10 μM of CPPs were mixed with siRNA to form CPP/siRNA complexes. (a) 24 h and (b) 72 h. Then 0.5 mg/ml MTT was added to the media. The formazan crystals that developed were solubilized with, and absorbance was measured at 560 nm using the ELISA reader. n = 3. (a) For 24 h, #$p < 0.05$ and the rest of the groups have $p < 0.5$. (b) For 72 h, #$p < 0.05$, *$p < 0.01$. Error bars represent standard deviation.

7.6 Conclusions

The newly identified CPP; VVNKLIRNNKMNC, from 30Kc19 protein was analyzed for its ability to penetrate and deliver cargo molecules *in vitro* by non-covalent method. When compared with the conjugated approach, the method itself is easier as mixing between the cargo and CPP is all that is needed prior to the addition to cell culture media. However, limitation lies in that cargo has to have negative charge for Pep-c19 to form a CPP/siRNA complex like other CPPs, such as 11R. Similar gene silencing effect was seen for Pep-c19 and 11R, and slight cytotoxicity was seen for both CPP/siRNA complexes when treated for longer period of time (72 h). The results strongly suggest that Pep-c19 has a great potential for the efficient delivery of siRNA *in vitro*, however, further study needs to be carried out for its applicability *in vivo*. Moreover, it would be interesting to perform conjugation approach, as to which method is more efficient in delivering siRNAs into cells.

Chapter 8.

Overall discussion and further suggestions

Chapter 8. Overall discussion and further suggestions

8.1 Overall discussion

Several studies have examined the functional properties for 30Kc6 and 30Kc19, and it was demonstrated that silkworm hemolymph and 30K proteins exhibit an anti-apoptotic effect in various cells by adding the protein to culture or medium by gene expression. 30K proteins also enhanced productions of recombinant erythropoietin, interferon-β, and monoclonal antibody, as well as increasing glycosylation, cell growth, and viability in various cells, and also had enzyme-stabilizing effects.

Due to many phenomenal effects of the 30K proteins, mass production of the proteins was desired and thus *E. coli* was selected as host for recombinant protein expression. However, difficulty lied for the 30Kc6 protein, an anti-apoptotic protein, because it was expressed as inclusion bodies. Generally, inclusion bodies are not sought because the misfolded proteins require refolding into bioactive forms, which are time-consuming and economically not viable. Hence, soluble forms of proteins are preferred over insoluble proteins. This is where the 30Kc19 comes in. Recently, the 30Kc19 protein has been studied in a great deal because it is expressed as soluble form in *E. coli*. Getting in hold of a large quantity of soluble recombinant 30Kc19 protein was definitely useful because it enabled researchers to perform numerous experiments on finding out the actual role and function of the protein.

This was the reason why the 30Kc19 protein was chosen as the raw material for research. During literature review, 30Kc19 protein, among the 30K proteins

(30Kc6, 30Kc12, 30Kc19, 30Kc21 and 30Kc23), was reported to be the most abundant among 30K proteins in the hemolymph of *Bombyx mori*. In the 5th instar larva to early pupa stage, these 30K proteins are synthesized in fat body cells and accumulate in the hemolymph. They are then transferred from the hemolymph to fat body cells during metamorphosis from larva to pupa, and are deposited there until later use. Then it came as a wonder why the 30Kc19 was vastly available in the silkworm hemolymph and why it was in the form of soluble protein. Only recently, the biological functions of the 30Kc19 protein started to unravel.

A recent study has shown that 30Kc19 protein has a cell-penetrating property when supplemented to the culture medium. In accordance with previous research, the 30Kc19 protein was found to be a very unique multi-functional protein. However, the exact mechanism of penetration to animal cells had not been fully determined and hence was necessary to understand the molecular mechanism of cell penetration for the practical use of the 30Kc19 protein. In parallel with the cell-penetrating property, dimerization propensity was seen for the 30Kc19 protein in the presence of sodium dodecyl sulfate (SDS). Native PAGE was carried out and showed that the 30Kc19 monomer formed a dimer when SDS or phospholipid was present. This dimerization phenomenon of the 30Kc19 protein in the presence of amphiphilic moieties; SDS or phospholipid, was key to explanation of the mechanism of entry. This led to perform GST pull-down assay, where supplementation of the 30Kc19 protein to mammalian cell culture medium showed dimerization and penetration; due to phospholipids at the cell membrane, the main components of the lipid bilayer. Through this

analysis, it was certain that the 30Kc19 protein formed dimer at phospholipid of the cell membrane and thus the 30Kc19 protein existed as dimer inside the cell. However, how the 30Kc19 protein homodimerizes during penetration was still unsure. A similar result was demonstrated with the peptide hormone resistin in which a disulfide-linked homodimer was converted to a monomer under reducing conditions and conversion of a single cysteine to alanine abolished the dimerization. Thus, mutagenesis was performed, and penetration was observed by 30Kc19 C76A and not 30Kc19 C57A, which meant Cys-57 is involved in dimerization of the 30Kc19 at the cell membrane during penetration.

Based on the cell-penetrating mechanism and cargo-delivering ability, hypothetical presence of cell-penetrating peptide (CPP) was assumed and strived for the identification of a CPP of the 30Kc19 protein, originating from the silkworm. First, N- and C-terminal truncated forms of 30Kc19 protein were expressed and purified. When cells were incubated with soluble form of N-terminal truncated 30Kc19 ($30Kc19_{1-120}$) at both 37 ℃ and 4 ℃, $30Kc19_{1-120}$ protein was found in the cell. This confirmed that CPP exist in the N-terminal of the 30Kc19 protein. However, for the practical use in delivery of cell-impermeable cargo molecules, the size of the truncated protein was still large. It was necessary to find a cell-penetrating domain, a minimal effective partial sequence of the parent cell-penetrating protein that can efficiently deliver cargo molecules into cells. A domain was selected as the most probable candidate from the result of helix motif, positive surface charge, hydrophobicity, and relative surface accessibility. The hydrophobic amino acid was thought to be an important factor because $Antp_{43-58}$ sequence (RQIKIWFQNRRMKWKK)

contains 6 hydrophobic amino (Ile, Ile, Trp, Phe, Met, Trp) acids in total. In addition, it was expected that cysteine may be an important factor because of previous report that it may be involved in the process of internalization via formation of dimer. Several CPP candidates were tested for cell-penetrating property and from this, a new CPP; VVNKLIRNNKMNC, from 30Kc19 protein (Pep-c19) was identified. It demonstrated that 30Kc19 exhibited a cell-penetrating property due to the presence of a cell-penetrating peptide at 45-57. On the other hand, other peptides; encompassing Val-41 and Ile-42 formed membrane-bound aggregates. The formation of aggregates could have risen from the hydrophobic amino acids in those peptides because of too many hydrophobic amino acids that allow stability and solubility in the culture medium.

Then, the mode of intracellular penetration was evaluated by the use of inhibitors of endocytosis to find out how the Pep-c19 penetrates into cells. Sucrose was treated to give cells a hyperosmolar condition, but no markedly difference in the penetration ability of the Pep-c19 was seen. This showed that Pep-c19 does not penetrate by clathrin-mediated endocytosis. However, when cytochalasin B or nystatin was treated to cells, slightly lowered cell-penetrating ability of the Pep-c19 was seen, which demonstrates that it penetrates cells by macropinocytosis and caveolin-mediated endocytosis.

Subsequently, Pep-c19 was compared with other CPPs. In terms of the primary structure, Pep-c19 CPP contains less positive amino acids (3 in the sequence) than other CPPs (TAT has 8, VP22 has 9, Antp; has 7). Instead, Pep-c19 has more hydrophobic acids (6 in the sequence) than the most of other

CPPs (TAT has 0, VP22 has 1, Antp has 6). With the secondary structure, Antp's homeodomain is comprised of 60 residues and it is consisted of 3 alpha-helices. Third alpha-helix is responsible for penetration (Antp), which is similar to our Pep-c19, because it is also from the third alpha helix of the 30Kc19 protein. HSV-1 protein has a size that is a little bigger than the 30Kc19 protein, 38 kDa, and VP22 is located at the very last 34 residues. These CPPs have been used to transduce proteins into cells and tissues and for some (Tat and Antp) even across blood brain barrier but efficiency various depending on the cargo that is attached to the CPPs. Whatever the differences are, among the CPPs, the major advantage of Pep-c19 is that it is not a virus-derived cell-penetrating peptide meaning it is applicable as a therapeutic tool, short length, and is not toxic.

In addition, efficiency and toxicity of this CPP was investigated in comparison with its original protein, 30Kc19, both *in vitro* and *in vivo* and showed its superiority over its parent protein in terms of efficiency. However, cargo was delivered in all the tissues except the brain, isolated from the mice that were injected with GFP-30Kc19 or GFP-Pep-c19, although the fluorescence intensities varied among tissues. No fluorescence was detected for all groups in the brain tissue, indicating the both the 30Kc19 and Pep-c19 are unable to penetrate and deliver cargos across the blood brain barrier (BBB). Toxicity of Pep-c19 was tested *in vivo*, and measured the toxicity parameters that represent toxicity in kidney and liver. Toxicity in kidney is shown by increase in the levels of blood urea nitrogen (BUN) and creatinine, whereas toxicity on liver is shown by increase in the levels of aspartate aminotransferase (ALT) and alanine aminotransferase (AST). Toxicity results showed that high

dose and long-term administration of Pep-c19 did not cause statistically significant or meaningful differences between 30Kc19 protein and Pep-c19 from all four toxicity parameter and demonstrated that Pep-c19 is non-toxic *in vivo*. Regarding the mechanism of entry for 30Kc19 and Pep-c19, it was found that Cys-57 plays a crucial role in the dimerization and penetration and because Cys-57 is the final jigsaw puzzle of the Pep-c19 sequence, the mode of penetration is expected to be similar for both cases.

Finally, the Pep-c19 was used for therapeutic application; non-covalent approach for the delivery of siRNA was tested. The results showed that Pep-c19 was able to deliver siRNAs and have gene silencing effect along with 11R, other widely recognized CPP. These results demonstrate that Pep-c19 can be applied for therapeutic applications. With regards to cell penetration, cell-penetrating mechanism of Pep-c19 is thought to be similar with 30Kc19 protein as mentioned previously, hence is expected to form a dimer at the cell membrane during penetration. When siRNA is mixed with Pep-c19, a non-covalent CPP/siRNA complex is formed prior to internalization. However, for Pep-c19/siRNA complex, it is thought to form a dimer with one another by Pep-c19.

The 30Kc19 protein and Pep-c19 are a non-virus derived (e.g. TAT) and non-cytotoxic (polyarginine) cell-penetrating protein/peptide. The protein transduction method is advantageous over virus-based method in that it does not cause tumorigenicity, because genetic modification of host cells does not occur and permanent expression can be solved. This study may open up new approaches and provide beneficial effects for the delivery of therapeutics in

bioindustries, such as pharma- and cosmeceuticals.

8.2 Conclusion and further suggestions

In this work, cell-penetrating mechanism was studied for the 30Kc19 protein when supplemented to the culture medium. In accordance with previous research, the 30Kc19 protein was found to be a very unique multi-functional protein. However, the exact mechanism of penetration to animal cells had not been fully determined and hence was necessary to understand the molecular mechanism of cell penetration for the practical use of the 30Kc19 protein. In parallel with the cell-penetrating property, dimerization propensity was seen for the 30Kc19 protein in the presence of amphiphilic moieties; SDS or phospholipid, which was the key to explanation of the mechanism of entry. Through further analysis, the results showed that the 30Kc19 protein formed dimer at phospholipid of the cell membrane and thus the 30Kc19 protein existed as dimer inside the cell. This was resolved by mutagenesis. Penetration was observed by 30Kc19 C76A and not 30Kc19 C57A, which meant Cys-57 is involved in dimerization of the 30Kc19 at the cell membrane during penetration.

Based on the cell-penetrating mechanism and cargo-delivering ability, hypothetical presence of cell-penetrating peptide (CPP) was assumed. Even for the practical use in delivery of cell-impermeable cargo molecules, the size of the whole protein was still large. Through multiple analyses, a minimal effective partial sequence of the parent cell-penetrating protein that can efficiently deliver cargo molecules into cells was found. A new CPP; VVNKLIRNNKMNC, from 30Kc19 protein (Pep-c19) was identified. It

demonstrated that 30Kc19 exhibited a cell-penetrating property due to the presence of a cell-penetrating peptide at 45-57.

Then, the mode of intracellular penetration was evaluated. Sucrose was treated to give cells a hyperosmolar condition, but no markedly difference in the penetration ability of the Pep-c19 was seen. This showed that Pep-c19 does not penetrate by clathrin-mediated endocytosis. However, when cytochalasin B or nystatin was treated to cells, slightly lowered cell-penetrating ability of the Pep-c19 was seen, which demonstrates that it penetrates cells by macropinocytosis and caveolin-mediated endocytosis.

The efficiency and toxicity of this CPP was investigated in comparison with its original protein, 30Kc19, both *in vitro* and *in vivo* and showed its superiority over its parent protein in terms of efficiency. However, cargo was delivered in all the tissues except the brain, isolated from the mice that were injected with GFP-30Kc19 or GFP-Pep-c19, although the fluorescence intensities varied among tissues. No fluorescence was detected for all groups in the brain tissue, indicating the both the 30Kc19 and Pep-c19 are unable to penetrate and deliver cargos across the blood brain barrier (BBB). Toxicity of Pep-c19 was tested in vivo, and measured the toxicity parameters that represent toxicity in kidney and liver and showed that high dose and long-term administration of Pep-c19 did not cause statistically significant or meaningful differences between 30Kc19 protein and Pep-c19 from all four toxicity parameter and demonstrated that Pep-c19 is non-toxic *in vivo*.

The Pep-c19 was used for therapeutic application; non-covalent approach for the delivery of siRNA. The results showed that Pep-c19 was able to deliver

siRNAs and have gene silencing effect along with 11R, other widely recognized CPP. The protein transduction method is advantageous over virus-based method in that it does not cause tumorigenicity, because genetic modification of host cells does not occur and permanent expression of reprogramming factors can be solved.

In terms of the primary structure, when Pep-c19 is compared with other CPPs, it contains less positive amino acids (3 in the sequence) than other CPPs (TAT has 8, VP22 has 9, Antp; has 7). Instead, Pep-c19 has more hydrophobic acids (6 in the sequence) than the most of other CPPs (TAT has 0, VP22 has 1, Antp has 6). With the secondary structure, Antp's homeodomain is comprised of 60 residues and it is consisted of 3 alpha-helices. Third alpha-helix is responsible for penetration (Antp), which is similar to our Pep-c19, because it is also from the third alpha helix of the 30Kc19 protein. These CPPs have been used to transduce proteins into cells and tissues and for some (Tat and Antp) even across blood brain barrier but not Pep-c19. Whatever the differences are, among the CPPs, the major advantage of Pep-c19 is that it is not a virus-derived cell-penetrating peptide meaning it is applicable as a therapeutic tool, short length, and is not toxic. Unlike other CPPs, Pep-c19 cannot go across the BBB, hence can be applicable for delivery of cargos into other parts of the organs and not the brain.

30Kc19 protein, among the 30K proteins (30Kc6, 30Kc12, 30Kc19, 30Kc21 and 30Kc23), was reported to be the most abundant among 30K proteins in the hemolymph of *Bombyx mori*. In the 5th instar larva to early pupa stage, these 30K proteins are synthesized in fat body cells and accumulate in the

hemolymph. They are then transferred from the hemolymph to fat body cells during metamorphosis from larva to pupa, and are deposited there until later use. It came as a wonder why the 30Kc19 was vastly available in the silkworm hemolymph and why it was in the form of soluble protein. Moreover, the cell-penetrating property and enzyme-stabilizing properties have now come to be important in the development of silkworm. With the start of metamorphosis from larvae to pupae, 30K proteins are translocated from the hemolymph to fat body cells, which was recently unraveled. Only recently, the biological functions of the 30Kc19 protein started to unravel. Metamorphosis is a very intense process which is achieved in a very short period of time and thus a high number of enzymatic reactions occur simultaneously at once. Therefore, it is believed that cell-penetrating peptide within the 30Kc19 protein enables quick and steady penetration, and the enzyme-stabilizing property of the 30K19 enables and maintains steady metabolism during the metamorphosis.

The 30Kc19 protein and Pep-c19 are a non-virus derived (e.g. TAT) and non-cytotoxic (polyarginine) cell-penetrating protein/peptide that is naturally found in nature. That may be the reason why cytotoxicity was not observed. From the identification Pep-c19, peptide engineering can be performed in relationship with other CPPs and further optimized Pep-c19 in terms of cell-penetrating and cargo-delivery efficiencies can be anticipated. In all, this study may open up new approaches and provide beneficial effects for the delivery of therapeutics in bioindustries, such as pharma- and cosmeceuticals.

Bibliography

[1] Izumi S, Fujie J, Yamada S, Tomino S. Molecular properties and biosynthesis of major plasma proteins in *Bombyx mori*. Biochimica et Biophysica Acta (BBA)-Protein Structure. 1981;670:222-9.

[2] Mori S, Izumi S, Tomino S. Structures and organization of major plasma protein genes of the silkworm *Bombyx mori*. Journal of Molecular Biology. 1991;218:7-12.

[3] Bosquet G, Guillet C, Calvez B, Chavancy G. The regulation of major haemolymph protein synthesis: Changes in mRNA content during the development of *Bombyx mori* larvae. Insect Biochemistry. 1989;19:29-39.

[4] Mori S, Izumi S, Tomino S. Complete nucleotide sequences of major plasma protein genes of *Bombyx mori*. Biochimica et Biophysica Acta (BBA)-Gene Structure and Expression. 1991;1090:129-32.

[5] Mine E, Izumi S, Katsuki M, Tomino S. Developmental and sex-dependent regulation of storage protein synthesis in the silkworm, *Bombyx mori*. Developmental Biology. 1983;97:329-37.

[6] Zhong BX, Li JK, Lin JR, Liang JS, Su SK, Xu HS, Yan HY, Zhang PB, Fujii H. Possible effect of 30K proteins in embryonic development of silkworm *Bombyx mori*. Acta Biochimica et Biophysica Sinica. 2005;37:355-61.

[7] Ogawa N, Kishimoto A, Asano T, Izumi S. The homeodomain protein PBX participates in JH-related suppressive regulation on the expression of major plasma protein genes in the silkworm, *Bombyx mori*. Insect Biochemistry and Molecular Biology. 2005;35:217-29.

[8] Rhee WJ, Kim EJ, Park TH. Kinetic effect of silkworm hemolymph on the delayed host cell death in an insect cell-baculovirus system. Biotechnology Progress. 1999;15:1028-32.

[9] Rhee WJ, Park TH. Silkworm hemolymph inhibits baculovirus-induced insect cell apoptosis. Biochemical and Biophysical Research Communications. 2000;271:186-90.

[10] Kim EJ, Rhee WJ, Park TH. Isolation and characterization of an apoptosis-inhibiting component from the hemolymph of *Bombyx mori*. Biochemical and Biophysical Research Communications. 2001;285:224-8.

[11] Choi SS, Rhee WJ, Park TH. Inhibition of human cell apoptosis by silkworm hemolymph. Biotechnology Progress. 2002;18:874-8.

[12] Rhee WJ, Kim EJ, Park TH. Silkworm hemolymph as a potent inhibitor of apoptosis in Sf9 cells. Biochemical and Biophysical Research Communications. 2002;295:779-83.

[13] Kim EJ, Park HJ, Park TH. Inhibition of apoptosis by recombinant 30K protein originating from silkworm hemolymph. Biochemical and Biophysical Research Communications. 2003;308:523-8.

[14] Kim EJ, Park TH. Anti-apoptosis engineering. Biotechnology and Bioprocess Engineering. 2003;8:76-82.

[15] Park HJ, Kim EJ, Koo TY, Park TH. Purification of recombinant 30K protein produced in *Escherichia coli* and its anti-apoptotic effect in mammalian and insect cell systems. Enzyme and Microbial Technology. 2003;33:466-71.

[16] Kim EJ, Rhee WJ, Park TH. Inhibition of apoptosis by a *Bombyx mori* gene. Biotechnology Progress. 2004;20:324-9.

[17] Choi SS, Rhee WJ, Kim EJ, Park TH. Enhancement of recombinant protein production in Chinese hamster ovary cells through anti-apoptosis engineering using *30Kc6* gene. Biotechnology and Bioengineering. 2006;95:459-67.

[18] Park JH, Park HH, Park TH. Cellular engineering for the high-level production of recombinant proteins in mammalian cell systems. Korean Journal of Chemical Engineering. 2010;27:1042-8.

[19] Wang Z, Ma X, Fan L, Rhee WJ, Park TH, Zhao L, Tan W-S. Understanding the mechanistic roles of *30Kc6* gene in apoptosis and specific productivity in antibody-producing Chinese hamster ovary cells. Applied Microbiology and Biotechnology. 2012;94:1243-53.

[20] Wang Z, Ma X, Zhao L, Fan L, Tan W-S. Expression of anti-apoptotic *30Kc6* gene inhibiting hyperosmotic pressure-induced apoptosis in antibody-producing Chinese hamster ovary cells. Process Biochemistry. 2012;47:735-41.

[21] Ha SH, Park TH, Kim S-E. Silkworm hemolymph as a substitute for fetal bovine serum in insect cell culture. Biotechnology Techniques. 1996;10:401-6.

[22] Ha S, Park T. Efficient production of recombinant protein in *Spodoptera frugiperda*/AcNPV system utilizing silkworm hemolymph. Biotechnology Letters. 1997;19:1087-91.

[23] Choi SS, Park TH. Enhancement of sialyltransferase-catalyzed transfer of sialic acid onto glycoprotein oligosaccharides using silkworm hemolymph and its 30K protein. Journal of Molecular Catalysis B: Enzymatic. 2006;43:128-32.

[24] Koo TY, Park JH, Park HH, Park TH. Beneficial effect of *30Kc6* gene expression on production of recombinant interferon-β in serum-free suspension culture of CHO cells. Process Biochemistry. 2009;44:146-53.

[25] Wang Z, Park JH, Park HH, Tan W, Park TH. Enhancement of therapeutic monoclonal antibody production in CHO cells using *30Kc6* gene. Process Biochemistry. 2010;45:1852-6.

[26] Wang Z, Park JH, Park HH, Tan W, Park TH. Enhancement of recombinant human EPO production and sialylation in Chinese hamster ovary cells through *Bombyx mori 30Kc19* gene expression. Biotechnology and Bioengineering. 2011;108:1634-42.

[27] Park JH, Park HH, Choi SS, Park TH. Stabilization of enzymes by the recombinant 30Kc19 protein. Process Biochemistry. 2012;47:164-9.

[28] Park JH, Wang Z, Jeong H-J, Park HH, Kim B-G, Tan W-S, Choi SS, Park TH. Enhancement of recombinant human EPO production and glycosylation in serum-free suspension culture of CHO cells through expression and supplementation of 30Kc19. Applied Microbiology and Biotechnology. 2012;96:671-83.

[29] Choi SS, Rhee WJ, Park TH. Beneficial effect of silkworm hemolymph on a CHO cell system: Inhibition of apoptosis and increase of EPO production. Biotechnology and Bioengineering. 2005;91:793-800.

[30] Robbins PD, Ghivizzani SC. Viral vectors for gene therapy. Pharmacology & Therapeutics. 1998;80:35-47.

[31] Straubinger RM, Düzgünes N, Papahadjopoulos D. pH-sensitive liposomes mediate cytoplasmic delivery of encapsulated macromolecules. FEBS Letters. 1985;179:148-54.

[32] Arnheiter H, Haller O. Antiviral state against influenza virus neutralized by microinjection of antibodies to interferon-induced Mx proteins. The EMBO Journal. 1988;7:1315.

[33] Chakrabarti R, Wylie DE, Schuster SM. Transfer of monoclonal antibodies into mammalian cells by electroporation. Journal of Biological Chemistry. 1989;264:15494-500.

[34] El-Andaloussi S, Holm T, Langel U. Cell-penetrating peptides:

mechanisms and applications. Current Pharmaceutical Design. 2005;11:3597-611.

[35] Zorko M, Langel Ü. Cell-penetrating peptides: mechanism and kinetics of cargo delivery. Advanced Drug Delivery Reviews. 2005;57:529-45.

[36] Frankel AD, Pabo CO. Cellular uptake of the tat protein from human immunodeficiency virus. Cell. 1988;55:1189-93.

[37] Green M, Loewenstein PM. Autonomous functional domains of chemically synthesized human immunodeficiency virus tat *trans*-activator protein. Cell. 1988;55:1179-88.

[38] Mann DA, Frankel AD. Endocytosis and targeting of exogenous HIV-1 Tat protein. The EMBO Journal. 1991;10:1733.

[39] Perez F, Joliot A, Bloch-Gallego E, Zahraoui A, Triller A, Prochiantz A. Antennapedia homeobox as a signal for the cellular internalization and nuclear addressing of a small exogenous peptide. Journal of Cell Science. 1992;102:717-22.

[40] Derossi D, Joliot AH, Chassaing G, Prochiantz A. The third helix of the Antennapedia homeodomain translocates through biological membranes. Journal of Biological Chemistry. 1994;269:10444-50.

[41] Elliott G, O'Hare P. Intercellular trafficking and protein delivery by a herpesvirus structural protein. Cell. 1997;88:223-33.

[42] Phelan A, Elliott G, O'Hare P. Intercellular delivery of functional p53 by the herpesvirus protein VP22. Nature Biotechnology. 1998;16:440-3.

[43] Eiríksdóttir E, Myrberg H, Hansen M, Langel U. Cellular uptake of cell-penetrating peptides. Drug Design Reviews-Online. 2004;1:161-73.

[44] Schmidt MC, Rothen-Rutishauser B, Rist B, Beck-Sickinger A, Wunderli-Allenspach H, Rubas W, Sadée W, Merkle HP. Translocation of human calcitonin in respiratory nasal epithelium is associated with self-assembly in lipid membrane. Biochemistry. 1998;37:16582-90.

[45] Mitchell D, Steinman L, Kim D, Fathman C, Rothbard J. Polyarginine enters cells more efficiently than other polycationic homopolymers. The Journal of Peptide Research. 2000;56:318-25.

[46] Rothbard JB, Garlington S, Lin Q, Kirschberg T, Kreider E, McGrane PL, Wender PA, Khavari PA. Conjugation of arginine oligomers to cyclosporin A facilitates topical delivery and inhibition of inflammation. Nature Medicine. 2000;6:1253-7.

[47] Zhou X, Klibanov AL, Huang L. Lipophilic polylysines mediate

efficient DNA transfection in mammalian cells. Biochimica et Biophysica Acta (BBA)-Biomembranes. 1991;1065:8-14.

[48] Ramsay E, Hadgraft J, Birchall J, Gumbleton M. Examination of the biophysical interaction between plasmid DNA and the polycations, polylysine and polyornithine, as a basis for their differential gene transfection in-vitro. International Journal of Pharmaceutics. 2000;210:97-107.

[49] Oehlke J, Scheller A, Wiesner B, Krause E, Beyermann M, Klauschenz E, Melzig M, Bienert M. Cellular uptake of an α-helical amphipathic model peptide with the potential to deliver polar compounds into the cell interior non-endocytically. Biochimica et Biophysica Acta (BBA)-Biomembranes. 1998;1414:127-39.

[50] Pooga M, Hällbrink M, Zorko M. Cell penetration by transportan. The FASEB Journal. 1998;12:67-77.

[51] Vives E, Brodin P, Lebleu B. A truncated HIV-1 Tat protein basic domain rapidly translocates through the plasma membrane and accumulates in the cell nucleus. Journal of Biological Chemistry. 1997;272:16010-7.

[52] Soomets U, Lindgren M, Gallet X, Hällbrink M, Elmquist A, Balaspiri L, Zorko M, Pooga M, Brasseur R, Langel Ü. Deletion analogues of transportan. Biochimica et Biophysica Acta (BBA)-Biomembranes. 2000;1467:165-76.

[53] Drin G, Mazel M, Clair P, Mathieu D, Kaczorek M, Temsamani J. Physico-chemical requirements for cellular uptake of pAntp peptide. European Journal of Biochemistry. 2001;268:1304-14.

[54] Elmquist A, Lindgren M, Bartfai T, Langel Ü. VE-cadherin-derived cell-penetrating peptide, p VEC, with carrier functions. Experimental Cell Research. 2001;269:237-44.

[55] Kilk K, Magzoub M, Pooga M, Eriksson LG, Langel Ü, Gräslund A. Cellular internalization of a cargo complex with a novel peptide derived from the third helix of the islet-1 homeodomain. Comparison with the penetratin peptide. Bioconjugate Chemistry. 2001;12:911-6.

[56] Pooga M, Kut C, Kihlmark M, Hällbrink M, Fernaeus S, Raid R, Land T, Hallberg E, Bartfai T, Langel Ü. Cellular translocation of proteins by transportan. The FASEB Journal. 2001;15:1451-3.

[57] Suzuki T, Futaki S, Niwa M, Tanaka S, Ueda K, Sugiura Y. Possible existence of common internalization mechanisms among arginine-rich

peptides. Journal of Biological Chemistry. 2002;277:2437-43.

[58] Violini S, Sharma V, Prior JL, Dyszlewski M, Piwnica-Worms D. Evidence for a plasma membrane-mediated permeability barrier to Tat basic domain in well-differentiated epithelial cells: lack of correlation with heparan sulfate. Biochemistry. 2002;41:12652-61.

[59] Elmquist A, Langel Ü. In vitro uptake and stability study of pVEC and its all-D analog. Biological Chemistry. 2003;384:387-93.

[60] Richard JP, Melikov K, Vives E, Ramos C, Verbeure B, Gait MJ, Chernomordik LV, Lebleu B. Cell-penetrating peptides A reevaluation of the mechanism of cellular uptake. Journal of Biological Chemistry. 2003;278:585-90.

[61] Thorén PE, Persson D, Isakson P, Goksör M, Ö nfelt A, Nordén B. Uptake of analogs of penetratin, Tat (48–60) and oligoarginine in live cells. Biochemical and Biophysical Research Communications. 2003;307:100-7.

[62] Lindgren M, Hallbrink M, Elmquist A, Langel U. Passage of cell-penetrating peptides across a human epithelial cell layer in vitro. Biochemical Journal. 2004;377:69-76.

[63] Leifert JA, Whitton JL. "Translocatory proteins" and "protein transduction domains": a critical analysis of their biological effects and the underlying mechanisms. Molecular Therapy. 2003;8:13-20.

[64] Vives E, Rispal C, Lebleu B. TAT peptide internalization: seeking the mechanism of entry. Current Protein and Peptide Science. 2003;4:125-32.

[65] Drin G, Cottin S, Blanc E, Rees AR, Temsamani J. Studies on the internalization mechanism of cationic cell-penetrating peptides. Journal of Biological Chemistry. 2003;278:31192-201.

[66] Krämer S, Wunderli-Allenspach H. No entry for TAT (44–57) into liposomes and intact MDCK cells: novel approach to study membrane permeation of cell-penetrating peptides. Biochimica et Biophysica Acta (BBA)-Biomembranes. 2003;1609:161-9.

[67] Morris M, Vidal P, Chaloin L, Heitz F, Divita G. A new peptide vector for efficient delivery of oligonucleotides into mammalian cells. Nucleic Acids Research. 1997;25:2730-6.

[68] Wadia JS, Stan RV, Dowdy SF. Transducible TAT-HA fusogenic peptide enhances escape of TAT-fusion proteins after lipid raft macropinocytosis. Nature Medicine. 2004;10:310-5.

[69] Kaplan IM, Wadia JS, Dowdy SF. Cationic TAT peptide transduction domain enters cells by macropinocytosis. Journal of Controlled Release. 2005;102:247-53.

[70] Lindberg M, Jarvet J, Langel Ü, Gräslund A. Secondary structure and position of the cell-penetrating peptide transportan in SDS micelles as determined by NMR. Biochemistry. 2001;40:3141-9.

[71] Gazit E, Lee W-J, Brey PT, Shai Y. Mode of action of the antibacterial cecropin B2: a spectrofluorometric study. Biochemistry. 1994;33:10681-92.

[72] Zemel A, Fattal DR, Ben-Shaul A. Energetics and self-assembly of amphipathic peptide pores in lipid membranes. Biophysical Journal. 2003;84:2242-55.

[73] Ziegler A. Thermodynamic studies and binding mechanisms of cell-penetrating peptides with lipids and glycosaminoglycans. Advanced Drug Delivery Reviews. 2008;60:580-97.

[74] Fittipaldi A, Ferrari A, Zoppé M, Arcangeli C, Pellegrini V, Beltram F, Giacca M. Cell membrane lipid rafts mediate caveolar endocytosis of HIV-1 Tat fusion proteins. Journal of Biological Chemistry. 2003;278:34141-9.

[75] El-Andaloussi S, Johansson HJ, Lundberg P, Langel Ü. Induction of splice correction by cell-penetrating peptide nucleic acids. The Journal of Gene Medicine. 2006;8:1262-73.

[76] Nakase I, Niwa M, Takeuchi T, Sonomura K, Kawabata N, Koike Y, Takehashi M, Tanaka S, Ueda K, Simpson JC. Cellular uptake of arginine-rich peptides: roles for macropinocytosis and actin rearrangement. Molecular Therapy. 2004;10:1011-22.

[77] Magzoub M, Sandgren S, Lundberg P, Oglęcka K, Lilja J, Wittrup A, Göran Eriksson L, Langel Ü, Belting M, Gräslund A. N-terminal peptides from unprocessed prion proteins enter cells by macropinocytosis. Biochemical and Biophysical Research Communications. 2006;348:379-85.

[78] Takeuchi T, Kosuge M, Tadokoro A, Sugiura Y, Nishi M, Kawata M, Sakai N, Matile S, Futaki S. Direct and rapid cytosolic delivery using cell-penetrating peptides mediated by pyrenebutyrate. ACS Chemical Biology. 2006;1:299-303.

[79] Liu BR, Huang Y-w, Winiarz JG, Chiang H-J, Lee H-J. Intracellular delivery of quantum dots mediated by a histidine-and arginine-rich

HR9 cell-penetrating peptide through the direct membrane translocation mechanism. Biomaterials. 2011;32:3520-37.

[80] Berlose JP, Convert O, Derossi D, Brunissen A, Chassaing G. Conformational and associative behaviours of the third helix of antennapedia homeodomain in membrane-mimetic environments. European Journal of Biochemistry. 1996;242:372-86.

[81] Derossi D, Calvet S, Trembleau A, Brunissen A, Chassaing G, Prochiantz A. Cell internalization of the third helix of the Antennapedia homeodomain is receptor-independent. Journal of Biological Chemistry. 1996;271:18188-93.

[82] Kawamoto S, Takasu M, Miyakawa T, Morikawa R, Oda T, Futaki S, Nagao H. Inverted micelle formation of cell-penetrating peptide studied by coarse-grained simulation: Importance of attractive force between cell-penetrating peptides and lipid head group. The Journal of Chemical Physics. 2011;134:095103.

[83] Scheller A, Oehlke J, Wiesner B, Dathe M, Krause E, Beyermann M, Melzig M, Bienert M. Structural requirements for cellular uptake of α-helical amphipathic peptides. Journal of Peptide Science. 1999;5:185-94.

[84] Chellaiah MA, Soga N, Swanson S, McAllister S, Alvarez U, Wang D, Dowdy SF, Hruska KA. Rho-A is critical for osteoclast podosome organization, motility, and bone resorption. Journal of Biological Chemistry. 2000;275:11993-2002.

[85] Perez JL, De Oña M, Niubo J, Villar H, Melon S, Garcia A, Martin R. Comparison of several fixation methods for cytomegalovirus antigenemia assay. Journal of Clinical Microbiology. 1995;33:1646-9.

[86] DiDonato D, Brasaemle DL. Fixation methods for the study of lipid droplets by immunofluorescence microscopy. Journal of Histochemistry and Cytochemistry. 2003;51:773-80.

[87] Sebbage V. Cell-penetrating peptides and their therapeutic applications. Bioscience Horizons. 2009;2:64-72.

[88] Pietersz GA, Li W, Apostolopoulos V. A 16-mer peptide (RQIKIWFQNRRMKWKK) from antennapedia preferentially targets the Class I pathway. Vaccine. 2001;19:1397-405.

[89] Pooga M, Soomets U, Hallbrink M, Valkna A, Saar K, Rezaei K, Kahl U, Jing-Xia Hao X-JX. Cell penetrating PNA constructs regulate galanin receptor levels and modify pain. Nature Biotechnology.

1998;16.

[90] Bolton SJ, Jones DN, Darker JG, Eggleston DS, Hunter AJ, Walsh FS. Cellular uptake and spread of the cell-permeable peptide penetratin in adult rat brain. European Journal of Neuroscience. 2000;12:2847-55.

[91] Rousselle C, Clair P, Lefauconnier J-M, Kaczorek M, Scherrmann J-M, Temsamani J. New advances in the transport of doxorubicin through the blood-brain barrier by a peptide vector-mediated strategy. Molecular Pharmacology. 2000;57:679-86.

[92] Schwarze SR, Ho A, Vocero-Akbani A, Dowdy SF. In vivo protein transduction: delivery of a biologically active protein into the mouse. Science. 1999;285:1569-72.

[93] Lin Y-Z, Yao S, Veach RA, Torgerson TR, Hawiger J. Inhibition of nuclear translocation of transcription factor NF-κB by a synthetic peptide containing a cell membrane-permeable motif and nuclear localization sequence. Journal of Biological Chemistry. 1995;270:14255-8.

[94] Lin Y-Z, Yao S, Hawiger J. Role of the nuclear localization sequence in fibroblast growth factor-1-stimulated mitogenic pathways. Journal of Biological Chemistry. 1996;271:5305-8.

[95] Rojas M, Donahue JP, Tan Z, Lin Y-Z. Genetic engineering of proteins with cell membrane permeability. Nature Biotechnology. 1998;16:370-5.

[96] Mäe M, Langel Ü. Cell-penetrating peptides as vectors for peptide, protein and oligonucleotide delivery. Current Opinion in Pharmacology. 2006;6:509-14.

[97] Fawell S, Seery J, Daikh Y, Moore C, Chen LL, Pepinsky B, Barsoum J. Tat-mediated delivery of heterologous proteins into cells. Proceedings of the National Academy of Sciences of the United States of America. 1994;91:664-8.

[98] Zender L, Kühnel F, Köck R, Manns M, Kubicka S. VP22-mediated intercellular transport of p53 in hepatoma cells in vitro and in vivo. Cancer Gene Therapy. 2002;9:489-96.

[99] Do Kwon Y, Oh SK, Kim HS, Ku S-Y, Kim SH, Choi YM, Moon SY. Cellular manipulation of human embryonic stem cells by TAT-PDX1 protein transduction. Molecular Therapy. 2005;12:28-32.

[100] Myrberg H, Lindgren M, Langel Ü. Protein delivery by the cell-penetrating peptide YTA2. Bioconjugate Chemistry. 2007;18:170-4.

[101] Gupta B, Levchenko TS, Torchilin VP. Intracellular delivery of large molecules and small particles by cell-penetrating proteins and peptides. Advanced Drug Delivery Reviews. 2005;57:637-51.

[102] Veldhoen S, Laufer SD, Trampe A, Restle T. Cellular delivery of small interfering RNA by a non-covalently attached cell-penetrating peptide: quantitative analysis of uptake and biological effect. Nucleic Acids Research. 2006;34:6561-73.

[103] Chiu Y-L, Ali A, Chu C-y, Cao H, Rana TM. Visualizing a correlation between siRNA localization, cellular uptake, and RNAi in living cells. Chemistry & Biology. 2004;11:1165-75.

[104] Eguchi A, Meade BR, Chang Y-C, Fredrickson CT, Willert K, Puri N, Dowdy SF. Efficient siRNA delivery into primary cells by a peptide transduction domain–dsRNA binding domain fusion protein. Nature Biotechnology. 2009;27:567-71.

[105] Choi Y-S, Lee JY, Suh JS, Kwon Y-M, Lee S-J, Chung J-K, Lee D-S, Yang VC, Chung C-P, Park Y-J. The systemic delivery of siRNAs by a cell penetrating peptide, low molecular weight protamine. Biomaterials. 2010;31:1429-43.

[106] Anderson D, Nichols E, Manger R, Woodle D, Barry M, Fritzberg A. Tumor cell retention of antibody Fab fragments is enhanced by an attached HIV TAT protein-derived peptide. Biochemical and Biophysical Research Communications. 1993;194:876-84.

[107] Hu M, Chen P, Wang J, Scollard DA, Vallis KA, Reilly RM. 123I-labeled HIV-1 tat peptide radioimmunoconjugates are imported into the nucleus of human breast cancer cells and functionally interact in vitro and in vivo with the cyclin-dependent kinase inhibitor, p21WAF-1/Cip-1. European Journal of Nuclear Medicine and Molecular Imaging. 2007;34:368-77.

[108] Lewin M, Carlesso N, Tung C-H, Tang X-W, Cory D, Scadden DT, Weissleder R. Tat peptide-derivatized magnetic nanoparticles allow in vivo tracking and recovery of progenitor cells. Nature Biotechnology. 2000;18:410-4.

[109] Derfus AM, Chan WC, Bhatia SN. Intracellular delivery of quantum dots for live cell labeling and organelle tracking. Advanced Materials. 2004;16:961-6.

[110] Santra S, Yang H, Dutta D, Stanley JT, Holloway PH, Tan W, Moudgil BM, Mericle RA. TAT conjugated, FITC doped silica nanoparticles for bioimaging applications. Chemical Communications. 2004:2810-1.

[111] Zhang K, Fang H, Chen Z, Taylor J-SA, Wooley KL. Shape effects of nanoparticles conjugated with cell-penetrating peptides (HIV Tat PTD) on CHO cell uptake. Bioconjugate Chemistry. 2008;19:1880-7.

[112] Nagahara H, Vocero-Akbani AM, Snyder EL, Ho A, Latham DG, Lissy NA, Becker-Hapak M, Ezhevsky SA, Dowdy SF. Transduction of full-length TAT fusion proteins into mammalian cells: TAT-p27Kip1 induces cell migration. Nature Medicine. 1998;4:1449-52.

[113] Ganz T, Lehrer RI. Antimicrobial peptides of vertebrates. Current Opinion in Immunology. 1998;10:41-4.

[114] Simmaco M, Mignogna G, Barra D. Antimicrobial peptides from amphibian skin: what do they tell us? Peptide Science. 1998;47:435-50.

[115] Walum E, Peterson A, Erkell L. Photometric recording of cell viability using trypan blue in perfused cell cultures. Xenobiotica. 1985;15:701-4.

[116] Mosmann T. Rapid colorimetric assay for cellular growth and survival: application to proliferation and cytotoxicity assays. Journal of Immunological Methods. 1983;65:55-63.

[117] Hällbrink M, Floren A, Elmquist A, Pooga M, Bartfai T, Langel Ü. Quantification of cellular uptake and comparison of some cell penetrating peptides. Biochimica et Biophysica Acta. 2001;1515:101.

[118] Joliot A, Triller A, Volovitch M, Pernelle C, Prochiantz A. alpha-2, 8-Polysialic acid is the neuronal surface receptor of antennapedia homeobox peptide. The New Biologist. 1991;3:1121-34.

[119] Prochiantz A. Messenger proteins: homeoproteins, TAT and others. Current Opinion in Cell Biology. 2000;12:400-6.

[120] Park I-W, Ullrich CK, Schoenberger E, Ganju RK, Groopman JE. HIV-1 Tat induces microvascular endothelial apoptosis through caspase activation. The Journal of Immunology. 2001;167:2766-71.

[121] Ramirez SH, Sanchez JF, Dimitri CA, Gelbard HA, Dewhurst S, Maggirwar SB. Neurotrophins prevent HIV Tat-induced neuronal apoptosis via a nuclear factor-κB (NF-κB)-dependent mechanism. Journal of Neurochemistry. 2001;78:874-89.

[122] Ensoli B, Barillari G, Salahuddin SZ, Gallo RC, Wong-Staal F. Tat protein of HIV-1 stimulates growth of cells derived from Kaposi's sarcoma lesions of AIDS patients. Nature. 1990;345:84-6.

[123] Jia H, Lohr M, Jezequel S, Davis D, Shaikh S, Selwood D, Zachary I. Cysteine-rich and basic domain HIV-1 Tat peptides inhibit angiogenesis and induce endothelial cell apoptosis. Biochemical and Biophysical

Research Communications. 2001;283:469-79.

[124] Gavin JR, Roth J, Jen P, Freychet P. Insulin receptors in human circulating cells and fibroblasts. Proceedings of the National Academy of Sciences of the United States of America. 1972;69:747-51.

[125] Lorenz D, Wiesner B, Zipper J, Winkler A, Krause E, Beyermann M, Lindau M, Bienert M. Mechanism of peptide-induced mast cell degranulation translocation and patch-clamp studies. The Journal of General Physiology. 1998;112:577-91.

[126] Lum BL, Gosland MP, Kaubisch S, Sikic BI. Molecular targets in oncology: implications of the multidrug resistance gene. Pharmacotherapy: The Journal of Human Pharmacology and Drug Therapy. 1993;13:88-109.

[127] Hawiger J. Cellular import of functional peptides to block intracellular signaling. Current Opinion in Immunology. 1997;9:189-94.

[128] Mahat R, Monera O, Smith L, Rolland A. Peptide-based gene delivery. Current Opinion in Molecular Therapeutics. 1999;1:226-43.

[129] White SH, Wimley WC. Membrane protein folding and stability: physical principles. Annual Review of Biophysics and Biomolecular Structure. 1999;28:319-65.

[130] Wender PA, Mitchell DJ, Pattabiraman K, Pelkey ET, Steinman L, Rothbard JB. The design, synthesis, and evaluation of molecules that enable or enhance cellular uptake: peptoid molecular transporters. Proceedings of the National Academy of Sciences of the United States of America. 2000;97:13003-8.

[131] Bremner K, Seymour L, Pouton C. Harnessing nuclear localization pathways for transgene delivery. Current Opinion in Molecular Therapeutics. 2001;3:170-7.

[132] Fraile-Ramos A, Kledal TN, Pelchen-Matthews A, Bowers K, Schwartz TW, Marsh M. The human cytomegalovirus US28 protein is located in endocytic vesicles and undergoes constitutive endocytosis and recycling. Molecular Biology of the Cell. 2001;12:1737-49.

[133] Lango MN, Shin DM, Grandis JR. Targeting growth factor receptors: integration of novel therapeutics in the management of head and neck cancer. Current Opinion in Oncology. 2001;13:168-75.

[134] Josephson L, Tung C-H, Moore A, Weissleder R. High-efficiency intracellular magnetic labeling with novel superparamagnetic-Tat peptide conjugates. Bioconjugate Chemistry. 1999;10:186-91.

[135] Eguchi A, Akuta T, Okuyama H, Senda T, Yokoi H, Inokuchi H, Fujita S, Hayakawa T, Takeda K, Hasegawa M. Protein transduction domain of HIV-1 Tat protein promotes efficient delivery of DNA into mammalian cells. Journal of Biological Chemistry. 2001;276:26204-10.

[136] Kaufman CL, Williams M, Ryle LM, Smith TL, Tanner M, Ho C. Superparamagnetic iron oxide particles transactivator protein-fluorescein isothiocyanate particle labeling for in vivo magnetic resonance imaging detection of cell migration: uptake and durability. Transplantation. 2003;76:1043-6.

[137] Polyakov V, Sharma V, Dahlheimer JL, Pica CM, Luker GD, Piwnica-Worms D. Novel Tat-peptide chelates for direct transduction of technetium-99m and rhenium into human cells for imaging and radiotherapy. Bioconjugate Chemistry. 2000;11:762-71.

[138] Lindgren M, Gallet X, Soomets U, Hällbrink M, Bråkenhielm E, Pooga M, Brasseur R, Langel Ü. Translocation properties of novel cell penetrating transportan and penetratin analogues. Bioconjugate Chemistry. 2000;11:619-26.

[139] Park JH, Lee JH, Park HH, Rhee WJ, Choi SS, Park TH. A protein delivery system using 30Kc19 cell-penetrating protein originating from silkworm. Biomaterials. 2012.

[140] Yang J-P, Ma X-X, He Y-X, Li W-F, Kang Y, Bao R, Chen Y, Zhou C-Z. Crystal structure of the 30K protein from the silkworm *Bombyx mori* reveals a new member of the β-trefoil superfamily. Journal of Structural Biology. 2011;175:97-103.

[141] Pietrzyk AJ, Panjikar S, Bujacz A, Mueller-Dieckmann J, Lochynska M, Jaskolski M, Bujacz G. High-resolution structure of *Bombyx mori* lipoprotein 7: crystallographic determination of the identity of the protein and its potential role in detoxification. Acta Crystallographica Section D: Biological Crystallography. 2012;68:1140-51.

[142] Åmand HL, Nordén B, Fant K. Functionalization with C-terminal cysteine enhances transfection efficiency of cell-penetrating peptides through dimer formation. Biochemical and Biophysical Research Communications. 2012;418:469-74.

[143] Song HS, Lee SH, Oh EH, Park TH. Expression, solubilization and purification of a human olfactory receptor from *Escherichia coli*. Current Microbiology. 2009;59:309-14.

[144] Banerjee RR, Lazar MA. Dimerization of resistin and resistin-like molecules is determined by a single cysteine. Journal of Biological

Chemistry. 2001;276:25970-3.

[145] Patel SD, Rajala MW, Rossetti L, Scherer PE, Shapiro L. Disulfide-dependent multimeric assembly of resistin family hormones. Science. 2004;304:1154-8.

[146] Lewis UJ, Peterson S, Bonewald L, Seavey B, VanderLaan W. An interchain disulfide dimer of human growth hormone. Journal of Biological Chemistry. 1977;252:3697-702.

[147] You M, Spangler J, Li E, Han X, Ghosh P, Hristova K. Effect of pathogenic cysteine mutations on FGFR3 transmembrane domain dimerization in detergents and lipid bilayers. Biochemistry. 2007;46:11039-46.

[148] Stewart KM, Horton KL, Kelley SO. Cell-penetrating peptides as delivery vehicles for biology and medicine. Organic and Biomolecular Chemistry. 2008;6:2242-55.

[149] Chen J, Li G, Lu J, Chen L, Huang Y, Wu H, Zhang J, Lu D. A novel type of PTD, common helix–loop–helix motif, could efficiently mediate protein transduction into mammalian cells. Biochemical and Biophysical Research Communications. 2006;347:931-40.

[150] Morris MC, Deshayes S, Heitz F, Divita G. Cell-penetrating peptides: from molecular mechanisms to therapeutics. Biology of the Cell. 2008;100:201-17.

[151] Gump JM, Dowdy SF. TAT transduction: the molecular mechanism and therapeutic prospects. Trends in Molecular Medicine. 2007;13:443-8.

[152] Johansson HJ, El-Andaloussi S, Holm T, Mäe M, Jänes J, Maimets T, Langel Ü. Characterization of a novel cytotoxic cell-penetrating peptide derived from p14ARF protein. Molecular Therapy. 2008;16:115-23.

[153] Ignatovich IA, Dizhe EB, Pavlotskaya AV, Akifiev BN, Burov SV, Orlov SV, Perevozchikov AP. Complexes of plasmid DNA with basic domain 47-57 of the HIV-1 Tat protein are transferred to mammalian cells by endocytosis-mediated pathways. Journal of Biological Chemistry. 2003;278:42625-36.

[154] Meade AJ, Meloni BP, Mastaglia FL, Knuckey NW. The application of cell penetrating peptides for the delivery of neuroprotective peptides/proteins in experimental cerebral ischaemia studies. Journal of Experimental Stroke and Translational Medicine. 2009;2:22-40.

[155] Lundberg M, Wikström S, Johansson M. Cell surface adherence and endocytosis of protein transduction domains. Molecular Therapy.

2003;8:143-50.

[156] Tünnemann G, Martin RM, Haupt S, Patsch C, Edenhofer F, Cardoso MC. Cargo-dependent mode of uptake and bioavailability of TAT-containing proteins and peptides in living cells. The FASEB Journal. 2006;20:1775-84.

[157] Cai S-R, Xu G, Becker-Hapak M, Ma M, Dowdy SF, McLeod HL. The kinetics and tissue distribution of protein transduction in mice. European Journal of Pharmaceutical Sciences. 2006;27:311-9.

[158] Choi J-M, Ahn M-H, Chae W-J, Jung Y-G, Park J-C, Song H-M, Kim Y-E, Shin J-A, Park C-S, Park J-W. Intranasal delivery of the cytoplasmic domain of CTLA-4 using a novel protein transduction domain prevents allergic inflammation. Nature Medicine. 2006;12:574-9.

[159] Borstad GC, Bryant LR, Abel MP, Scroggie DA, Harris MD, Alloway JA. Colchicine for prophylaxis of acute flares when initiating allopurinol for chronic gouty arthritis. The Journal of Rheumatology. 2004;31:2429-32.

[160] Lee CK, Son SH, Park KK, Park JHY, Lim SS, Kim SH, Chung WY. Licochalcone A inhibits the growth of colon carcinoma and attenuates cisplatin-induced toxicity without a loss of chemotherapeutic efficacy in mice. Basic and Clinical Pharmacology and Toxicology. 2008;103:48-54.

[161] Torchilin VP, Levchenko TS, Rammohan R, Volodina N, Papahadjopoulos-Sternberg B, D'Souza GG. Cell transfection in vitro and in vivo with nontoxic TAT peptide-liposome–DNA complexes. Proceedings of the National Academy of Sciences of the United States of America. 2003;100:1972-7.

[162] Sugita T, Yoshikawa T, Mukai Y, Yamanada N, Imai S, Nagano K, Yoshida Y, Shibata H, Yoshioka Y, Nakagawa S. Comparative study on transduction and toxicity of protein transduction domains. British Journal of Pharmacology. 2008;153:1143-52.

[163] Akkarawongsa R, Cullinan AE, Zinkel A, Clarin J, Brandt CR. Corneal toxicity of cell-penetrating peptides that inhibit herpes simplex virus entry. Journal of Ocular Pharmacology and Therapeutics. 2006;22:279-89.

[164] Fire A, Xu S, Montgomery MK, Kostas SA, Driver SE, Mello CC. Potent and specific genetic interference by double-stranded RNA in *Caenorhabditis elegans*. Nature. 1998;391:806-11.

[165] Rana TM. Illuminating the silence: understanding the structure and function of small RNAs. Nature Reviews Molecular Cell Biology. 2007;8:23-36.

[166] Miller VM, Xia H, Marrs GL, Gouvion CM, Lee G, Davidson BL, Paulson HL. Allele-specific silencing of dominant disease genes. Proceedings of the National Academy of Sciences of the United States of America. 2003;100:7195-200.

[167] Santel A, Aleku M, Keil O, Endruschat J, Esche V, Durieux B, Löffler K, Fechtner M, Röhl T, Fisch G. RNA interference in the mouse vascular endothelium by systemic administration of siRNA-lipoplexes for cancer therapy. Gene Therapy. 2006;13:1360-70.

[168] Xia X, Zhou H, Huang Y, Xu Z. Allele-specific RNAi selectively silences mutant SOD1 and achieves significant therapeutic benefit in vivo. Neurobiology of Disease. 2006;23:578-86.

[169] Cardoso A, Simoes S, De Almeida L, Pelisek J, Culmsee C, Wagner E, Pedroso de Lima M. siRNA delivery by a transferrin-associated lipid-based vector: a non-viral strategy to mediate gene silencing. The Journal of Gene Medicine. 2007;9:170-83.

[170] Minakuchi Y, Takeshita F, Kosaka N, Sasaki H, Yamamoto Y, Kouno M, Honma K, Nagahara S, Hanai K, Sano A. Atelocollagen-mediated synthetic small interfering RNA delivery for effective gene silencing in vitro and in vivo. Nucleic Acids Research. 2004;32:e109-e.

[171] Song E, Zhu P, Lee S-K, Chowdhury D, Kussman S, Dykxhoorn DM, Feng Y, Palliser D, Weiner DB, Shankar P. Antibody mediated in vivo delivery of small interfering RNAs via cell-surface receptors. Nature Biotechnology. 2005;23:709-17.

[172] Takeshita F, Minakuchi Y, Nagahara S, Honma K, Sasaki H, Hirai K, Teratani T, Namatame N, Yamamoto Y, Hanai K. Efficient delivery of small interfering RNA to bone-metastatic tumors by using atelocollagen in vivo. Proceedings of the National Academy of Sciences of the United States of America. 2005;102:12177-82.

[173] Hammond SM, Bernstein E, Beach D, Hannon GJ. An RNA-directed nuclease mediates post-transcriptional gene silencing in *Drosophila* cells. Nature. 2000;404:293-6.

[174] Chien P-Y, Wang J, Carbonaro D, Lei S, Miller B, Sheikh S, Ali SM, Ahmad MU, Ahmad I. Novel cationic cardiolipin analogue-based liposome for efficient DNA and small interfering RNA delivery in vitro and in vivo. Cancer Gene Therapy. 2005;12:321-8.

[175] Grzelinski M, Urban-Klein B, Martens T, Lamszus K, Bakowsky U, Höbel S, Czubayko F, Aigner A. RNA interference-mediated gene silencing of pleiotrophin through polyethylenimine-complexed small interfering RNAs in vivo exerts antitumoral effects in glioblastoma xenografts. Human Gene Therapy. 2006;17:751-66.

[176] Pirollo KF, Zon G, Rait A, Zhou Q, Yu W, Hogrefe R, Chang EH. Tumor-targeting nanoimmunoliposome complex for short interfering RNA delivery. Human Gene Therapy. 2006;17:117-24.

[177] Ying R-S, Zhu C, Fan X-G, Li N, Tian X-F, Liu H-B, Zhang B-X. Hepatitis B virus is inhibited by RNA interference in cell culture and in mice. Antiviral Research. 2007;73:24-30.

[178] Moschos SA, Jones SW, Perry MM, Williams AE, Erjefalt JS, Turner JJ, Barnes PJ, Sproat BS, Gait MJ, Lindsay MA. Lung delivery studies using siRNA conjugated to TAT (48-60) and penetratin reveal peptide induced reduction in gene expression and induction of innate immunity. Bioconjugate Chemistry. 2007;18:1450-9.

[179] Davidson TJ, Harel S, Arboleda VA, Prunell GF, Shelanski ML, Greene LA, Troy CM. Highly efficient small interfering RNA delivery to primary mammalian neurons induces MicroRNA-like effects before mRNA degradation. The Journal of Neuroscience. 2004;24:10040-6.

[180] Muratovska A, Eccles MR. Conjugate for efficient delivery of short interfering RNA (siRNA) into mammalian cells. FEBS Letters. 2004;558:63-8.

[181] Turner JJ, Jones S, Fabani MM, Ivanova G, Arzumanov AA, Gait MJ. RNA targeting with peptide conjugates of oligonucleotides, siRNA and PNA. Blood Cells, Molecules, and Diseases. 2007;38:1-7.

[182] Meade BR, Dowdy SF. Exogenous siRNA delivery using peptide transduction domains/cell penetrating peptides. Advanced Drug Delivery Reviews. 2007;59:134-40.

[183] Unnamalai N, Kang BG, Lee WS. Cationic oligopeptide-mediated delivery of dsRNA for post-transcriptional gene silencing in plant cells. FEBS Letters. 2004;566:307-10.

[184] Wang Y-H, Hou Y-W, Lee H-J. An intracellular delivery method for siRNA by an arginine-rich peptide. Journal of Biochemical and Biophysical Methods. 2007;70:579-86.

[185] Simeoni F, Morris MC, Heitz F, Divita G. Insight into the mechanism of the peptide-based gene delivery system MPG: implications for

delivery of siRNA into mammalian cells. Nucleic Acids Research. 2003;31:2717-24.

[186] Lundberg P, El-Andaloussi S, Sütlü T, Johansson H, Langel Ü. Delivery of short interfering RNA using endosomolytic cell-penetrating peptides. The FASEB Journal. 2007;21:2664-71.

[187] Eguchi A, Dowdy SF. siRNA delivery using peptide transduction domains. Trends in Pharmacological Sciences. 2009;30:341-5.

국 문 초 록

30Kc19 단백질의 세포투과 펩타이드 동정과 특성 분석 및 단백질과 유전자 전달을 위한 응용

박 희 호
서울대학교 대학원
화학생물공학부

30Kc19 단백질은 누에 체액에 존재하는 유사한 구조의 단백질의 모임인 30K 단백질 그룹의 일원이다. 이 단백질들은 30 kDa 정도의 분자량을 지니며, 30Kc19 단백질은 누에 채액 내에 존재하는 30K 단백질들 (30Kc6, 30Kc12, 30Kc19, 30Kc21, 30Kc23) 중 가장 많은 비중을 차지한다. 30K 단백질의 누에 내 생물학적인 기능은 완벽히 알려지지 않았으나, 최근 30Kc6와 30Kc19의 기능적 특성을 밝히는 연구들이 수행된 바 있다. 이전의 연구에서, 누에 체액과 30K 단백질은 단백질을 배양 배지에 첨가 혹은 30K 단백질 유전자를 발현하는 방법으로 여러 종류의 세포에서 항 아폽토시스 효과를 나타냄을 보였다. 또한, 30K 단백질은 재조합 에리스로포이에틴, 인터페론-β, 단클론 항체의 생산량과 당쇄화를 증대시키고, 여러 세포에서 세포 성장 및 생존을 증대시켰으며, 효소 안정화 효과 또한 보였다. 최근의 연구에서는 30Kc19 단백질이 세포 배양 배지에

첨가될 경우, 세포투과 효과를 보임을 밝히기도 하였다. 따라서, 30Kc19 단백질은 매우 독특한 특성을 지니는 다기능 단백질이며, 세포막을 투과하고 운반한 단백질을 안정시킬 수 있기 때문에 효소를 포함한 치료용 단백질의 전달에 활용될 수 있다.

이 연구의 목적은 30Kc19 단백질의 이합체화 경향 및 세포투과 기작 연구와 목적 물질을 운반하는 데 필요한 30Kc19 단백질내의 세포투과 펩타이드를 찾는 것이다. 먼저, 양친성 물질, 즉 SDS 혹은 인지질 존재 하에서의 30Kc19 단백질의 이합체화 경향을 연구하였다. Native 폴리아크릴아미드겔전기영동 결과를 통하여 30Kc19 단량체가 SDS나 인지질이 존재할 경우 이합체화가 되는 것을 보였다. GST pull-down 분석을 통하여 동물 세포 배양 배지에 30Kc19가 첨가될 경우, 세포막에 존재하는 지질 이중막의 주 성분인 인지질에 의하여 30Kc19가 이합체를 형성하며 세포 내로 투과하는 것을 관찰할 수 있었다. 돌연변이 생성 수행 결과 30Kc19 C76A에서 세포투과가 관찰된 반면 30Kc19 C57A에서는 관찰되지 않았으며, 이는 Cys-57이 세포투과 과정 중 세포막에서 이합체화가 되는 데 관여함을 의미한다. 다음으로는, 단백질 전달 시스템에 이용하기 위하여 세포를 투과하는 30Kc19 단백질이 어떻게 주요 세포막 구성 성분인 인지질과 연관되어 있는지 와 30Kc19 단백질이 동물 세포 내로 진입하는 기작을 밝히는 연구가 진행되었다.

세포투과 기작과 물질 수송 능력에 기반을 두어, 누에 유래 30Kc19 단백질 내에 세포투과 펩타이드 (CPP) 가 존재할 것이라 가정하였고, 이를 확인하기 위한 연구를 시도하였다. 실제로 세포를 투과할 수 없는 물질을 세포 내에 전달하기 위해서는 30Kc19내에서 효율적인 물질 전달에 사용되는 여타 세포투과 단백질과 유사한 세포투과 영역을 찾는 것이

필요하다. 30Kc19 내에서 가장 CPP일 가능성이 높은 후보 영역이 선정되었으며, 여러 CPP 후보들의 세포투과 특성을 시험하였다. 이를 통하여 30Kc19 내의 45-57번째 아미노산인 VVNKLIRNNKMNC 이 새로운 CPP (Pep-c19) 로 규명되었다. 또한 이 CPP의 세포투과 효율과 독성 여부를 30Kc19의 기능과 비교 실험한 결과, 생체외와 생체내 모두에서 원 단백질에 비해 효율성이 우수함을 관찰하였다. 또한 치료 목적으로의 응용을 위하여, siRNA 전달을 위한 비공유결합적 접근을 시도하였다. 이 결과, Pep-c19이 siRNA를 세포 내로 성공적으로 운반하여, 널리 사용되는 CPP인 11R을 사용하였을 때와 유사한 유전자 침묵화 효과를 확인하였다. Pep-c19은 최초의 곤충 체액 유래의 세포투과 단백질에서 얻은 세포투과 펩타이드이기 때문에, 이 발견을 통하여 다른 곤충 유래의 단백질에서 Pep-c19과 유사한 특성을 갖는 다른 세포투과 펩타이드를 발견할 수 있을 것으로 기대된다.

30Kc19 단백질과 Pep-c19는 TAT와 달리 비-바이러스 유래 물질이며, 세포 독성이 없는 세포투과 단백질/펩타이드로서 응용 가능하다. 이 연구를 통하여 제약, 화장품과 같은 생물 산업에서의 효율적인 치료 물질 전달을 위한 이로운 효과를 미치는 새로운 접근 방법을 열어 줄 수 있을 것으로 기대된다.

주요어: 30Kc19 단백질, 이합체화, 세포투과 펩타이드, 방해 리보 핵산, 재조합 단백질 생산, *생체내* 전달

학번: 2007-30849